Dividing Time – An Absolute Chronological Study of Material Culture from Early Iron Age Urnfields in Denmark

Helene Rose * and John Meadows

Posted Date: 28 November 2023

doi: 10.20944/preprints202311.1702.v1

Keywords: Archaeology; Early Iron Age; typology; cremated bone; radiocarbon dating; Bayesian chronological modelling

Article

Dividing Time – An Absolute Chronological Study of Material Culture from Early Iron Age Urnfields in Denmark

Helene Agerskov Rose [1,2,*] and John Meadows [1,3]

[1] Centre for Baltic and Scandinavian Archaeology, Foundation of Museums of the State of Schleswig-Holstein, Germany; ORCID id 0000-0003-1061-3129; ORCID id 0000-0002-4346-5591
[2] Department of Historical Studies, University of Gothenburg, Sweden
[3] Leibniz-Laboratory for AMS Dating and Stable Isotope Research, Kiel University, Germany
* Correspondence: helene.agerskov.rose@gu.se (HAR)

Abstract: Chronological frameworks based on artefact typologies are essential for interpreting the archaeological record, but they inadvertently treat transitions between phases as abrupt events and disregard the temporality of transformation processes within and between individual phases. This study presents an absolute chronological investigation of a dynamic material culture from Early Iron Age urnfields in Denmark. The chronological framework of Early Iron Age in Southern Scandinavia is largely unconstrained by absolute dating, primarily due to it coinciding with the so-called 'Hallstatt calibration plateau' (c.750 to 400 cal BC), and it is difficult to correlate it with Central European chronologies due to a lack of imported artefacts. This study applies recent methodological advances in radiocarbon dating and Bayesian chronological modelling, specifically a statistical model for wood-age offsets in cremated bone and presents the first large-scale radiocarbon investigation of regional material culture from Early Iron Age in Southern Jutland, Denmark. Dated material is primarily cremated bone from 111 cremation burials from three urnfields. The study presents absolute date ranges for 16 types of pottery and 15 types of metalwork, which include most of the recognised metalwork types from the period. This provides new insights into gradual change in material culture, when certain artefact types were in production and primary use, how quickly types were taken up and later abandoned, and distinguishing periods of faster and slower change. The study also provides the first absolute chronology for the period, enabling correlation with chronologies from other regions. Urnfields were introduced at the Bronze-Iron Age transformation, which is often assumed to have occurred c.530-500 BC. We demonstrate that this transformation took place in the 7th century BC, however, which revives the discussion of whether the final Bronze Age period VI should be interpreted as a transitional phase to the Iron Age.

Keywords: archaeology; Early Iron Age; typology; cremated bone; radiocarbon dating; Bayesian chronological modelling

Introduction

Time and culture are old concepts within the discipline of archaeology, but how these are approached differs across the globe and has also changed over time, reflecting the emerging 'schools of thought'. A common approach is the construction of chronological frameworks based on systematized observations of stratigraphy and typology, such as Thomsen's Three Age System (e.g. 1, 2). In the 20th century, Scandinavian archaeology strived toward increasing the chronological resolution of material culture within (3, 4, 5). Early Central European researchers were more focused on defining cultural groups or 'people' (e.g. 6, 7), and today the concepts of period, culture and even geography have been ingrained into the discipline. This has caused some confusion because it can be difficult to distinguish the terms 'urnfield period', 'urnfield culture(s)' and 'urnfield area' that are used interchangeably in the literature (8). This study investigates artefact assemblages from three

 doi:10.20944/preprints202311.1702.v1

urnfield cemeteries in Denmark (Figure 1) and uses the term 'urnfield' to describe the specific funerary practice present in northern Europe during the first millennium BC, without any assumptions regarding chronology or ethnicity.

Figure 1. Location of Aarupgaard, Aarre and Søhale urnfields in south-west Jutland, Denmark (map: GIS, ZBSA).

The earlier part of the Iron Age in Southern Scandinavian, which is defined as 'Pre-Roman' (i.e., 'before the Roman Empire'), began in c.500 BC The relative chronological framework of the Pre-Roman Iron Age (PRIA) is traditionally based on typo-chronological studies of urnfield artefact assemblages (4, 9, 10), and presently two chronological systems are used in Danish archaeology: Becker's from 1961 and Jensen's from 2005 (Figure 2). Becker divided the PRIA into three periods, corresponding to Central European La Tène periods I-III (4), but Jensen demonstrated how this produced an uneven distribution of pottery and metalwork over the period, along with difficulties in harmonizing the materials, possibly because of divergent chronological sensitivities (11, 12). Metalwork typology has been assumed to be chronologically sensitive, with more rapidly changing typological traits, whereas pottery types are considered to be more 'conservative' and longer-lasting (13). Jensen (5) revised the chronological framework, specifically avoiding the use of 'type fossils' and divided the PRIA into two main chronological periods: Early PRIA (c.500-250 BC) and Late PRIA (c.250 BC – AD 1) (14), with further divisions into sub-periods and phases specific to the geographical area.

Preprints (www.preprints.org) | NOT PEER-REVIEWED | Posted: 28 November 2023 doi:10.20944/preprints202311.1702.v1

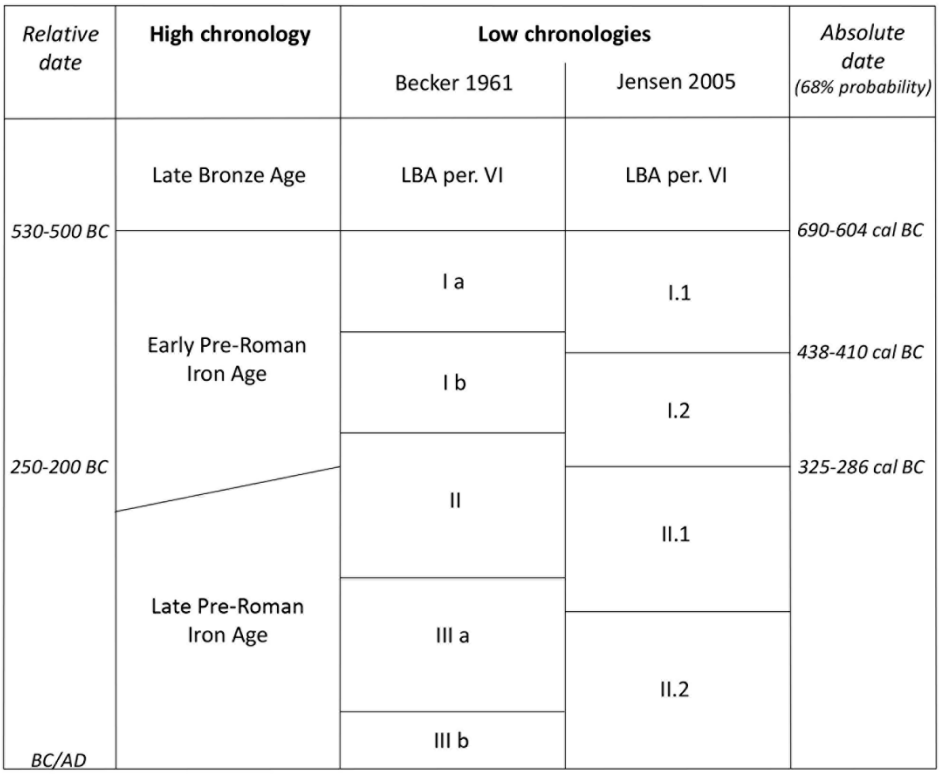

Figure 2. Chronological framework of the Pre-Roman Iron Age in Southern Scandinavia (4, 5). Absolute dates at 68% probability are based on results presented in this paper.

It is difficult to correlate the relative chronologies of Southern Scandinavia and Central European due to a lack of imported artefacts, but the Early Pre-Roman Iron Age has been suggested to coincide with Ha D in Central Europe, based on a few Wendel rings and eyelet rings from depot finds and two North European Certosa-type fibulae from a flat grave (15, 16, 17). The chronological framework of Southern Scandinavia is largely unconstrained by absolute dating (although see 18). This is partly due to difficulties associating features dated by radiocarbon (^{14}C) or dendrochronology with typo-chronological phases, but primarily due to the longstanding perception that between c.750 and 400 cal BC the ^{14}C calibration curve is too flat to justify ^{14}C dating (19). It is only with relatively recent developments in ^{14}C dating techniques that it has become possible to date the bio-apatite of fully calcined bone (20), which is of great importance for research into the Late Bronze Age-Early Iron Age in north-western Europe when cremation was the dominant burial rite (e.g. 21). Experimental studies have however shown that significant carbon exchange occurs between bone-apatite and the pyre atmosphere during cremation, which can cause a calendar date offset between the ^{14}C event and the date of cremation (22, 23, 24, 25). If the effects of wood-age offsets on ^{14}C dates from cremated bone are corrected with a statistical outlier model (25), it will date the cremation event and thus the deposition date of the associated artefacts. From an archaeological perspective, the cremation is a separate event occurring after death and before burial, but these events cannot have been separated by more than a few days or weeks. The production date of an artefact must have occurred sometime before deposition, and for the present purpose, it is assumed that part of the metalwork might have a discernible residence time, but that most of the funerary urns were made less than a decade before the cremation.

Dividing time and identifying change

How archaeology as a discipline divides time and approaches chronology is largely defined by principles arising from cultural history that assume similarities and differences in material culture can be employed to define discrete and relatively homogenous social entities (26). Cultural history was critiqued by New Archaeology for being descriptive rather than explaining human beliefs and

 doi:10.20944/preprints202311.1702.v1

behaviours (27, 28), but the methodological basis for placing research in space and time remained. This approach privileges certain research questions and has a great influence on how we write archaeological narratives (29).

Chronological frameworks remain essential for interpreting the archaeological record, but although they may appear to be neutral and unbiased, they present subjective interpretations of the past (30). Such frameworks have inherent linear and successive structures and assume change occurs at a constant rate in a progressive step-wise sequence (26). The uniformitarian nature of their construction leads to the creation of non-overlapping chronological units, where generally, short time spans are thought to reflect dynamic societies in more troubled times, whereas longer time spans reflect peaceful periods (31). Transitions between non-overlapping chronological units are inadvertently treated as abrupt, disregarding the temporality of transformation processes within and between periods. More detailed chronologies, with shorter periods, can be created when material culture changed relatively quickly, whereas slower change leads to the creation of longer periods (31).

Artefact typologies describe and create entities according to a set of formal morphological characteristics (e.g. weight, height and colour). These entities can be ordered by seriation, which is a heuristic tool, aiming to describe a specific artefact as opposed to similar objects that preceded it and followed it (32), creating schemes of relatedness of types (33). Seriation relies on the idea that every artefact is a copy of an 'ideal' (34), but Fowler has suggested ideals did not exist but to rather perceive artefact types as arising from similar iterative processes in the past (32). Several different types might be contemporaneous, as their 'relatedness' does not imply a linear chronological sequence (33). Typology has an inherent risk of forcing artefacts into rigid schemes, obscuring or even erasing their differences (35), but typology is nonetheless indispensable for understanding change and continuity in the past (32).

The construction of relative chronologies relies on three basic principles: all artefacts from a 'closed find' are contemporaneous; layers are deposited in stratigraphic succession with the oldest at the bottom and the youngest at the top; change in material culture occurs gradually and artefacts close in time are more likely to look similar than chronologically distant artefacts (36, 37). Sorting large numbers of attributes or variables into is computationally demanding and since the 1980s has often been carried out using correspondence analysis (38, 39, 40). Established artefact seriations can then be grouped into relative chronological units of periods, phases or horizons, and archaeologists have since the 19th century strived to construct increasingly detailed chronologies (e.g. 37, 41, 42). Sequential ordering of archaeological material into relative typological chronologies or typo-chronologies is a vital part of the cultural history methodology and a fundamental part of interpreting change in the past (43, 44), although it is debatable whether the chronological divisions carry real cultural meaning (45). Typo-chronologies are good at showing long-term and geographically broad patterns of change in the archaeological record and they can help us understand how change in one domain of a society, such as change in the material culture or the introduction of a new burial practice, might be linked to broader transformations in the society and its environment. Typo-chronologies are constructed in response to different needs, be that to date an archaeological culture, define a material culture or reveal economic and technical changes regarding data selection, analysis and interpretation, causing every system to present a different version of the past. A version dependent on arbitrary geographical constrains such as modern countries or regions, obscuring spatial differences within the selected area and between different areas.

Burials have traditionally provided closed-context material for typo-chronological analyses (e.g. 4), but because mortuary practices are often conservative in nature (46, 47), the temporal scale of grave-good chronologies might not equal the temporal scale otherwise observable at contemporaneous settlement sites (48). Another challenge to chronological analyses of burial assemblages is the possibility of objects being passed between generations as heirlooms (37). It has been suggested that pottery from graves is not representative of the style otherwise in use at the time of death, but rather a style produced or selected specifically for funerary purposes (49). There are demonstrated difficulties in correlating metalwork and pottery typologies from the PRIA in Denmark

 doi:10.20944/preprints202311.1702.v1

(11). This may be due to different temporal sensitivity, where metalwork patterns are intrinsically more fluid than pottery shapes, leading to expected higher rates of change in metalwork types. Pottery typology was also regarded as more conservative in Early Iron Age urnfield material from Schleswig-Holstein (13). There is a need to evaluate existing typo-chronologies and resolve possible temporal discrepancies using absolute dating, but this is not a straightforward process, as evidenced by ^{14}C dating of sequential cultural layers with diagnostic pottery, whose results can be difficult to reconcile with existing chronological frameworks (e.g. 50). Such studies commonly use pottery types as markers of certain periods or phases, but without investigating the currencies of the individual types it is not possible to conclude whether it is the chronology or the typologies, or indeed both, that are in need of a revision.

Modelling change within a Bayesian framework

Bayesian statistics offers a coherent statistical framework for evaluating and interpreting statistically independent likelihoods for the calendar dates of events associated with an archaeological phenomenon in view of our relative dating information (51). Calendar information will often be calibrated ^{14}C ages, but thermoluminescence dates, dendrochronological dates, numismatic or historical dates can equally be included. A Bayesian chronological model combines probability distributions of calibrated dates with prior information consisting of expert observations obtained independently of the likelihoods. This 'prior information' can either take the form of informative priors based on the temporal relationships between samples, such as relative dating based on traditional stratigraphy or typology, or as uninformative priors that impose a statistical distribution on the dated events, e.g. assuming that the calendar dates of potential ^{14}C samples are uniformly distributed between start and end boundaries (52, 53). The model uses this prior information to constrain the statistically most likely date ranges (*posterior density estimates*) of the ^{14}C samples. Bayesian chronological models can estimate dates of events that cannot be dated directly, such as when burial activity started at a cemetery, or when an artefact type came into use, which allows us to investigate change as a process and to test existing interpretations of causal processes. The introduction of an artefact type at more sites can be modelled individually but modelling its spatio-temporal progress across the landscape using geography as prior information, remains challenging in spite of recent progress (e.g. 54).

In most cases, a Bayesian chronological model will significantly improve the overall precision of directly dated events compared to individual calibrated ^{14}C dates, but studies coinciding with plateaus in the ^{14}C calibration curve remain challenging. Here even relatively precise ^{14}C ages for short-lived samples can produce calibrated date ranges spanning the whole plateau, or at best, give multimodal distributions offering alternative solutions in different centuries. This study is concerned with the ^{14}C plateau c.750-400 BC (55, 56), also known as the Hallstatt plateau (57, 58). The Hallstatt plateau has been detrimental to studies of Early Iron Age chronologies in Europe (59), but with recent developments in ^{14}C science it might no longer be a 'catastrophe' for archaeological chronology (19). Developments include ^{14}C measurements with increasing precisions (e.g. 60) and new algorithms applying less smoothing to the new IntCal20 calibration dataset (61). Finally, IntCal20 include calibration data at single-year resolution for the first half of the Hallstatt plateau (62, 63, 64), although not for the second half, which coincides with the Danish urnfields. Recent studies using Bayesian chronological modelling have demonstrated that is possible to model case studies on ^{14}C calibration plateaus, although applications tend to target materials whose dates are constrained by strong prior information based e.g. on stratigraphy (65, 66), floating tree-ring series (67, 68), or archaeogenetic evidence (69). This study however employs relatively weak constraints, assuming that artefacts sharing certain characteristics (i.e. of the same type) are more likely to date close to each other than far apart, and if a representative number of samples are dated from each type, their currency can be modelled, i.e. the period a certain artefact type was in production and in primary use. There is no available prior information from traditional stratigraphy, e.g. constructional or depositional sequences, although urnfield site formation has been described using horizontal stratigraphy (e.g. 70).

 doi:10.20944/preprints202311.1702.v1

A majority of published Bayesian chronological models assume that change occurred too rapidly to detect within the resolution of the ^{14}C dating method. Although this is a useful working assumption and probably not grossly misleading in most cases (71), cultural change is an ongoing process and whether that is visible in the archaeological record depends on the temporal resolution of the available data. This is certainly true for the material record and Brainerd stated that "*Each type originates at a given time in a given place, is made gradually in increasing numbers as time goes on, then decreases in popularity until it becomes forgotten, never to reoccur in an identical form*" (43). Brainerd's statement has been demonstrated using known-age datasets (72, 73), but is not supported by the commonly used uniform distribution bounded-phase model, which assumes that archaeological activity began and ended abruptly (74). The Bayesian community has been long been aware of this (75), but there was no better alternative available before Lee and Bronk Ramsey (76) developed a trapezoidal distribution model, which was introduced in OxCal v.4.2 (77). They based it on earlier works by Karlsberg (75), who found that assuming different *a priori* information about the rate of deposition has a significant influence on the posterior density estimates and the archaeological interpretations thereof. The trapezoidal model splits the distribution into three parts: a gradual increase (introductory period), a period with a constant rate of activity (blooming period), and finally a gradual demise (period of decline). This distribution corresponds well with the currency model suggested by Trachsel based on his re-evaluation of Hallstatt chronology (37). The trapezium model provides an alternative approach for modelling transitional processes, allowing the transition to have a duration without having prior knowledge of which dated cases belong in the introductory period, blooming period or period of decline (76, 78). It remains a more demanding model in terms of computational time and number of dated cases required to reach useful posterior estimates, but the current study aims to apply it whenever it is suitable and possible.

A single ^{14}C age can be associated with more items from the same context, e.g. the death of an individual, the decline of artefact type A, the blooming of artefact B and the introduction of artefact type C. Cross-referencing events between different elements in the model is a powerful tool that allows a single likelihood to be evaluated over a range of prior information (e.g. 79). Extensive use of cross-referencing do however remain computationally challenging and it can be necessary to duplicate posterior estimates using the OxCal function Prior, which allows the same likelihood to be sampled multiple times (B-R 2009: 351-2).

Early Pre-Roman Iron Age in Southern Scandinavia

In Southern Scandinavia, and in particular southern Jutland, the PRIA appears to be a hybrid cultural group sharing traits of material culture, house types, economy and funerary practices with the Jastorf core area in Holstein and Mecklenburg (80), and the Lower Rhine area (81). Around the start of the PRIA, iron began to be extracted locally in Denmark, substituting the previous dependence of imported bronze and limiting the import of artefacts with a wider European distribution (14). Jutland is divided into three regional groups, based on differences in material culture and funerary practices: southern Jutland, middle Jutland and northern Jutland (4). The Early PRIA (c.500-250 BC) appears to have been a peaceful period, although it coincides with a peak in deposition of human bodies in bogs (82), which might indicate inter-personal or even religiously or societally initiated violence. It is difficult to detect any social stratification in this period (83), but rather than being a truly egalitarian society, social hierarchy was likely expressed in ways that are not archaeologically recognisable. This argument is supported by an ongoing reorganisation of the cultural landscape in the Early PRIA, as demonstrated by the introduction of Celtic fields demarcating land ownership (84), pit alignments with possible implications of fortification, control of movement of people and cattle (85), and the first fortified settlements (86).

The urnfield funerary tradition

In Denmark, funerary practices changed from inhumation to cremation around the transition from Early to Late Bronze Age (c.1100 BC), but burials continued to take place at the large Early Bronze Age burial mounds. This practice continued into the Early Iron Age, but in parallel with this,

 doi:10.20944/preprints202311.1702.v1

the urnfield funerary tradition was introduced in Southern Jutland at the beginning of the PRIA and the large collective burial grounds mark a fundamental break with earlier funerary practices (14). The Danish urnfield tradition is a late part of a wider European tradition, but unlike in Continental Europe, it does not define the period or its cultural affiliation (81).

The urnfields were first described at the end of the 19th century, when the small burial mounds were still visible in the landscape (9, 10). Madsen and Neergaard excavated the central part of close to 500 urnfield graves and although largely ignoring the rest of the burial mounds, they concluded that the character of the urnfield were so homogenous that future excavations were unlikely to alter this picture (9). More urnfields were however excavated during the first half of the 20th century to obtain datable material for typo-chronological studies (4, 87, 88). New urnfields continue to be recorded through development-led excavations, aerial photography and LiDAR remote sensing (e.g. 89) and to date, 66 certain and another 22 possible urnfields have been identified (18). The urnfields are primarily situated in south-west Jutland, where the landscape is characterized by outwash plains with primarily nutrient-poor sandy soil. The topography is low-lying and smaller rivers, lakes and bogs are scattered across the landscape, which to the west is bordered by the Wadden Sea (90). The urnfields are often constructed in the vicinity of Neolithic or Bronze Age burial mounds, continuing the Bronze Age tradition of demarcating major routes of transport by lines of burial mounds, but at the same time separate from contemporaneous settlements (91).

Following the Danish urnfield tradition, the deceased were cremated, and fragments of calcinated bone were deposited in ceramic vessels along with metal objects and buried individually under a small burial mound or 'hillock' (Figure 3). Approximately 1/3 of burials contained metal objects regarded as possible dress accessories. At some sites, a small part of the pyre debris (i.e. charcoal and other charred archaeobotanical remains) was also transferred to the urn. There is no evidence of cremation pyres near the urnfields and in fact, few prehistoric pyre sites are known from Denmark. Pyres can be preserved if they are covered shortly after the cremation event, e.g. by a burial mound, but even then, it can be difficult to identify them archaeologically, as evidenced by experimental cremation studies (92). A smaller number of other grave types also occur, such as 'bone-layer graves' without a (discernible) container, 'urn-bone layer graves' as a hybrid burial form containing cremated bone and pottery sherds (grave types after 93), and at some sites graves are covered by a stone paving rather than a hillock (94). A key feature of the urnfield tradition is that each grave is encircled by a ditch with a varying number of interruptions, forming bridges into the central hillock (4). The hillocks were created by using the soil from the circular ditch, and have estimated original heights of 1-2 m and diameters from a few meters up to 11 m. At some urnfields, the hillocks were further demarcated by kerbstones or wooden posts (70).

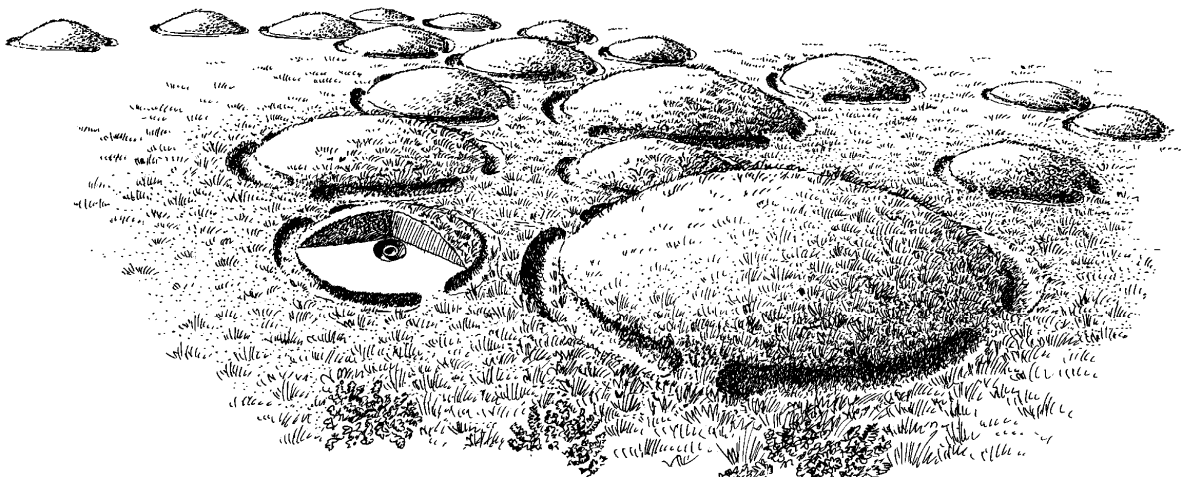

Figure 3. Reconstruction of urnfield in Kelstrup plantation forest, Southern Jutland. The small mounds are encircled by ditches with interruptions, cross-section of one mound to show the central urn grave (drawing: J Andersen, Museum Sønderjylland).

Preprints (www.preprints.org) | NOT PEER-REVIEWED | Posted: 28 November 2023 doi:10.20944/preprints202311.1702.v1

The urnfields vary from a few and up to around 1500 closely spaced graves. The graves are clearly demarcated by open circular ditches and generally do not inter-cut (70), making it difficult to determine any direct stratigraphic relationship between graves. Horizontal stratigraphy has however been observed at several urnfields (4, 11, 70, 95).

Material record

Urnfield artefact assemblages only represents part of the PRIA material record, but the relative chronological framework of the period has historically been based on typo-chronological studies of these assemblages. There are no weapon graves from the period and all artefacts of metal are related to the personal dress attire, representing a limited range of dress accessories and other related adornments. Dress pins from the LBA are made in bronze, but with the onset of PRIA, the pins are primarily made of iron. Neck rings and certain pin types do however continue to be made of bronze. The repertoire of pins and belt equipment is similar to but more restricted than material from Schleswig-Holstein (13, 96, 97, 98, 99, 100). A list of type names in English and Danish is provided in the Supporting Information. According to the typo-chronology of Jensen (5), the earliest pin type has a coiled head and a bend in the upper part of the pin, just beneath the head. In period I.1b-I.2a, the bend moves down the needle, creating a neck beneath the head. Pins with circular head and bomb-shaped head are introduced in period I.2. In period II.1, Holstein pins, pins with grooved head, winged head pins and pins with rod-shaped head appear. Different types of iron belt equipment appear from period I.1 onwards, starting with iron rings with eyelets. In period I.1b, belt hooks with protruding clasps are introduced, initially with a tongue-shaped outline, followed by a triangular outline, before becoming narrow in outline by period II.1. Also occurring in period II.1 are iron rings with shank (5).

One exception from Jensen's typology (5) is made regarding the subdivision of pins with circular head based on the size of the head. Pins with 'large' heads (diameter >2x pin width) are supposedly introduced a little earlier than pins with 'small' head (diameter <2x pin width). We however only found one pin, from Aarupgaard grave U123, with a small circular head following this definition. When the head size index (diameter of inner head/pin width) of all the pins with circular heads from Aarupgaard is plotted, they demonstrate a continuous distribution without any clear typological categories (Figure 4). This analysis only considers material from Aarupgaard, and warrants further investigation, but for the present study, we suggest that pins with circular head belong to a single typological group, and we will treat them as such in the following.

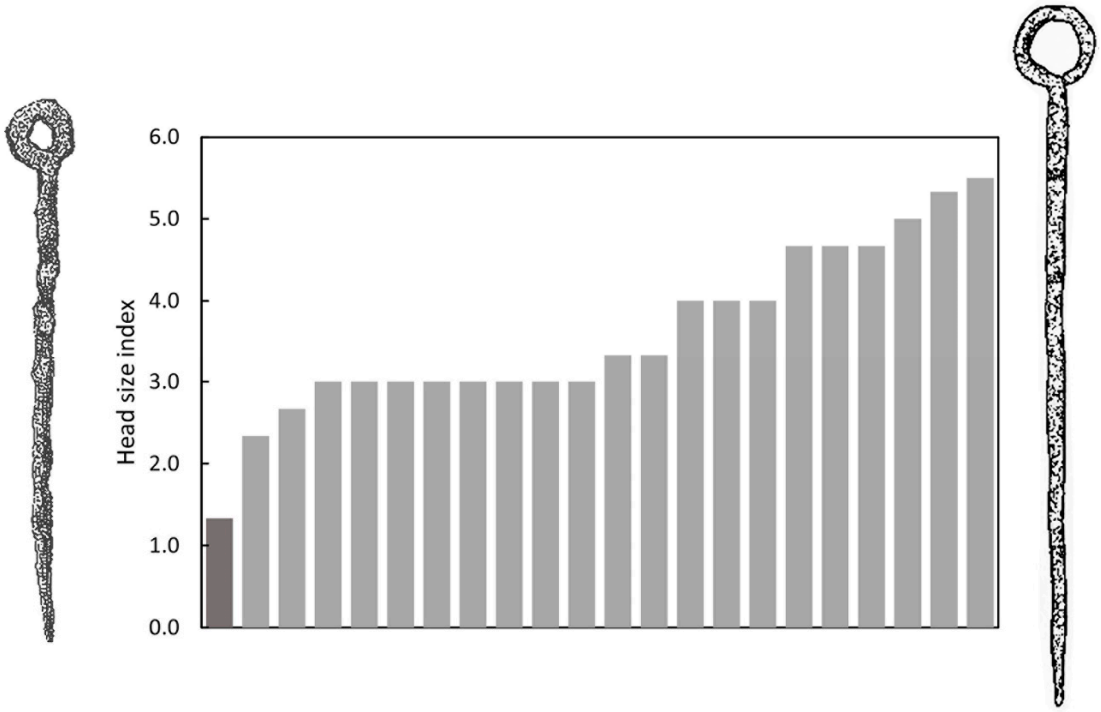

 doi:10.20944/preprints202311.1702.v1

Figure 4. Distribution of head size index (inner head diameter divided by pin width) of 22 pins with circular head from 11 graves from Aarupgaard urnfield. Each column presents a single pin and only one pin from grave U123 qualifies as having a small head (darker grey column and depicted to the left of the plot). To the right of the plot is depicted the pin with the largest head size, from grave U500.

The full pottery repertoire found at settlement sites includes a range of vessels in different sizes, but at burial sites, most pots are large-medium sized storage vessels used as funerary urns, and small bowls and cups used as accompanying vessels (Figure 5). Ornamentation is rare and although vessel rim shapes are chronologically sensitive (11), they have often been destroyed by agricultural activity, making them ill-suited for chronological studies. Instead, typological division is based on vessel proportions (height and width) (5). Individual types are designated by a number referring to the shape of the vessel body, and a capital letter referring to the shape of the vessel neck (see Supporting Information). Some of the types remained in use for most of the Early PRIA and then disappeared at the transition to Late PRIA, when several new types were introduced. Vessel shapes 11, 12 and 13, with cylindrical or concave necks, were most prevalent in the Early PRIA, with early types 11A, 11D, 12A, 13A and 13C, and late types 13B, 13D, 15B, 15C and 18C. Vessel shapes 16, 17 and 20, with no necks, were most prevalent in Late PRIA (5).

Figure 5. Pottery from Aarupgaard urnfield on exhibition at Haderslev Museum. Medium-large sized vessels are funerary urns, with and without handles and lids, small bowls and cups are accompanying vessels from either the burial pit or the circular ditches (photo: HA Rose).

Aarre urnfield

Aarre urnfield is situated on Esbjerg Bakkeø, a low hill island surrounded by wetlands. The site was first investigated by antiquarians in the 1890s, and it came to play an important role in the definition of a chronological framework for the PRIA in Southern Scandinavia (4, 5, 9). Following recent rescue excavations, it is estimated that approximately half of the original burial ground of c.10,000 m^2 with up to 1000 burials has been archaeologically investigated, making it the second largest urnfield in Denmark (heritage registration: VAM 1600, ARV 113, ARV 115; Figure 6). Three

 doi:10.20944/preprints202311.1702.v1

main lines of large burial mounds converge at Aarre, and at least 10 Neolithic and Bronze Age burial mounds are located within the urnfield (101). The urnfield burial organization has been described using horizontal stratigraphy, with the earliest urn burials located around a small group of these older burial mounds, and from this point, the urnfield expanded outwards in several directions (4). Approximately 1/3 of the urn burials contained metal objects primarily in the form of dress pins of either iron or bronze, different types of belt hooks, chains and O-rings. The site is estimated to have been in use c.500-250 BC, based on metalwork typo-chronology (4, 101).

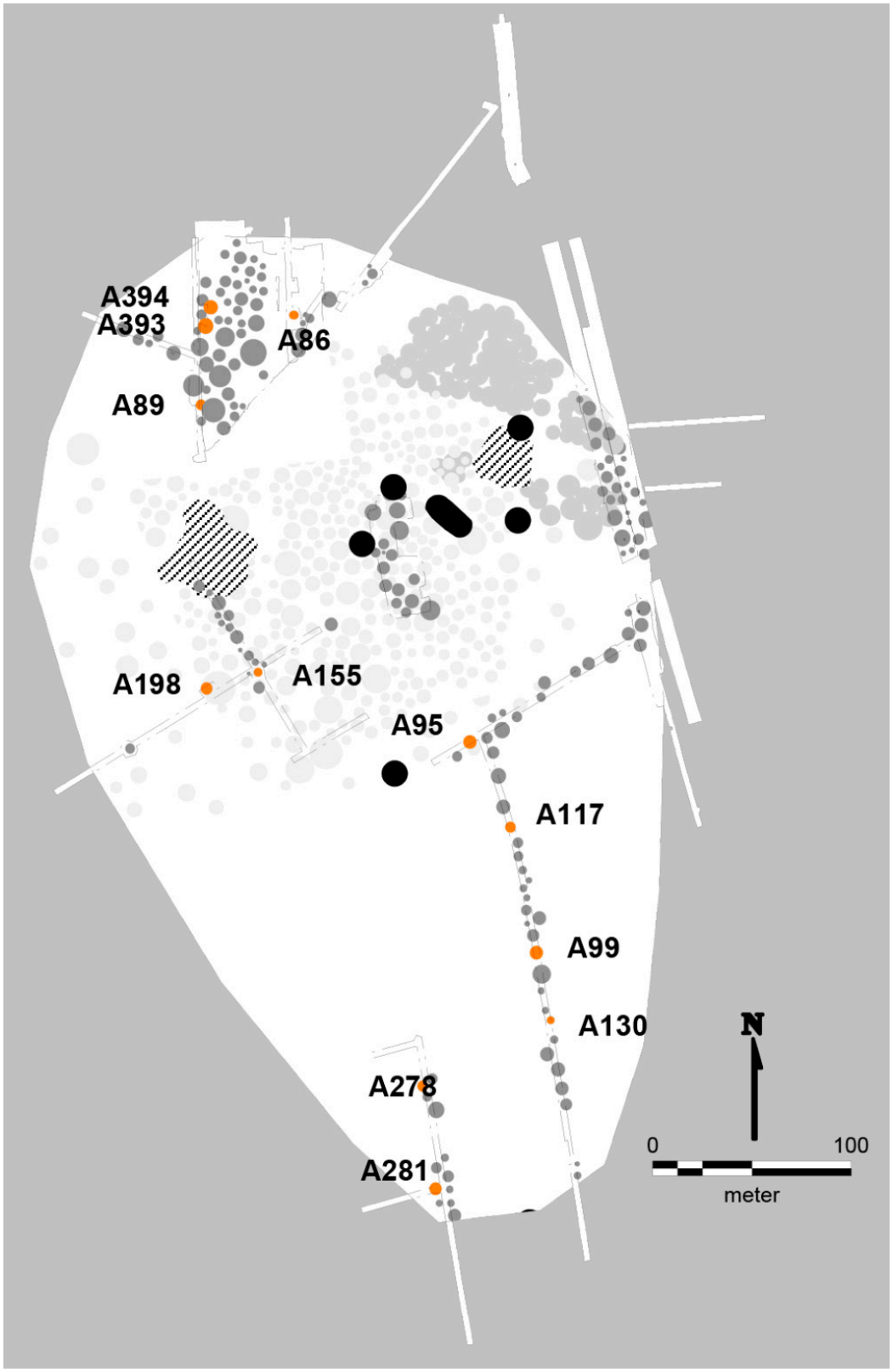

Preprints (www.preprints.org) | NOT PEER-REVIEWED | Posted: 28 November 2023 doi:10.20944/preprints202311.1702.v1

Figure 6. Layout of Aarre urnfield. ^{14}C dated burials are marked in orange and with corresponding A numbers (map: ARKVEST – Arkæologi i Vestjylland/LC Bentsen).

Søhale urnfield

Søhale urnfield is situated 10 km inland on a plateau, delimited by streams and wetlands to the east, north and west. 700 m east of the site is a line of burial mounds demarcating a major transport route. Some 30 m northeast of the site are two large, older burial mounds that might have served as a point of origin, but a modern road prevents further investigation. The site was excavated in 1996 as part of a development-led excavation in advance of gravel extraction, and the extent of the burial ground to the west, south and east was documented, whereas a modern road cuts it to the north (heritage registration: ESM 2139; Figure 7). 93 urnfield mounds were recovered and 73 of these contained a centrally placed urn burial enclosed by a circular or slightly oval ditch with a diameter of 2-10 m. Besides the standard urn burial, the local burial tradition also includes bone-layer burials, urn-bone layer burials, and possible cenotaphs with and without mound and circular ditch (18). According to Møller et al., the cemetery started out as two separate burial groups differentiated by burial types, and although the burial groups merged over time, the differences remain, possibly reflecting different communities sharing the burial ground (18).

Approximately 1/3 of the urn burials contained a limited range of metal objects, primarily in the form of dress pins and different types of belt equipment. Following excavation, the recovered cremation urns were left in museum storage, with their contents still intact, but they have recently been computed tomography (CT)-scanned and analysed as part of a renewed investigation of the Danish urnfield tradition (18). Based on diagnostic artefacts and 22 ^{14}C dates on cremated bone from 21 burials, they find that Søhale was established at the beginning of the PRIA and continued in use for c. 300 years.

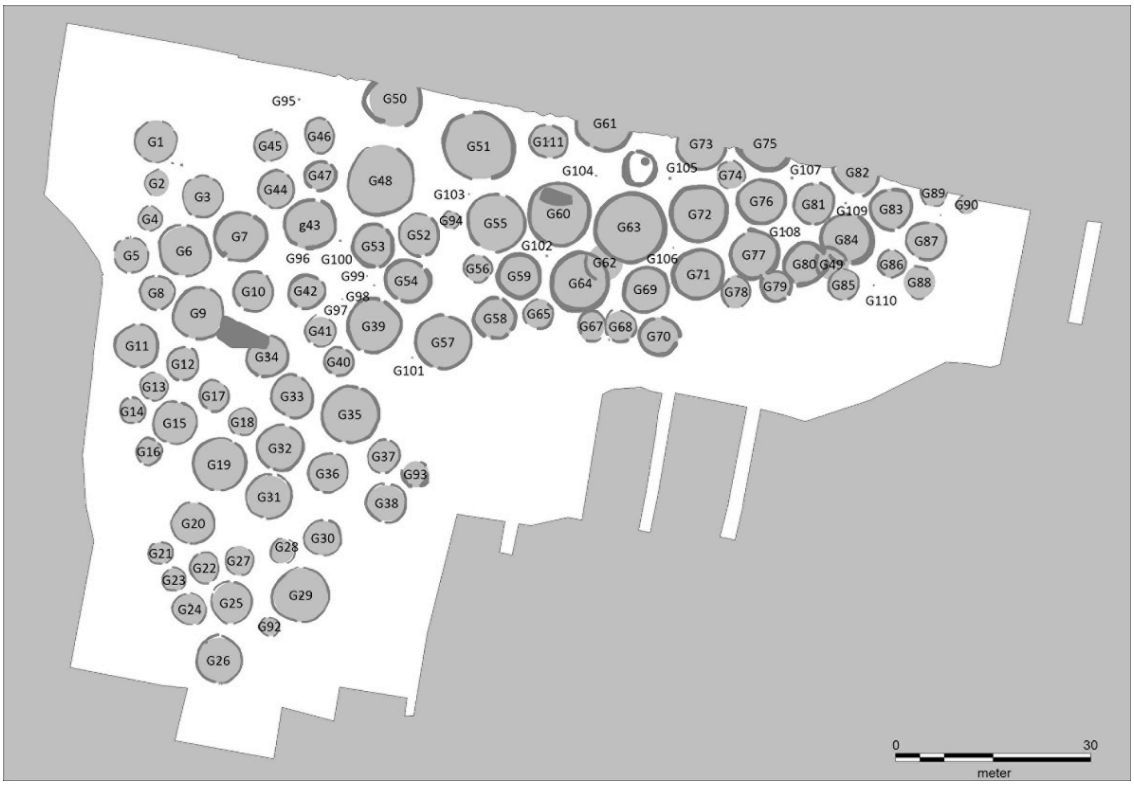

Figure 7. Layout of Søhale urnfield (18).

Aarupgaard urnfield

Aarupgaard urnfield is situated on the western point of a low hill, bordered by two streams, Gram Å to the north and Gels Å to the south. The site was first registered in the late 19th century and

later totally excavated in 1970-72 (heritage registration: HAM 1070) (70, 88). A Bronze Age burial mound serves as point of origin for up to 1500 urn burials, and although this mound was largely destroyed before excavation, within it were found three urns typologically dating to the transition period LBA-PRIA (burials U3330, U3342 and U3869). They are probably among the first burials at the site, and from their location the cemetery expanded southwards, which can best be described using horizontal stratigraphy. Aarupgaard is by far the largest urnfield in Denmark and covers an area of c.60.000 m², measuring c.100-200 m across (E-W) and c.450 from north to south. It can be divided into a large western group (orange circles, Figure 8) and a smaller eastern group (light yellow circles, Figure 8), both spreading out from the Bronze Age burial mound (red circle, Figure 8) and in use throughout the chronological sequence of the site, albeit with differing burial tempi. Approximately 30% of the burials contained metalwork and based on diagnostic artefacts, horizontal stratigraphy and other architectural features of the burial monuments, it has been suggested that Aarupgaard urnfield was in use c.500-100 BC and that it can be divided into a number of phases (11, 70, 83).

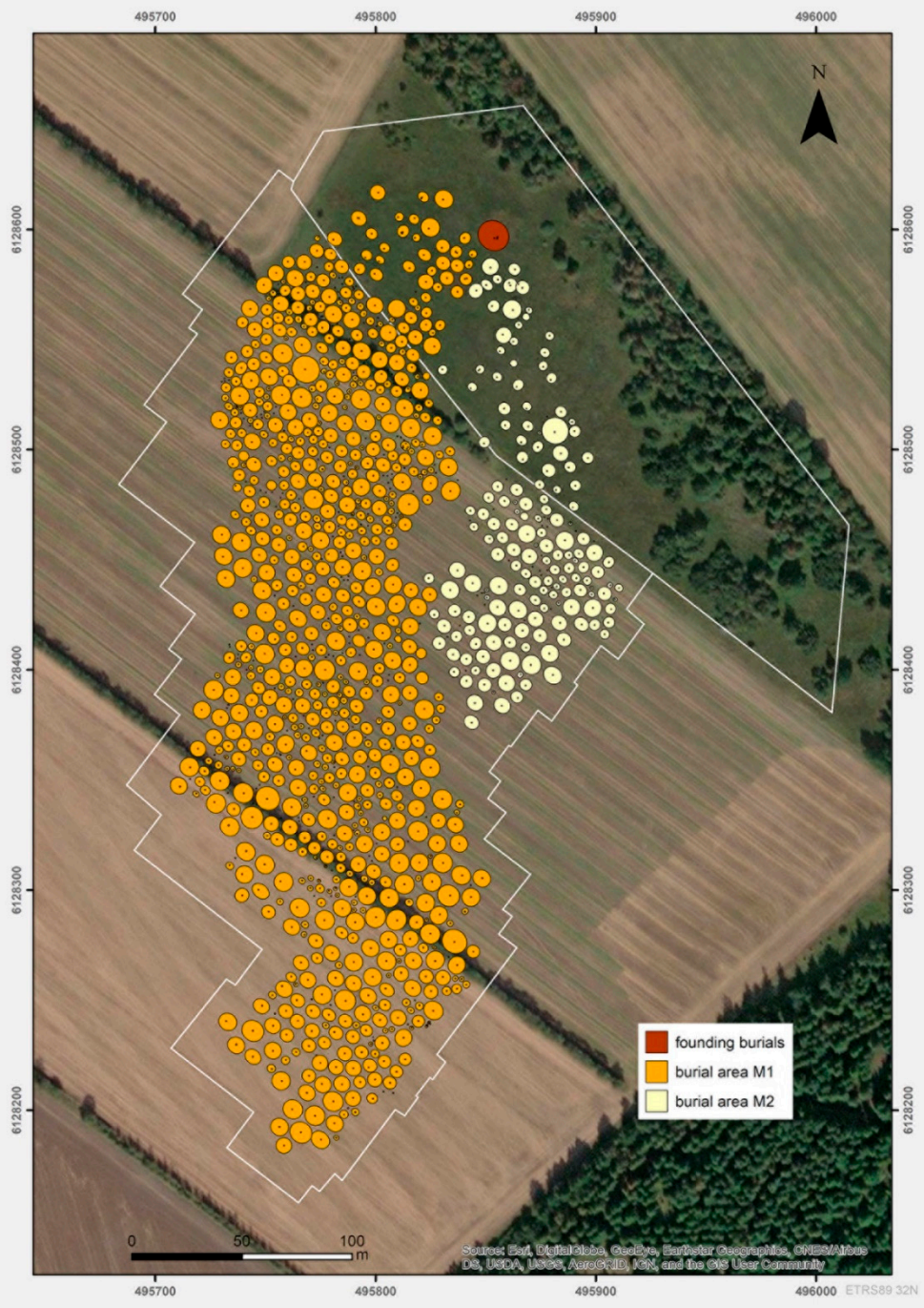

 doi:10.20944/preprints202311.1702.v1

Figure 8. Layout of Aarupgaard urnfield. ^{14}C dated burials are marked in red (map: K. Göbel, ZBSA and K. Terkildsen).

Osteological profile of urnfield burials

Osteological analyses of cremated human remains have been carried out for 67 burials from Søhale urnfield (18) and 58 burials from Aarupgaard urnfield (report by Harvig, 2019). Burials from Aarupgaard were selected to include varying amounts of bone, degree of preservation and from the entire chronological sequence. Results show that bone is fully cremated with a white to greyish-white colour, reflecting consistent pyre temperatures around 800 °C. The homogenous material reveals that a highly standardized modus operandi of both cremation and post-cremation handling was in place at both sites. Each burial is anatomically representative of a single individual and individuals of both sexes and from all age groups were identified. The majority lived to full adulthood, but 28% of the burials from Søhale contained sub-adults, as did 20 out of 58 burials from Aarupgaard. This is remarkable, because sub-adult individuals are often poorly represented or even missing from archaeological contexts (102), although significant numbers of sub-adults in relation to adults from cemeteries dating to the PRIA have been noted elsewhere (e.g. 103). Even though only part of the c.900 burials from Aarupgaard with preserved cremated human remains have been osteologically analysed, whereas all available material was analysed from Søhale, the funerary practices appear to be comparable between the two sites. It is not possible to compare the demographic profiles, beyond noting the large proportion of sub-adults at both sites.

Research questions

Bayesian chronological modelling is used extensively in archaeology today to construct fine-grained regional chronologies (e.g. 40), and it enables the correlation of chronological frameworks across larger regions with no shared material culture. This has made it abundantly clear that the past is more complex than previously anticipated, e.g. the origin and spread of megaliths in Northern Europe (104, 105), but also that the rate of change has increased and decreased over time, questioning the uniformitarian nature of chronological frameworks (e.g. 106). This study presents a dynamic chronological examination of PRIA artefact assemblages from Aarre, Søhale and Aarupgaard urnfields, all located within the core urnfield area in south-west Jutland, Denmark. It continues a long history of chronological research into the urnfields, but brings it up to date by applying a research approach that combines archaeological expert knowledge with ^{14}C data in a Bayesian framework. We model the temporal distributions of a range of artefact types, i.e. their currencies, spanning more archaeological phases in order to identify possible periods with varying rates of change in the material culture. Building on this, we provide an absolute chronological framework for the PRIA, enabling correlation with chronologies from other regions.

This study is concerned with temporal changes in a regional material culture, but rather than viewing these as isolated incidents, they can be linked to changes in other spheres of society, indicating major turning points in prehistory. Without a detailed understanding of the chronological framework and the material culture on which it hinges, it is difficult to address overarching questions regarding for example social structure, economy and religion.

Material and Methods

Sample selection

Ideally, we only wish to include urnfield graves containing mixed find assemblages of diagnostic pottery and metalwork, along with cremated human remains that can be ^{14}C dated and thus provide an indirect date for the artefacts. Up until the 1980s, urnfield excavations generally produced well-preserved material, but cremated human remains were not routinely archived before the 1970s. Agricultural activity over the last four decades has had a severe impact on these shallow structures, and although new urnfields are continuously recorded, they are increasingly poorly preserved (18). This leaves a narrow timeframe for urnfield excavations that could provide enough

 doi:10.20944/preprints202311.1702.v1

material for this study, which is even further limited by only about 1/3 of the burials containing metalwork.

Fragments of cremated bone were sampled from Aarre, Søhale and Aarupgaard urnfields, preferably cortical bone from diaphyses of major long bones (humerus, femur and tibia), but in cases of heavy fragmentation other skeletal elements were selected. Aarupgaard was excavated in the early 1970s and was the only site that provided well-preserved, mixed find assemblages. Aarre and Søhale urnfields were excavated more recently, and here pottery was preserved well enough to be included in only a few cases. Metalwork was also rather poorly preserved, but urns were micro-excavated in a controlled indoor environment after CT scanning. CT is in principle digital x-ray performed in 3D and it has in recent years been applied to prehistoric cremation urns more regularly (e.g. 107). In this case, the CT images enabled the identification of even very fragmented artefacts (Figure 9).

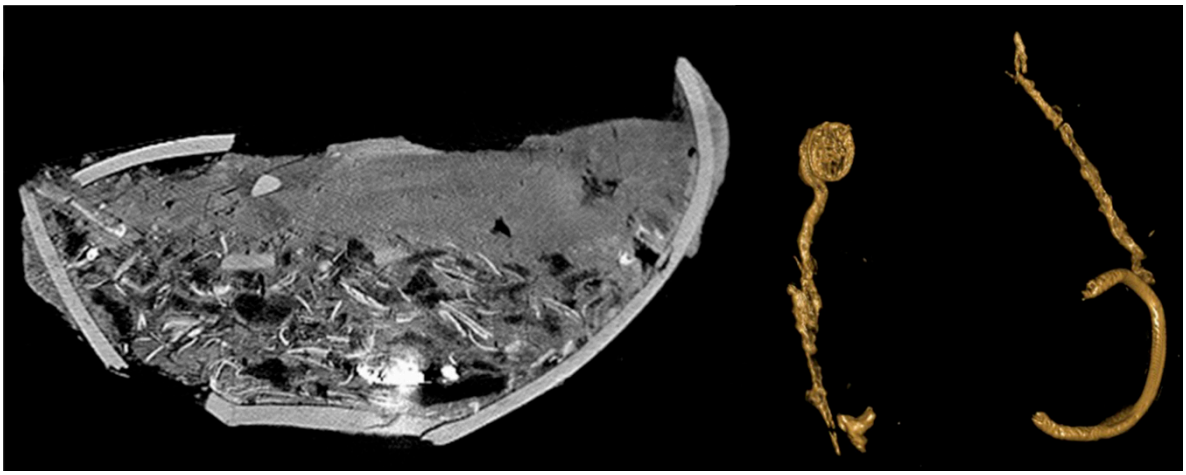

Figure 9. CT images of urn grave A278 from Aarre urnfield. To the left is a cross section of the fragmented urn that contain a bottom layer of cremated bone and some fragments of metal. To the right the metal has been isolated and it is possible to determine a bronze ring and two pins with disc-shaped head. Urn and artefacts are not to scale. (Hjertecenter Vest/ARKVEST - Arkæologi i Vestjylland).

Laboratory analyses

Samples of white cremated bone (CB) were selected for dating. To confirm they were fully calcined, aliquots of powdered untreated CB were analysed by Fourier-transform infrared spectroscopy (FTIR). The crystallinity index (CI) was estimated as the splitting factor between the two absorption bands at ca. 603 and ca. 565 cm^{-1} ($CI = (A_{603}+A_{565})/A_{valley}$) (108, 109). The samples were dated by the Leibniz-Laboratory (KIA-), Kiel, Germany, the Center for Isotope Research (GrM-), Groningen University, the Netherlands, and the Royal Institute for Cultural Heritage (RICH-), Brussels, Belgium. Pretreatment of samples of cremated bone varied between the laboratories, with Groningen using the traditional acetic acid treatment and Brussels and Kiel using variations of an acid-leaching treatment. A comparison study has however demonstrated these differences to have no influence on the results (110).

Pretreatment and combustion

Brussels leached ca. 30% by weight of each solid sample of cremated bone in 1% HCl, before it was powdered and treated with 1% acetic acid (24 hr) to remove calcite (111, 112). Kiel crushed each sample before treating it with 0.6% (1M) acetic acid (5 ×30min) and leaching ca. 50% with 1% HCl (22). Groningen treated the samples with 1.5% sodium hypochlorite (NaOCl, 48 hr, 20°C), followed by 6% (1M) acetic acid (24 hr, 20°C) (20, 113). All extracts were reacted with phosphoric acid to produce CO_2

 doi:10.20944/preprints202311.1702.v1

Graphitization and AMS measurement

Purified CO_2 was reduced to graphite for AMS measurement. Kiel measured double targets on samples from 17 later burials from Aarupgaard urnfield to reduce measurements uncertainty; this does not equal full replication including new extractions, but we know that a large part of the final uncertainty comes from the combustion, graphitisation and uncertainty in the standards measured concurrently, and these errors are independent between the paired targets. Measurements in Brussels were performed on a Micadas (195.5 kV) AMS system (114), Kiel used a HVEE 3MV Tandetron 4130 AMS system (115), and Groningen used a Micadas (180 kV) AMS system (113). All resulting ^{14}C-contents was corrected for fractionation using the simultaneously AMS measured $^{13}C/^{12}C$ isotope ratios (116).

Results

Artefact frequencies

Typological analysis of pottery and metalwork rely on published data on pottery by Jensen (5), registrations by Terkildsen (master thesis, Aarhus University), and supplemented by analyses carried out by the first author. Some of the burials from Aarupgaard contain small accompanying vessels, but for this study, we focus on the large funerary vessels. Frequencies of metalwork (n=129) and pottery (n=53) from Aarre, Søhale and Aarupgaard urnfields are sorted by type and illustrated in Figure 10a,b. The study includes 15 types of pottery with 14 types at Aarupgaard and 4 types at Søhale, and 15 types of metalwork with 14 types at Aarupgaard, 4 types at Aarre and 7 types at Søhale. Metalwork has higher frequencies than pottery, because burials from all three sites contain metalwork, but only burials from Aarupgaard contain pottery in larger numbers.

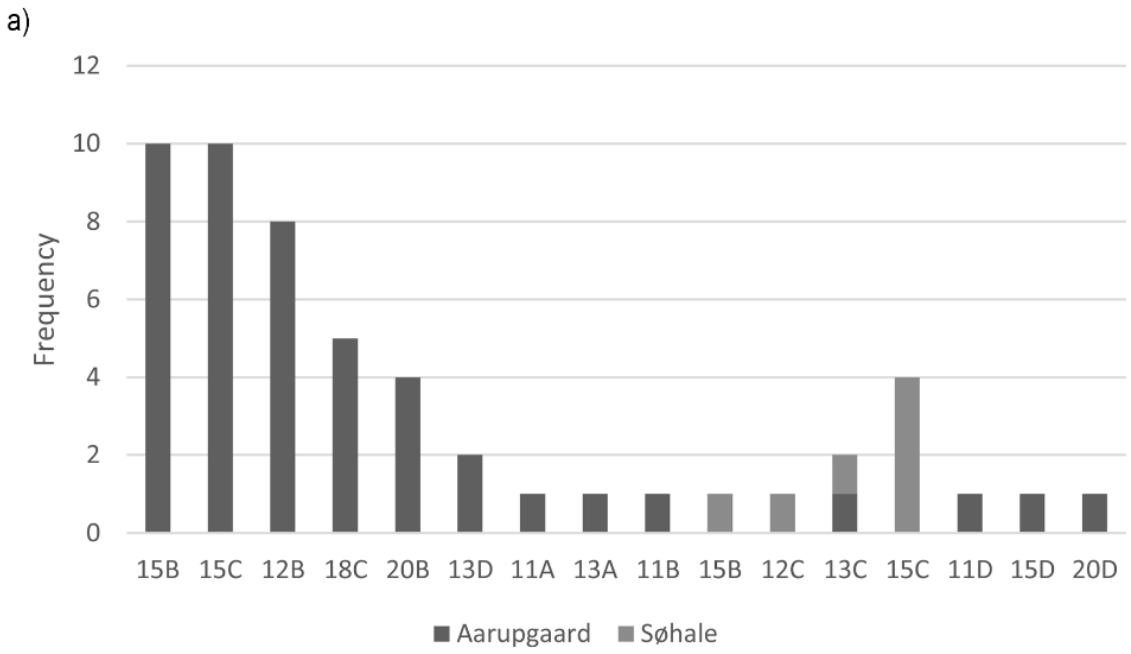

Preprints (www.preprints.org) | NOT PEER-REVIEWED | Posted: 28 November 2023 doi:10.20944/preprints202311.1702.v1

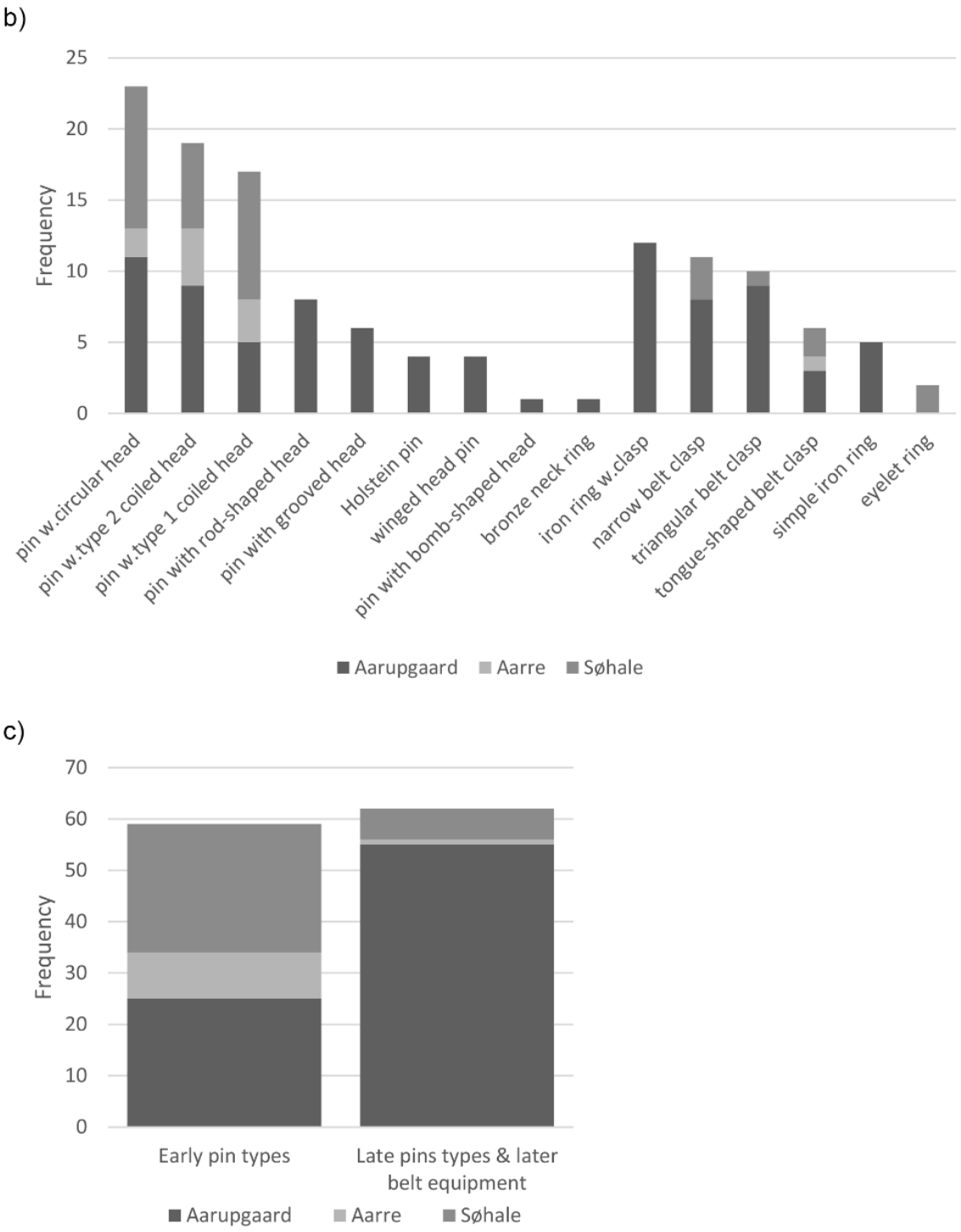

Figure 10. Frequency histogram of artefact types from Aarupgaard, Aarre and Søhale urnfields. Depicting types of a) metalwork, b) pottery, c) number of burials containing early pin types (pins with type 1 and 2 coiled head, pins with circular head), and later occurring pin types (Holstein pin, pin with bomb-shaped head, pin with rod-shaped head, pin with grooved head, winged-head pin) and belt equipment (iron ring with shanks, all types of belt clasps). Typology after Jensen (5).

The dataset is dominated by burials from Aarupgaard urnfield with more metalwork types and almost all pottery types only coming from this site. This is partly explained by Aarupgaard having a longer duration than Aarre and Søhale, but also better preservation. The differential site contributions have implications for the representations of particularly younger burials in the dataset, as illustrated by comparing frequencies of early pin types (n = 59; pin with type 1 coiled head, pin with type 2

 doi:10.20944/preprints202311.1702.v1

coiled head, pin with circular head) with later occurring types of pins and belt equipment (n = 62; Holstein pin, pin with bomb-shaped head, pin with rod-shaped head, pin with grooved head, winged-head pin, tongue-shaped belt clasp, triangular belt clasp, narrow belt clasp, iron ring with clasp; Figure 10c). Søhale and Aarupgaard contribute with near equal number of burials containing early pin types, whereas the later types of pins and belt equipment, and thereby the dataset, are dominated by burials from Aarupgaard.

Radiocarbon results

We report 66 new AMS ^{14}C ages from Aarupgaard, Aarre and Søhale urnfields, which are compiled in a dataset with previously published ^{14}C ages from the same sites, giving a total of 170 ^{14}C dates on 111 urnfield burials (Aarre: 12 burials, 46 ^{14}C dates; Søhale: 37 burials, 41 ^{14}C dates; Aarupgaard: 62 burials, 83 ^{14}C dates; Table 1) (18, 25, 110). The burials are primarily dated on samples of cremated bone, with additional dates on archaeobotanical remains associated with 10 burials from Aarre urnfield. Samples of cremated bone dated in Kiel, Groningen and Brussels have acceptable CI values >5, indicating they were fully cremated and suitable for ^{14}C dating. Excepted from this is Aarupgaard U884 (KIA-55391) with CI value 4.8, but because the ^{14}C date does not contradict the archaeological prior information we choose to accept the date regardless. There are no available CI values on cremated bone dated in Aarhus and it was not possible to replicate any of the dates. There does however not appear to be no systematic difference between the dates measured in Aarhus and the dates measured in Kiel, Groningen and Brussels. The cremated bone samples have mean values of $\delta^{13}C$ (Aarre mean = -23.4 ± 2.1 $\delta^{13}C$; Søhale mean = -24.8 ± 2.2 $\delta^{13}C$; Aarupgaard mean = -23.5 ± 3.0 $\delta^{13}C$), and %C (Aarre mean = 0.18 ± 0.09%C; Søhale mean = 0.23 ± 0.13%C; Aarupgaard mean = 0.18 ± 0.10 %C) that fall within expected ranges. However, all $\delta^{13}C$ values are measured by AMS and results will be affected by fractionation during acid extraction, graphitization and AMS measurement, and thus are not comparable between laboratories. Equally, %C can vary between laboratories, because pretreatment methods vary and %C is calculated at different steps in the process (Rose et al. 2019).

Table 1. Radiocarbon results and associated artefacts from Aarupgaard, Aarre and Søhale urnfields. Replicate measurements have been tested for consistency and combined following Ward and Wilson (117).

Lab code	Sample ID	Material	Diagnostic artefacts	Entrances / burial group	CI	%C of extract	Corrected pMC	AMS δ13C (‰VPDB)[1]	^{14}C Age (BP)	Reference
Aarupgaard urnfield cemetery (HAM 1070)										
KIA-51892	U34x34-1	Cremated bone (human)	Urn type 20B, 2 pins with type 2 coiled heads	>2 entrances, M1_CC2,	6.4	0.24	74.68 ± 0.26	-24.4	2346 ± 28	
KIA-51893	U36x36-1	Cremated bone (human)	Urn type 20B, 2 pins with type 2 coiled heads	>2 entrances, M1_CC2	5.9	0.23	73.81 ± 0.19	-24.6	2439 ± 21	
GrM-15072	U51x51-1	Cremated bone (human)	Urn type 15B, 2 pins with coiled heads and incomplete neck bends	>2 entrances, M1_CC1	5.9	0.11	73.77 ± 0.26	-30.3 ± 0.4	2445 ± 20	Rose et al. (2019)
KIA-52339	U51x51-1	Cremated bone (human)	-	-	-	0.38	73.73 ± 0.24	-26.8 ± 0.3	2448 ± 26	Rose et al. (2019)
Weighted mean U51x51-1: T′ = 0.0, T′ (5%) = 3.8, ν = 1, 2446 ± 16 BP										
GrM-14589	U81x81-1	Cremated bone (human)	Urn type 12B, 2 pins with type 2 coiled heads, iron chain corroded together with pins	>2 entrances, M1_CC1	5.9	0.06	73.93 ± 0.20	-27.5	2425 ± 30	Rose et al. (2019)
KIA-52819	U81x81-81	Replicate of GrM-14589; apatite pretreated at CIO, CO2 extracted and dated at KIA.	-	-	-	0.19	74.37 ± 0.20	-23.0	2379 ± 22	Rose et al. (2019)
Weighted mean U81x81-81: T′ = 1.5, T′ (5%) = 3.8, ν = 1, 2395 ± 18 BP										
GrM-15078	U83x83-1	Cremated bone (human)	Urn type 12B, 2 pins with type 2 coiled heads, pin of unknown type	>2 entrances, M1_CC1	6.0	0.06	73.42 ± 0.30	-28.1	2485 ± 30	Rose et al. (2019)
KIA-52825	U83x83-1	Replicate of GrM-15078; apatite pretreated at CIO, CO2 extracted and dated at KIA.	-	-	-	0.17	74.09 ± 0.25	-20.7	2409 ± 27	Rose et al. (2019)
Weighted mean U83x83-1: T′ = 3.5, T′ (5%) = 3.8, ν = 1, 2443 ± 21 BP										
KIA-51894	U123x123-1	Cremated bone (human)	Urn type 20B, triangular belt clasp, pin with circular head	>2 entrances, M1_CC2	6.4	0.29	75.32 ± 0.25	-22.6	2277 ± 26	
KIA-51895	U183x183-1	Cremated bone (human)	Urn type 12B, tongue-shaped belt clasp, 2 pins with circular heads	2 entrances, M2_CC1-3	6.6	0.21	75.64 ± 0.21	-23.4	2243 ± 23	
GrM-14704	U230x230-1	Cremated bone (human)	Urn type 12B, 2 pins with circular heads	>2 entrances, M1_CC2	5.4	0.07	72.83 ± 0.12	-21.7	2546 ± 19	Rose et al. (2019)
KIA-52826	U230x230-1	Replicate of GrM-14704; apatite pretreated at CIO, CO2 extracted and dated at KIA.	-	-	-	0.19	74.53 ± 0.23	-20.9	2362 ± 25	Rose et al. (2019)
Weighted mean U230x230-1: T′ = 34.1, T′ (5%) = 3.8, ν = 1, 2480 ± 16 BP										

doi:10.20944/preprints202311.1702.v1

GrM-14588	U280x280-1	Cremated bone (human)	Urn type 15B, 2 pins with type 2 coiled heads	>2 entrances, M1_CC2	6.2	0.08	74.12 ± 0.14	-25.1	2405 ± 20	Rose et al. (2019)
KIA-52820	U280x280-1	Replicate of GrM-14588; apatite pretreated at CIO, CO2 extracted and dated at KIA.	-	-	-	0.27	74.16 ± 0.21	-22.7	2402 ± 22	Rose et al. (2019)
Weighted mean U280x280-1: T′ = 0.0, T′ (5%) = 3.8, v = 1, 2404 ± 15 BP										
KIA-51896	U293x293-1	Cremated bone (human)	Urn type 20B, 3 pins with circular heads	>2 entrances, M1_CC2	6.9	0.22	74.38 ± 0.21	-22.8	2378 ± 23	
KIA-51897	U346x346-1	Cremated bone (human)	Urn type 15C, tongue-shaped belt clasp	2 entrances, M2_CC1-3	6.3	0.18	75.61 ± 0.22	-21.9	2246 ± 24	
GrM-14596	U382x382-1	Cremated bone (human)	Urn type 15C, narrow belt clasp	2 entrances, M2_CC1-3	7.3	0.08	75.29 ± 0.14	-24.8 ± 0.2	2280 ± 20	Rose et al. (2019)
KIA-52827	U382x382-1	Replicate of GrM-14596; apatite pretreated at CIO, CO2 extracted and dated at KIA.	-	-	-	0.27	75.77 ± 0.24	-22.5 ± 0.3	2229 ± 25	Rose et al. (2019)
Weighted mean U382x382-1: T′ = 2.5, T′ (5%) = 3.8, v = 1, 2260 ± 16 BP										
KIA-55388	U427x427-1	Cremated bone (human)	Holstein pin, triangular belt clasp, tweezer	2 entrances, M2_CC1-3	6.2	0.26	75.66 ± 0.22	-21.0	2241 ± 17	
KIA-51898	U500x500-1	Cremated bone (human)	Urn type 12B, 3 pins with circular heads	>2 entrances, M1_CC3	7.6	0.21	75.30 ± 0.21	-26.7	2278 ± 23	
GrM-14705	U681x681-1	Cremated bone (human)	Urn type 13D, 2 pins with type 2 coiled heads, simple iron ring	>2 entrances, M1_CC3	6.0	0.08	75.01 ± 0.12	-22.3	2310 ± 19	Rose et al. (2019)
KIA-53094	U681x681-1	Replicate of GrM-14705; apatite pretreated at CIO, CO2 extracted and dated at KIA.	-	-	-	0.24	75.05 ± 0.19	-22.5	2305 ± 20	Rose et al. (2019)
Weighted mean U681x681-1: T′ = 0.0, T′ (5%) = 3.8, v = 1, 2308 ± 14 BP										
RICH-25343	U752x752-1	Cremated bone (human)	Urn type 12B, 2 pins with circular heads	>2 entrances, M1_CC3	5.7	0.28	74.94	-24.2	2317 ± 26	
GrM-14589	U766x766-1	Cremated bone (human)	Urn type 15B, 3 pins with circular heads	>2 entrances, M1_CC3	5.5	0.16	75.24 ± 0.14	-26.4	2285 ± 20	Rose et al. (2019)
KIA-52821	U766x766-1	Replicate of GrM-14589; apatite pretreated at CIO, CO2 extracted and dated at KIA.	-	-	-	0.39	75.55 ± 0.21	-25.2	2252 ± 23	Rose et al. (2019)
Weighted mean U766x766-1: T′ = 1.2, T′ (5%) = 3.8, v = 1, 2271 ± 16 BP										
RICH-24151	U797x797-1	Cremated bone (human)	Urn type 13C, 2 pins with circular heads, narrow belt clasp	>2 entrances, M1_CC3	6.7	0.03	75.53	-27.9	2255 ± 28	
KIA-51899	U858x858-1	Cremated bone (human)	Urn type 15B, pin with rod-shaped head, narrow belt clasp	2 entrances, M2_CC4	6.2	0.41	75.49 ± 0.21	-21.5	2258 ± 23	

doi:10.20944/preprints202311.1702.v1

KIA-55389	U867x867-1	Cremated bone (human)	Urn type 15D, winged head pin	2 entrances, M2_CC4	6.0	0.28	75.93 ± 0.23	-17.9	2219 ± 12	
KIA-55390	U871x871-1	Cremated bone (human)	Pin with grooved head, iron ring with shank	2 entrances, M2_CC4	5.7	0.35	75.63 ± 0.22	-21.5	2239 ± 17	
KIA-55391	U884x884-1	Cremated bone (human)	Urn type 15D, winged head pin	2 entrances, M2_CC4	4.8	0.22	75.95 ± 0.21	-21.7	2211 ± 16	
RICH-24150	U928x928-1	Cremated bone (human)	Urn type 15B, pin with type 2 coiled head, pin with circular head	2 entrances, M1_CC3	7.3	0.05	75.13	-20.6	2297 ± 25	
GrM-14599	U1001x1001-1	Cremated bone (human)	Urn types 18C and 15B, pin of unknown type, iron ring with shank	2 entrances, M1_CC4	6.2	0.08	75.71 ± 0.14	-23.0	2235 ± 20	Rose et al. (2019)
KIA-53095	U1001x1001-1	Replicate of GrM-14599; apatite pretreated at CIO, CO2 extracted and dated at KIA.	-	-	-	0.22	75.54 ± 0.19	-20.1	2253 ± 21	Rose et al. (2019)
Weighted mean U1001x1001-1: T′ = 0.4, T′ (5%) = 3.8, v = 1, 2244 ± 15 BP										
KIA-51900	U1016x1016-1	Cremated bone (human)	Urn type 15B, iron ring with shank	2 entrances, M1_CC4	6.7	0.23	75.85 ± 0.24	-23.7	2220 ± 25	
KIA-55392	U1018x1018-1	Cremated bone (human)	Urn type 15B, winged head pin, iron ring with shank	2 entrances, M1_CC4	5.3	0.21	75.63 ± 0.22	-17.6	2242 ± 17	
GrM-14592	U1076x1076-1	Cremated bone (human)	Urn type 18C, narrow belt clasp, bronze neck ring	2 entrances, M1_CC4	6.4	0.08	75.47 ± 0.14	-27.8	2260 ± 20	Rose et al. (2019)
KIA-52822	U1076x1076-1	Replicate of GrM-14592; apatite pretreated at CIO, CO2 extracted and dated at KIA.	-	-	-	0.18	76.05 ± 0.28	-25.3	2199 ± 29	Rose et al. (2019)
RICH-25340	U1076x1076-1	Cremated bone (human)	-	-		0.12	76.06 ± 0.26	-25.5	2198 ± 27	Rose et al. (2019)
Weighted mean U1076x1076-1: T′ = 4.8, T′ (5%) = 6.0, v = 2, 2229 ± 15 BP										
GrM-14597	U1186x1186-1	Cremated bone (human)	Urn type 13A, 2 pins with type 1 coiled heads, simple iron ring	>2 entrances, M1_CC1	5.8	0.12	73.58 ± 0.13	-24.7	2465 ± 20	Rose et al. (2019)
KIA-53096	U1186x1186-1	Replicate of GrM-14597; apatite pretreated at CIO, CO2 extracted and dated at KIA.	-	-	-	0.27	74.10 ± 0.18	-24.1	2408 ± 20	Rose et al. (2019)
Weighted mean U1186x1186-1: T′ = 4.1, T′ (5%) = 3.8, v = 1, 2437 ± 15 BP										
RICH-25332	U1232x1232-1	Cremated bone (human)	Urn type 15B, 2 pins with type 1 coiled heads	>2 entrances, M1_CC1	5.8	0.16	73.78	-21.4	2443 ±27	
RICH-24143	U1279x1279-1	Cremated bone (human)	Urn type 13A, 2 pins with type 2 coiled heads	>2 entrances, M1_CC1	5.7	0.21	73.56	-19.6	2467 ± 26	
GrM-14602	U1363x1363-1	Cremated bone (human)	Urn type 15B, triangular belt clasp	2 entrances, M1_CC4	6.5	0.07	75.79 ± 0.14	-30.3	2225 ± 20	Rose et al. (2019)

doi:10.20944/preprints202311.1702.v1

KIA-52828	U1363x1363-1	Replicate of GrM-14602; apatite pretreated at CIO, CO2 extracted and dated at KIA.	-	-	-	0.17	76.09 ± 0.23	-27.9	2195 ± 24	Rose et al. (2019)
Weighted mean U1363x1363-1: T′ = 0.9, T′ (5%) = 3.8, ν = 1, 2213 ± 16 BP										
RICH-25335	U1382x1382-1	Cremated bone (human)	Urn type 18C, 2 pins with circular heads, triangular belt clasp	2 entrances, M1_CC4	6.8	0.10	76.01	-26.2	2204 ± 27	
RICH-25357	U1422x1422-1	Cremated bone (human)	Urn type 13D, pin with grooved head, narrow belt clasp	2 entrances, M1_CC4	5.9	0.11	76.18	-23.5	2186 ± 26	
RICH-25333	U1436x1436-1	Cremated bone (human)	Urn type 15C, narrow belt clasp	2 entrances, M1_CC4	5.9	0.11	75.55	-25.3	2252 ± 28	
RICH-25334	U1617x1617-1	Cremated bone (human)	Urn type 18C, 2 pins with circular heads, bronze pin with grooved head, triangular belt clasp	2 entrances, M1_CC5	5.4	0.14	76.39	-25.6	2163 ± 28	
KIA-55393	U1654x1654-1	Cremated bone (human)	Pin with grooved head, iron ring with shank	2 entrances, M1_CC5	5.9	0.31	76.22 ± 0.24	-22.0	2183 ±14	
KIA-52340	U1678x1678-1	Cremated bone (human)	Urn type 15C, narrow belt clasp	2 entrances, M1_CC5	5.4	0.32	75.64 ± 0.23	-22.3	2243 ± 25	
GrM-15074	U1791x1791-1	Cremated bone (human)	Urn type 15C, triangular belt clasp	2 entrances, M1_CC5	5.7	0.07	75.78 ± 0.26	-30.0	2230 ± 25	Rose et al. (2019)
KIA-52341	U1791x1791-1	Cremated bone (human)	-	-	-	0.29	76.35 ± 0.23	-29.63	2167 ± 25	Rose et al. (2019)
Weighted mean U1791x1791-1: T′ = 3.2, T′ (5%) = 3.8, ν = 1, 2199 ± 18 BP										
RICH-24144	U1834x1834-1	Cremated bone (human)	Urn type 12B, tongue-shaped belt clasp	2 entrances, M1_CC5	6.5	0.09	74.89	-19.8	2322 ± 25	
KIA-55394	U1834x1834-1	Cremated bone (human), separate sample from RICH-24144	-	-	5.1	0.18	75.91 ± 0.23	-25.7	2216 ± 18	
Weighted mean U1834x1834-1: T′ = 11.9, T′ (5%) = 3.8, ν = 1, 2253 ± 15 BP										
GrM-15075	U1847x1847-1	Cremated bone (human)	Urn type 15C, triangular belt clasp	2 entrances, M1_CC5	6.1	0.08	75.53 ± 0.20	-25.4	2255 ± 20	Rose et al. (2019)
KIA-52342	U1847x1847-1	Cremated bone (human)	-	-	-	0.28	75.78 ± 0.24	-28.9	2228 ± 25	Rose et al. (2019)
Weighted mean U1847x1847-1: T′ = 0.7, T′ (5%) = 3.8, ν = 1, 2244 ± 16 BP										
KIA-55395	U1894x1894-1	Cremated bone (human)	Pin with rod-shaped head, iron ring with shank	2 entrances, M1_CC5	5.1	0.24	75.94 ± 0.21	-21.1	2211 ± 14	
KIA-52343	U1970x1970-1	Cremated bone (human)	Urn type 15C, bronze pin with grooved head, narrow belt clasp	2 entrances, M1_CC5	5.9	0.28	75.61 ± 0.22	-22.8	2246 ± 23	

doi:10.20944/preprints202311.1702.v1

KIA-55396	U1993x1993-1	Cremated bone (human)	Pin with grooved head, iron ring with shank	2 entrances, M1_CC5	5.1	0.35	75.82 ± 0.25	-21.6	2228 ±15	
KIA-52344	U1997x1997-1	Cremated bone (human)	Urn type 18C, bronze pin with grooved head, triangular belt clasp	2 entrances, M1_CC5	6.5	0.38	76.36 ± 0.26	-30.6	2167 ± 27	
KIA-55397	U2199x2199-1	Cremated bone (human)	Holstein pin	2 entrances, M1_CC6	5.3	0.15	75.59 ± 0.26	-20.4	2244 ± 17	
GrM-14593	U2262x2262-1	Cremated bone (human)	Urn type 11D, narrow belt clasp	2 entrances, M1_CC6	6.5	0.07	75.53 ± 0.16	-20.9	2255 ± 25	Rose et al. (2019)
KIA-52823	U2262x2262-1	Replicate of GrM-14593; apatite pretreated at CIO, CO2 extracted and dated at KIA.	-	-	-	0.24	75.92 ± 0.26	-19.0	2214 ± 28	Rose et al. (2019)
Weighted mean U2262x2262-1: T′ = 1.2, T′ (5%) = 3.8, ν = 1, 2237 ± 19 BP										
KIA-55398	U2293x2293-1	Cremated bone (human)	Urn type 15D, pin with rod-shaped head, iron ring with shank	2 entrances, M1_CC6	6.7	0.05	76.19 ± 0.31	-22.3	2185 ± 25	
KIA-55399	U2354x2354-1	Cremated bone (human)	Urn type 15C, pin with rod-shaped head, iron ring with shank	2 entrances, M1_CC6	7.9	0.12	75.70 ± 0.23	-22.6	2237 ± 18	
KIA-55400	U2366x2366-1	Cremated bone (human)	Urn type 20B, pin with rod-shaped head, simple iron ring	2 entrances, M1_CC6	5.8	0.22	75.75 ± 0.24	-18.9	2232 ± 15	
KIA-55401	U2455x2455-1	Cremated bone (human)	Pin with rod-shaped head, simple iron ring	2 entrances, M1_CC6	7.4	0.05	75.66 ± 0.30	-21.5	2240 ± 25	
KIA-55402	U2498x2498-1	Cremated bone (human)	Urn type 15D, winged head pin	2 entrances, M1_CC6	7.7	0.08	76.37 ± 0.31	-24.5	2165 ± 25	
RICH-24145	U2541x2541-1	Cremated bone (human)	Urn type 20D, Holstein pin, pin with flat pierced head, iron ring with shank,	2 entrances, M1_CC6	5.9	0.06	75.89	-22.7	2216 ± 26	
KIA-55403	U2545x2545-1	Cremated bone (human)	Pin with rod-shaped head, pin with small pierced head	2 entrances, M1_CC6	6.1	0.15	76.11 ± 0.24	-24.9	2194 ± 18	
RICH-24146	U2550x2550-1	Cremated bone (human)	Urn type 15D, iron ring with shank	2 entrances, M1_CC6	5.9	0.08	75.18	-22.3	2291 ± 26	
KIA-55404	U2593x2593-1	Cremated bone (human)	Urn type 17D, Holstein pin, iron ring with shank	2 entrances, M1_CC6	6.9	0.15	75.84 ± 0.23	-21.9	2222 ± 17	
RICH-25355	U2710x2710-1	Cremated bone (human)	Urn type 11A, pin with bomb-shaped head, possibly second pin of same type, unknown pin type with bend neck	>2 entrances, M1_CC1	5.5	0.12	74.07	-18.9	2411 ± 27	

doi:10.20944/preprints202311.1702.v1

GrM-14594	U3330x3330-1	Cremated bone (human)	Urn type 15? Iron pin with coiled head and no bend neck	Founding burial	6.8	0.10	72.96 ± 0.13	-21.0	2535 ± 20	Rose et al. (2019)
KIA-52824	U3330x3330-1	Replicate of GrM-14594; apatite pretreated at CIO, CO2 extracted and dated at KIA.	-	-	-	0.29	73.52 ± 0.24	-21.5	2471 ± 26	Rose et al. (2019)
KIA-51901	U3330x3330-1	Cremated bone (human), separate sample from KIA-52824 and GrM14594	-	-	-	0.28	73.23 ± 0.24	-21.9	2503 ± 27	Rose et al. (2019)
Weighted mean U3330x3330-1: T′ = 3.9, T′ (5%) = 6.0, v = 2, 2509 ± 14 BP										
RICH-25354	U3341x3341-1	Cremated bone (human)	Urn of Bronze Age period VI type, side urn of pre-Roman Iron Age style, swan neck pin	Founding burial	5.7	0.35	73.47	-21.5	2477±27	
RICH-24147	U3452x3452-1	Cremated bone (human)	Urn type 15B, 2 pins with type 1 coiled heads	>2 entrances, M1_CC1	6.2	0.12	73.03	-19.1	2525 ± 25	
RICH-24148	U3778x3778-1	Cremated bone (human)	Urn type 12B, 2 pins with type 2 coiled heads, simple iron ring	>2 entrances, M1_CC1	5.4	0.12	73.7	-18.1	2452 ± 25	
KIA-52345	U3822x3822-1	Cremated bone (human)	Urn type 11B, 2 pins with type 1 coiled heads	>2 entrances, M2_CC1-3	5.5	0.26	73.87 ± 0.24	-23.9	2433 ± 26	
GrM-15076	U3869x3869-1	Cremated bone (human)	Urn, open with no neck. Iron pin with round head and no neck bend	Founding burial	6.0	0.09	72.87 ± 0.16	-21.6	2540 ± 20	Rose et al. (2019)
KIA-52346	U3869x3869-1	Cremated bone (human)	-	-	-	0.21	73.66 ± 0.23	-25.9	2456 ± 25	Rose et al. (2019)
RICH-24152	U3869x3869-1	Cremated bone (human)	-	-	-	0.20	73.22 ± 0.24	-25.8	2504 ± 26	Rose et al. (2019)
Weighted mean U3869x3869-1: T′ = 6.9, T′ (5%) = 6.0, v = 2, 2507 ± 14 BP										
Aarre urnfield cemetery (VAM 1600)										
KIA-53941	A86x339 (urn)	*Acer* sp. trunk wood charcoal (Ø >10 cm)	-	-	-	63.96	73.60 ± 0.23	-25.3	2463 ± 25	Rose et al. (2020)
KIA-53942	A86x340 (urn)	Cremated bone (human)	-	-	5.4	0.35	74.37 ± 0.24	-19.7	2379 ± 26	Rose et al. (2020)
KIA-53942	A86x340 (urn)	Cremated bone (human), replicate	Urn of unknown type, 2 pins with type 2 coiled heads	-	-	-	74.31 ± 0.23	-22.8	2385 ± 25	Rose et al. (2020)
Weighted mean A86x340: T′ = 0.0, T′ (5%) = 3.8, v = 1, 2382 ± 19 BP										
RICH-25356	A89x311 (urn)	Cremated bone (human)	Urn type 13, 2 pins with type 1 coiled heads	-	6.4	0.16	-	-21.18	2464 ± 27	
KIA-53984	A95x368 no.1 (urn)	*Quercus* sp. twig charcoal (Ø <0.3 cm)	-	-	-	70.68	74.45 ± 0.23	-28.4	2370 ± 25	Rose et al. (2020)

doi:10.20944/preprints202311.1702.v1

KIA-53985	A95x368 no.3 (urn)	*Acer* sp. twig charcoal (Ø <0.5 cm)	-	-	-	70.49	73.90 ± 0.23	-27.7	2430 ± 26	Rose et al. (2020)
RICH-25342	A95x369 (urn)	Cremated bone (human)	Urn type 16?	-	7.8	0.11	73.90 ± 0.25	-24.3	2428 ± 27	Rose et al. (2020)
RICH-25071	A99x65 no.2 (pit)	*Alnus* sp. trunk wood charcoal (Ø 8-10 cm)	-	-	-	60.00	75.39 ± 0.28	-33.3	2269 ± 29	Rose et al. (2020)
RICH-25067	A99x65 no.3 (pit)	*Quercus* sp. trunk wood charcoal (Ø <10 cm)	-	-	-	61.00	67.85 ± 0.26	-31.6	3115 ± 31	Rose et al. (2020)
GrM-16774	A99x345 (urn)	Cremated bone (human)	Urn of unknown type, pin with type 1 coiled head	-	6.5	0.06	75.50 ± 0.17	-26.5	2255 ± 20	Rose et al. (2020)
RICH-25069	A99x346 no.1 (urn)	*Alnus* sp. twig charcoal (Ø <0.3 cm)	-	-	-	53.50	77.14 ± 0.28	-31.8	2085 ± 29	Rose et al. (2020)
RICH-25066	A99x346 no.27 (urn)	Alnus sp. trunk wood charcoal (Ø > 10 cm)	-	-	-	61.60	75.56 ± 0.28	-35.3	2251 ± 30	Rose et al. (2020)
GrM-14604	A117x762 (urn)	Cremated bone (human)	Urn type 12, elaborate set of chain and pins	-	6.0	0.10	73.75 ± 0.13	-25.7	2445 ± 20	Rose et al. (2019)
KIA-53098	A117x762 (urn)	Replicate of GrM-14604; apatite pretreated at CIO, CO2 extracted and dated at KIA.	-	-	-	0.28	74.03 ± 0.19	-22.1	2416 ± 20	Rose et al. (2019)
Weighted mean A117x762: T′ = 1.1, T′ (5%) = 3.8, v = 1, 2431 ± 15 BP										
KIA-53943	A117x769 (urn)	*Quercus* sp. charcoal (Ø >10 cm) 1 annual ring sampled	-	-	-	31.21	73.72 ± 0.23	-23.6	2449 ± 25	Rose et al. (2020)
KIA-53944	A117x774 (urn)	*Quercus* sp. charcoal (Ø >10 cm)	-	-	-	60.58	73.30 ± 0.22	-25.0	2495 ± 24	Rose et al. (2020)
KIA-53945	A130x82 no.1 (urn)	Charred grass stem	Pin of unknown type, tongue-shaped belt clasp,	-	-	68.30	72.49 ± 0.23	-25.1	2585 ± 25	Rose et al. (2020)
KIA-53946	A130x82 no.2 (urn)	*Triticum* cf. *aestivum*, charred cereal	-	-	-	64.19	76.46 ± 0.23	-28.5	2156 ± 24	Rose et al. (2020)
KIA-53947	A130x217 (urn)	Cremated bone (human)	-	-	5.8	0.24	75.57 ± 0.23	-20.9	2250 ± 25	Rose et al. (2020)
KIA-53947	A130x217 (urn)	Cremated bone (human), replicate	-	-	-	-	75.52 ± 0.23	-21.7	2255 ± 25	Rose et al. (2020)
Weighted mean A130x217: T′ = 0.0, T′ (5%) = 3.8, v = 1, 2253 ± 18 BP										
KIA-53948	A155x127 no.1 (urn)	cf. *Triticum* sp., charred cereal	-	-	-	50.00	73.31 ± 0.22	-26.4	2494 ± 24	Rose et al. (2020)

doi:10.20944/preprints202311.1702.v1

KIA-53949	A155x127 no.2 (urn)	*Arrhenatherum elatius* ssp. *Bulbosum*, charred grass bulb	-	-	-	65.52	73.56 ± 0.22	-28.2	2466 ± 24	Rose et al. (2020)
KIA-53950	A155x281 (urn)	Cremated bone (human)	Pin with circular head	-	6.1	0.26	74.55 ± 0.23	-23.6	2359 ± 25	Rose et al. (2020)
KIA-53950	A155x281 (urn)	Cremated bone (human), replicate	-	-	-	-	74.41 ± 0.23	-24.1	2374 ± 25	Rose et al. (2020)
Weighted mean A155x281: T′ = 0.2, T′ (5%) = 3.8, ν = 1, 2367 ± 18 BP										
KIA-53951	A198x338 (urn)	*Alnus* sp. trunk wood charcoal (Ø >10 cm)	-	-	-	57.02	69.12 ± 0.21	-24.9	2967 ± 24	Rose et al. (2020)
KIA-53952	A198x338 CB (urn)	Cremated bone (human)	Urn of unknown type, 2 pins with type 2 coiled heads	-	5.9	0.28	74.89 ± 0.24	-24.9	2323 ± 26	Rose et al. (2020)
KIA-53952	A198x338 CB (urn)	Cremated bone (human), replicate	-	-	-	-	74.82 ± 0.29	-25.9	2330 ± 35	Rose et al. (2020)
Weighted mean A198x338 CB: T′ = 0.0, T′ (5%) = 3.8, ν = 1, 2325 ± 21 BP										
GrM-14707	A281x484 (urn)	Cremated bone (human)	Urn type 15, 2 pins with circular heads	-	6.2	0.10	74.91 ± 0.13	-28.0	2320 ± 20	Rose et al. (2019)
KIA-53100	A281x484 (urn)	Replicate of GrM-14707; apatite pretreated at CIO, CO2 extracted and dated at KIA.		-	-	0.11	75.37 ± 0.19	-23.5	2271 ± 20	Rose et al. (2019)
Weighted mean A281x484: T′ = 3.9, T′ (5%) = 3.8, ν = 1, 2296 ± 15 BP										
KIA-53953	A278x782 no.1 (urn)	Charred grass stem	-	-	-	74.57	74.17 ± 0.23	-27.5	2400 ± 25	Rose et al. (2020)
KIA-53954	A278x782 no.2 (urn)	Charred grass, stem and root fragment	-	-	-	67.11	73.76 ± 0.23	-26.2	2445 ± 25	Rose et al. (2020)
KIA-53955	A278x783 (urn)	Cremated bone (human)	Urn of unknown type, 2 pins with disc-shaped heads, bronze ring	-	5.5	0.20	73.47 ± 0.24	-22.7	2477 ± 26	Rose et al. (2020)
KIA-53955	A278x783 (urn)	Cremated bone (human), replicate	-	-	-	-	73.71 ± 0.23	-22.9	2450 ± 25	Rose et al. (2020)
Weighted mean A278x783: T′ = 0.6, T′ (5%) = 3.8, ν = 1, 2463 ± 19 BP										
RICH-25068	A393x568 no.1 (pit)	*Triticum dicoccum*, charred cereal	-	-	-	61.10	69.69 ± 0.28	-29.9	2901 ± 32	Rose et al. (2020)
RICH-25070	A393x568 no.2 (pit)	*Hordeum vulgare nudum*, charred cereal	-	-	-	44.30	69.58 ± 0.28	-27.2	2914 ± 32	Rose et al. (2020)
RICH-25341	A393x561 CB (urn)	Cremated bone (human)	Urn of unknown type, 2 pins with type 1 coiled heads	-	6.4	0.16	73.90 ± 0.25	-25.3	2480 ± 27	Rose et al. (2020)

doi:10.20944/preprints202311.1702.v1

KIA-52411	A393x561 no.1 (urn)	*Hordeum vulgare nudum*, charred cereal	-	-	-	54.67	67.70 ± 0.21	-24.0	3134 ± 25	Rose et al. (2020)
KIA-52412	A393x561 no.3 (urn)	*Hordeum vulgare nudum*, charred cereal	-	-	-	32.35	67.57 ± 0.22	-21.9	3150 ± 27	Rose et al. (2020)
KIA-52413	A393x561 *Quercus* (urn)	*Quercus* sp. trunk wood charcoal (Ø >10 cm)	-	-	-	24.78	72.25 ± 0.24	-25.7	2611 ± 27	Rose et al. (2020)
KIA-52414	A394x556 no.1 (urn)	*Alnus* sp. charcoal from branch sapwood (Ø 3-5 cm)	-	-	-	26.74	70.77 ± 0.23	-24.9	2778 ± 27	Rose et al. (2020)
KIA-53983	A394x781 no.9 (urn)	*Acer* sp. trunk wood charcoal (Ø > 10 cm)	-	-	-	66.85	68.58 ± 0.21	-27.0	3029 ± 24	Rose et al. (2020)
GrM-14708	A394x785 CB (urn)	Cremated bone (human)	Urn of unknown type, 2 pins with type 2 coiled heads	-	6.3	0.10	73.57 ± 0.11	-21.2	2465 ± 18	Rose et al. (2019)
KIA-53099	A394x785 CB (urn)	Replicate of GrM-14708; apatite pretreated at CIO, CO2 extracted and dated at KIA.	-	-	-	0.14	73.97 ± 0.19	-22.7	2422 ± 20	Rose et al. (2019)
			Weighted mean A394x785 CB: T′ = 2.6, T′ (5%) = 3.8, ν = 1, 2446 ± 14 BP							
KIA-52415	A394x785 no.1 (urn)	*Triticum aestivum*, charred cereal	-	-	-	37.76	70.19 ± 0.23	-23.0	2843 ± 26	Rose et al. (2020)
KIA-52416	A394x785 no.4 (urn)	*Alnus* sp. heartwood charcoal (Ø 2-3 cm)	-	-	-	28.07	70.82 ± 0.23	-27.9	2772 ± 26	Rose et al. (2020)
KIA-52417	A394x786 no.1 (urn)	*Quercus* sp. trunk wood charcoal (Ø >10 cm)	-	-	-	51.01	71.29 ± 0.24	-25.2	2719 ± 27	Rose et al. (2020)
			Søhale urnfield cemetery (ESM 2139)							
AAR-25251	G3x22-III	Cremated bone (adult)	Urn of unknown type, unknown iron object	Multiple entrances	-	-	75.94 ± 0.26	-25	2211 ± 27	Møller et al. (2020)
AAR-25250	G5x21-III	Cremated bone, 25-40yrs (adult), female?	Belt clasp?	Multiple entrances	-	-	75.5 ± 0.25	-27	2258 ± 27	Møller et al. (2020)
KIA-53937	G7x37-III	Cremated bone (human)	Urn type 13C, pin with circular head	NNE-SSW entrances	5.1	0.38	75.86 ± 0.23	-21.9	2220 ± 20	
KIA-53936	G9x19-II	Cremated bone (human)	2 pins with large circular heads	NNE-SSW entrances	6.2	0.23	75.43 ± 0.24	-25.8	2265 ± 26	
RICH-26501	G10x23-II	Cremated bone (human)	Urn of unknown type, 2 pins with circular head	NNE-SSW entrances	-	0.10	74.97 ± 0.23	-22.8	2314 ± 24	
AAR-25249	G11x18-III	Cremated bone, 6-15yrs (infans)	Pin of unknown type, narrow belt clasp	N-S entrances	-	-	76.19 ± 0.26	-28	2185 ± 27	Møller et al. (2020)

doi:10.20944/preprints202311.1702.v1

AAR-25248	G12x17	Cremated bone (infans-adult)	None	NNE-SSW entrances	-	-	75.46 ± 0.37	-26	2262 ± 40	Møller et al. (2020)
AAR-25243	G19x10-II	Cremated bone, 2-10yrs. (infans)	Urn of unknown type	NNE-SSW entrances	-	-	75.93 ± 0.29	-24	2212 ± 30	Møller et al. (2020)
AAR-25244	G31x12/x25A	Cremated bone (adult)	None	NNE-SSW entrances	-	-	76.22 ± 0.36	-29	2181 ± 38	Møller et al. (2020)
AAR-25245	G31x12/x25B	Cremated bone (adult)	None	-	-	-	75.74 ± 0.32	-24	2232 ± 34	Møller et al. (2020)
Weighted mean G31x12: T′ = 1.0, T′ (5%) = 3.8, ν = 1, 2209 ± 26 BP										
AAR-25246	G32x14	Cremated bone (infans-adult)	Urn type 15C	NNE-SSW entrances	-	-	74.74 ± 0.25	-23	2339 ±26	Møller et al. (2020)
GrM-16770	G34x40-II	Cremated bone (human)	Urn of unknown type, pin with circular head	?-SSW entrances	-	0.10	75.79 ± 0.18	-23.5	2227 ± 19	
RICH-26493	G35x28-II	Cremated bone (human)	Urn of unknown type, tongue-shaped belt clasp	NNE-SSW entrances	-	0.26	75.62 ± 0.25	-26.3	2245 ± 27	
AAR-25253	G37x27-I	Cremated bone (infans-adult)	None	NNE-S entrances	-	-	75.7 ± 0.28	-24	2237 ± 30	Møller et al. (2020)
RICH-26494	G39x31-II	Cremated bone (human)	Urn type 15? Pin with circular head, pin with bend neck	NNE-SSW entrances	-	0.10	74.76 ± 0.25	-24.6	2337 ±27	
AAR-25254	G40x30-III	Cremated bone (infans-adult)	Eyelet ring, triangular belt clasp	NNE-SSW entrances	-	-	74.9 ± 0.26	-26	2322 ± 28	Møller et al. (2020)
RICH-26495	G44x38-II	Cremated bone (human)	Urn type 15, narrow belt clasp	NNE-SSW entrances	5.9	0.06	75.54 ± 0.24	-28.8	2254 ± 26	
KIA-53938	G44x38-II	Replicate of RICH-26495	-	-	-	0.22	76.12 ± 0.25	-21.5	2192 ± 27	
Weighted mean: G44x38-II: T′ = 2.7, T′ (5%) = 3.8, ν = 1, 2224 ± 19 BP										
AAR-25257	G48x35-II	Cremated bone, <20yrs (adult), male.	Urn type 12C	N entrance	-	-	73.54 ± 0.24	-26	2469 ± 26	Møller et al. (2020)
AAR-25258	G51x47-III	Cremated bone, <40yrs (matures), male?	Urn type 15, 2 pins with type 1 coiled heads	NNW-S entrances	-	-	73.98 ± 0.25	-19	2421 ± 27	Møller et al. (2020)
AAR-25256	G52x33-II	Cremated bone, <35yrs (maturus), male?	Urn of unknown type	NNE-SSE entrances	-	-	74.61 ± 0.25	-24	2353 ± 27	Møller et al. (2020)
RICH-26502	G53x34-II	Cremated bone (human)	Urn of unknown type, 2 pins with circular head	NNE-SSE entrances	-	0.37	74.71 ± 0.24	-25.8	2342 ± 26	
AAR-25255	G54x32-II	Cremated bone, <30yrs (adult)	Urn of unknown type, 2 pins with circular head	NNE-SSW entrances	-	-	74.15 ± 0.27	-29	2403 ± 29	Møller et al. (2020)

doi:10.20944/preprints202311.1702.v1

GrM-16771	G57x41-V	Cremated bone (human)	Urn 13C, narrow belt clasp, 1 pin with circular head, 1 pin of unknown type	NNE-SSW entrances	-	0.09	74.46 ± 0.19	-25.8	2370 ± 20	
GrM-16772	G59x44-II	Cremated bone (human)	2 pins with coiled head, type 1 and 2	No entrances	5.8	0.09	73.60 ±0.20	-26.5	2465 ±20	
KIA-53939	G59x44-II	Replicate of GrM-16772	-	-	-	0.34	73.55 ± 0.23	-24.1	2468 ± 25	
Weighted mean G59x44-II: T′ = 0.0, T′ (5%) = 3.8, v = 1, 2466 ± 16 BP										
GrM-16773	G60x49-III	Cremated bone (human)	Urn of unknown type, pin with type 1 coiled head, bronze ring with eyelet	No entrances	-	0.15	73.92 ±0.16	-25.5	2425 ±19	
AAR-25260	G63x51-IV	Cremated bone, <35yrs (maturus), male?	Urn type 15C, pin with type 1 coiled head, pin of unknown type	No entrances	-	-	73.8 ± 0.25	-25	2440 ± 27	Møller et al. (2020)
KIA-53431	G64x50-II	Cremated bone (human)	Urn type 15B, pin with type 2 coiled head, fragments of a pin of unknown type	No entrances	5.5	0.29	73.82 ±0.19	-21.9	2438 ±21	
AAR-25261	G69x52-II	Cremated bone, 12-18yrs (juvenilis)	Urn type 15C, pin with type 1 coiled head, minimum 2 pins with neck bend	No entrances	-	-	74.01 ± 0.28	-21	2418 ± 31	Møller et al. (2020)
AAR-25262	G70x55-II	Cremated bone, <35yrs (maturus), male?	Urn type 13	N-E entrances	-	-	74.68 ± 0.26	-26	2345 ± 27	Møller et al. (2020)
KIA-53435	G73x92-III	Cremated bone (human)	Urn of unknown type, pin with type 1 coiled head, pin with bend neck and head, imitation of pin x92-I?	No entrances?	6.0	0.39	73.93 ±0.19	-24.2	2427 ±21	
AAR-25263	G81x65-V	Cremated bone <35yrs (maturus), female?	Urn of unknown type, 2 pins with slightly coiled heads, iron ring with shank	N-S entrances	-	-	74.97 ± 0.26	-18	2314 ± 28	Møller et al. (2020)
AAR-25265	G82x93-II	Cremated bone, <25yrs (adult), male?	Urn type 15, 2 pins, hereof at least one with type 2 coiled head	?-S entrance(s)	-	-	74.3 ± 0.27	-24	2387 ± 29	Møller et al. (2020)
AAR-25264	G87x69-IV	Cremated bone, >25yrs (adult)	Urn of unknown type, pin with circular head, pin with neck bend	NNE-SSW entrances	-	-	75.08 ± 0.27	-26	2303 ± 28	Møller et al. (2020)
AAR-25252	G93x26-III	Cremated bone (infans-adult)	Pin with small circular head, tongue-shaped belt clasp	Multiple entrances	-	-	75.32 ± 0.36	-20	2277 ± 38	Møller et al. (2020)
KIA-53434	G105x76-II	Cremated bone (human)	Urn type 15C, pin with type 2 coiled head, pin with type 1 coiled head	No burial mound	6.0	0.24	73.86 ±0.19	-29.0	2434 ±21	
KIA-53940	G105x76-II	Replicate of KIA-53434	-	-	-	0.21	73.90 ± 0.24	-27.4	2429 ± 26	
Weighted mean G105x76-II: T′ = 0.0, T′ (5%) = 3.8, v = 1, 2432 ± 17 BP										

doi:10.20944/preprints202311.1702.v1

KIA-53433	G107x74-II	Cremated bone (human)	Urn of unknown type, pin with type 2 coiled head, pin with type 1 coiled head	No burial mound	5.9	0.33	74.42 ±0.19	-22.6	2373 ±21	
KIA-53432	G110x72-VII	Cremated bone (human)	Urn of unknown type, flat iron ring, 2 pins with type 2 coiled heads	No burial mound	6.4	0.44	74.34 ±0.19	-23.1	2382 ±21	
AAR-25259	G111x48-II	Cremated bone (adult)	Urn of unknown type	N-S entrances	-	-	73.62 ± 0.27	-26	2460 ± 30	Møller et al. (2020)

doi:10.20944/preprints202311.1702.v1

Replicate measurements are available on 17 sets of double targets and on separate extractions of samples from 26 burials. The 17 sets of double targets are all highly statistically consistent with mean T-value 0.01 (117). 21 paired results on separate extractions are statistically consistent at 95% confidence and another two paired results are close to being statistically consistent and we chose to accept them (Aarupgaard 1186: (T = 4.1, T′ (5%) = 3.8, v = 1); Aarre A281: (T = 3.9, T′ (5%) = 3.8, v = 1; Table 1). The three available dates on Aarupgaard U3869 are not in agreement (T = 6.9, T′ (5%) = 6.0, v = 1), although the two earlier dates and the two later dates are, respectively. It is difficult to conclude whether this is caused by a slight underestimation of errors, of if there is a real difference between the 14C ages of the extracts (110). We cannot reject any of the dates and choose to accept the combined date regardless. The two remaining paired results are highly statistically inconsistent (Aarupgaard U230: (T = 34.1, T′ (5%) = 3.8, v = 1); Aarupgaard U1834: (T = 11.9, T′ (5%) = 3.8, v = 1), but there is no reason to dismiss any of the dates based on values of CI, %C yield or $\delta^{13}C$. Instead, we evaluate the results based on the expected time range of the accompanying artefacts. Aarupgaard U230 contains pins with circular head and Aarupgaard U1834 contains a tongue-shaped belt clasp. In both cases, we reject the earlier date (GrM-14704 and RICH-24144, respectively) because they are considerably earlier than other dates on these artefact types. Results from Aarupgaard U1834 were measured on separate bone fragments, which might have different wood-age offsets due to differential uptake of carbon from the burning atmosphere (25), although the presence of multiple individuals in the grave cannot be excluded, as observed in Late Bronze Age cremation burials in Belgium (118). The laboratories have participated in more intercomparison studies, demonstrating results to be reproducible and comparable (110, 119).

Chronological Modelling

All dates are calibrated in OxCal v4.4 using the IntCal20 calibration curve (64, 77). All cremated bone samples gave ^{14}C ages between c.2550 and 2150 BP, equivalent to c. six centuries in the middle of the first millennium BC (64, 77). The ^{14}C dataset consists predominantly of dates measured on cremated bone, which have been demonstrated to be susceptible to wood-age offsets (22, 23, 25, 120). Modelling the cremated bone dates as simple *terminus post quem* (*TPQ)* is unhelpful and instead a Cremation Outlier_Model (OM) is applied to all dates on cremated bone (25). The Cremation OM is based on an existing OxCal OM for charcoal (121, 122), but the parameter values are changed to incorporate a minimum offset, a slightly faster exponential decay and a reduction of sub-decadal offsets. Chronological models discussed in the following are provided in Supporting Information S2 using the exact code in OxCal v4's Chronological Query Language (77).

Modelling burial activity

Initial modelling of burial activity at Aarre, Aarupgaard and Søhale urnfields imposes no constraints of the order of dated samples. Excepted from this are dates from Aarre urnfield on charcoal with potentially significant intrinsic age that are used as *TPQ*s of the associated burial, and where cremated bone dates from burials A95, A130 and A278 are combined with dates on contemporaneous, short-lived samples (25). Legacy dates from LBA periods V and VI (123) are modelled in two contiguous phases and the end boundary of period VI is used as *TPQ* to constrain the start of the urnfield model. The initial **urnfield model A** is compatible with the ^{14}C results ($A_{overall}$ = 80.5), and it estimates urnfield burials started *713-529 cal BC* (95.4% probability) and ended *212 cal BC – 47 cal AD* (95.4% probability). The model provides multimodal solutions for many burials, and estimated a much shorter use-life at Søhale than is indicated by typo-chronology. Based on this we reject the initial urnfield model A.

There are very limited stratigraphic relationships between urnfield burials that can be applied as dating constraints in a chronological model, although it has been discussed if urnfields might be described using horizontal stratigraphy (11, 70). To check the plausibility of these interpretations, we modified the basic structure of model A by adding the inferred site formation processes as dating constraints (urnfield model B). Søhale urnfield are modelled in three potentially overlapping bounded phases, based the orientation of interruptions of the circular ditches, which was thought to

 doi:10.20944/preprints202311.1702.v1

have changed over time: from no interruptions, followed by N-S orientated interruptions to NNE-SSW orientated interruptions (18). This interpretation was at least partly based on ^{14}C dating and we refrain from defining the sequence of entrance groups to avoid circular reasoning. Burials from Aarupgaard urnfield are modelled in a sequence based on typo-chronology with an initial 'founding phase' with burials U3330, U3341 and U3869 that were interred within an existing Bronze Age mound. Their funerary urns resemble LBA pottery, and although the pins are made of iron, they are typologically closer to LBA types. Remaining burials are modelled based on observations that the number of interruptions of the circular ditches changed over time (70, 83), starting with a phase with multiple interruptions, followed by a final phase with two interruptions. The transition between the latter two phases is modelled with trapezium priors, allowing it to have a duration. There is no architectural prior information available on the internal sequence of the burials from Aarre urnfield.

The **urnfield model B** is acceptable ($A_{overall}$ = 67.6), and it estimates urnfield burial activity to have started *709-571 cal BC* (95.4% probability), probably *662-588 cal BC* (68.3% probability), and to have ended *260-125 cal BC* (95.4% probability), *probably 234-114 cal BC* (68.3% probability). The cremation OM *estimates 1-60yr offsets* (95.4% probability), *probably 1-24yr* (68.3% probability). Aarre urnfield is estimated to be in use for 158-264yr (68.3% probability), starting *617-457 cal BC* (95.4% probability), or *572-499 cal BC* (68.3% probability), and ending *356-214 cal BC* (95.4% probability), or 348-307 cal BC (68.3% probability) (Figure 11, S1 Fig. Kernel density plot of Aarre urnfield). The use period of Aarre urnfield is credible, although, given the limited number of samples, it cannot be excluded that the cemetery might have lasted longer. Søhale urnfield is estimated to have been in use for *92-186yr* (68.3%), starting *555-423 cal BC* (95.4% probability), or *510-432 cal BC* (68.3% probability), and ending *360-277 cal BC* (95.4% probability), or *351-314 cal BC* (68.3% probability) (Figure 12, S1 Fig. Kernel density plot of_Søhale urnfield). The use period of Søhale urnfield is longer than estimated by urnfield model A, and now more consistent with the archaeological expectation. Aarupgaard urnfield is estimated to have been in use *344-404yr* (68.3% probability), starting *642-556 cal BC* (95.4% probability), or *616-571 cal BC* (68.3% probability), and ending *257-186 cal BC* (95.4% probability), or *238-201 cal BC* (68.3% probability) (Figure 13, S1 Fig. Kernel density plot of Aarupgaard urnfield). The use period of Aarupgaard urnfield is longer than that of the other urnfields, but this is in agreement with the occurrence of both earlier and later artefact types at Aarupgaard than at Aarre and Søhale. The model is able to constrain the end boundary and provides unimodal solutions for nearly all burial dates. Urnfield model B is our preferred chronological model for modelling burial activity at Aarre, Aarupgaard and Søhale urnfields, because it evaluates more prior information.

Preprints (www.preprints.org) | NOT PEER-REVIEWED | Posted: 28 November 2023 doi:10.20944/preprints202311.1702.v1

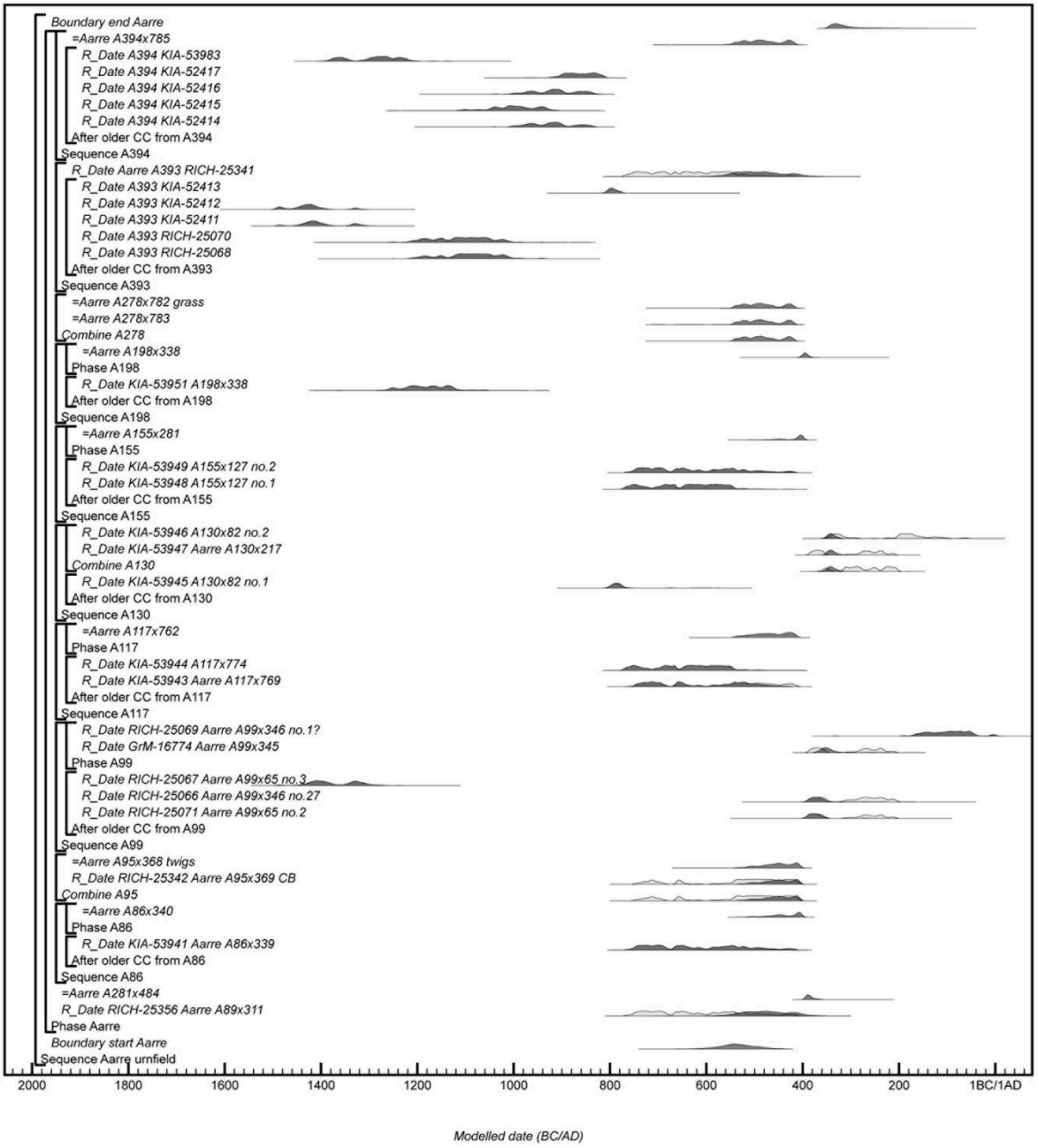

Figure 11. Chronological model of Aarre urnfield, based on the preferred urnfield model B.

Preprints (www.preprints.org) | NOT PEER-REVIEWED | Posted: 28 November 2023 doi:10.20944/preprints202311.1702.v1

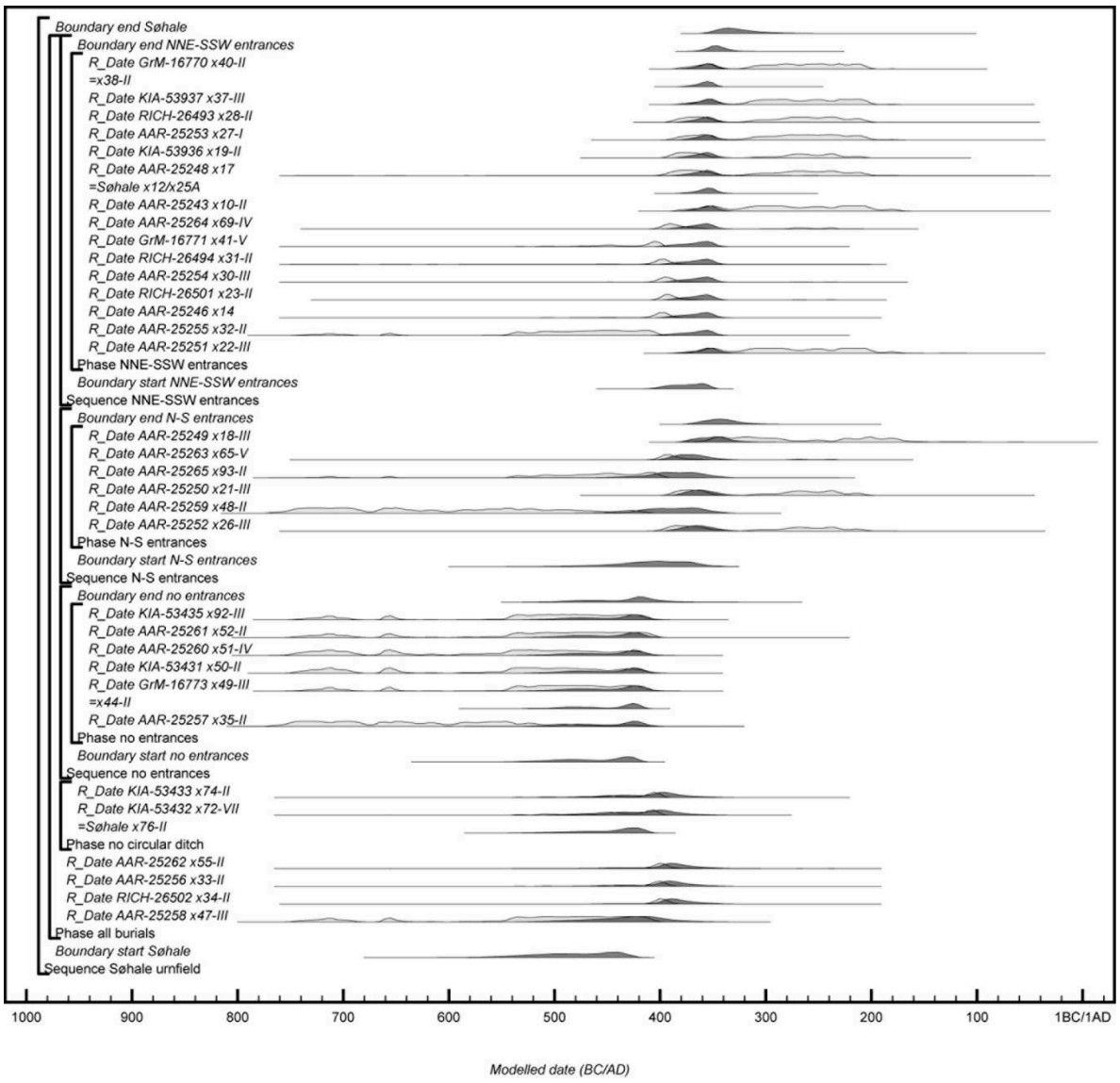

Figure 12. Chronological model of Søhale urnfield, based on the preferred urnfield model B.

Preprints (www.preprints.org) | NOT PEER-REVIEWED | Posted: 28 November 2023 doi:10.20944/preprints202311.1702.v1

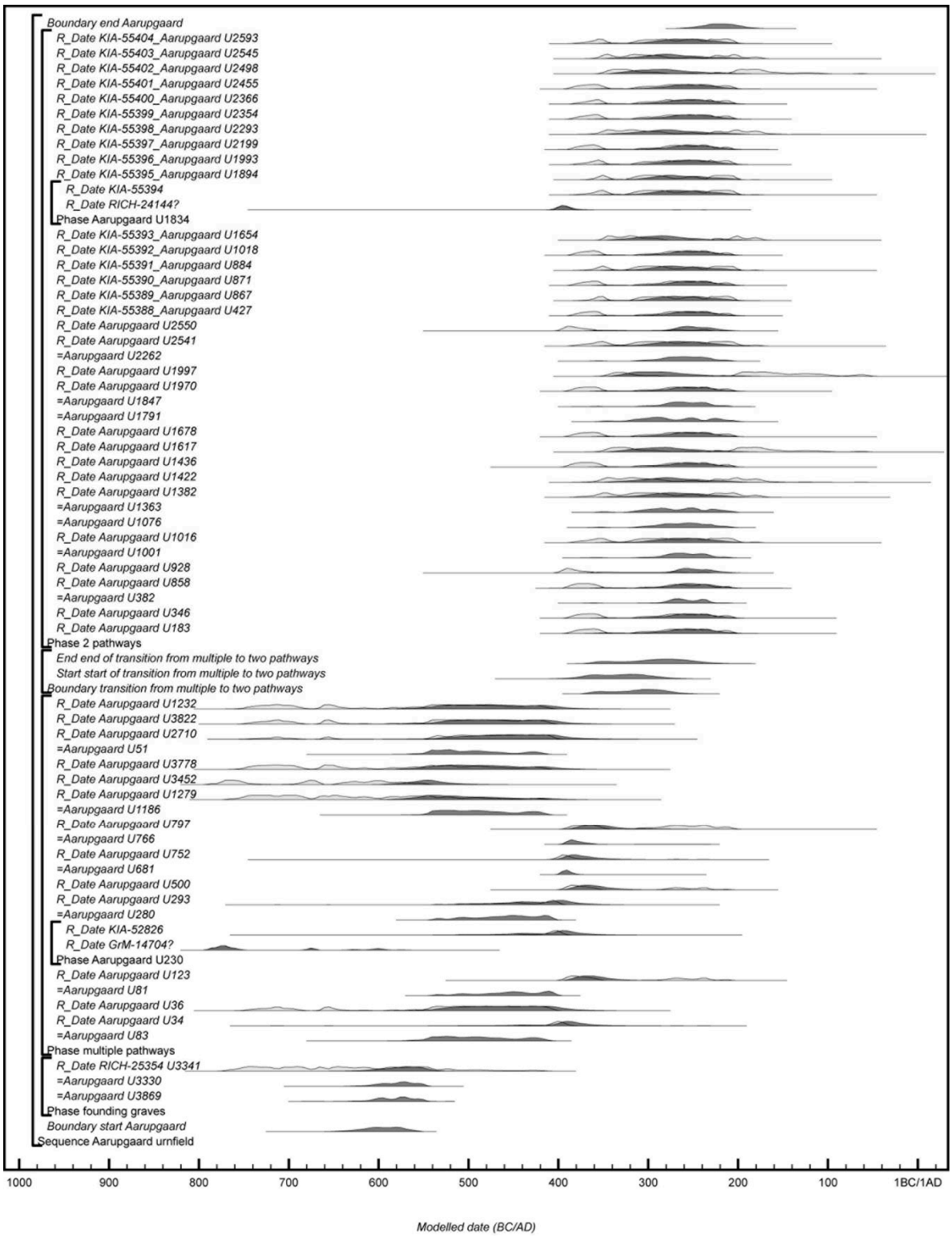

Figure 13. Chronological model of Aarupgaard urnfield, based on the preferred urnfield model B.

Spatio-temporal development

An alternative site model of Aarupgaard urnfield is based on earlier observations of horizontal stratigraphy (11, 70). Burials are divided into horizontal groups of c. 200 individuals based on distance to the founding burials in the northern end of the urnfield (H1-H6) and are further divided into a main western burial group (M1), and smaller eastern burial group (M2). The starts of the M1 horizontal groups are constrained to follow the sequence: M1-H1, M1-H2, M1-H3, M1-H4, M1-H5,

Preprints (www.preprints.org) | NOT PEER-REVIEWED | Posted: 28 November 2023 doi:10.20944/preprints202311.1702.v1

M1-H6. The model makes no assumptions about the sequence of M1 horizontal group ends, in order to allow for later infilling of burials. There are fewer burials in burial group M2, making it necessary to merge horizontal groups 1-3, and there are no burials beyond horizontal group 4. The start and end of the M2 horizontal groups are constrained to follow the sequence: M2-1-3, M2-4. The other components of the model (i.e. dated burials at Aarre and Søhale) correspond to the preferred urnfield model. The alternative model is acceptable ($A_{overall}$ = 83.7), confirming that site formation at Aarupgaard urnfield followed a north-southbound trajectory best described using horizontal stratigraphy (Figure 14 upper panel, S1 Fig. Summarized burial activity of arbitrary horizontal groups at Aarupgaard urnfield). The first 200 burials taking twice as long as the next 200 burials, indicating an increasing burial rate in the initial phase of the urnfield. The model estimates burial activity to have continued slightly later when compared to urnfield model B, but it also estimates more fluctuating burial rates (S1 Fig. Kernel density estimate of alternative horizontal model of Aarupgaard urnfield). Urnfield model B does not depend on these arbitrary divisions into horizontal groups, and it remains our preferred model.

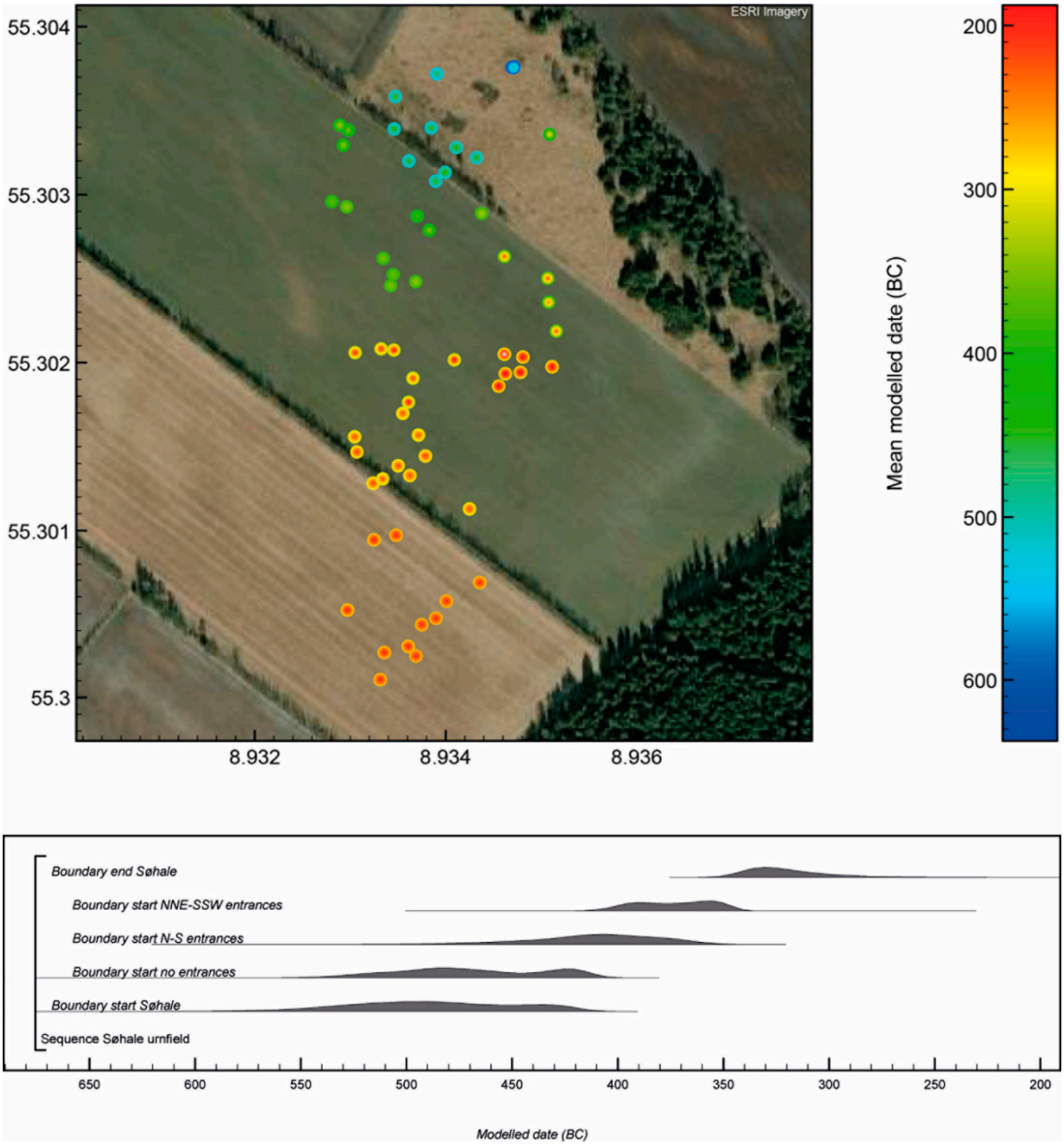

 doi:10.20944/preprints202311.1702.v1

Figure 14. Alternative chronological models. Upper panel: Spatio-temporal plot of Aarupgaard urnfield based on horizontal stratigraphy. Lower panel: Søhale urnfield, based on the orientation of the interruptions of the circular ditches.

Sensitivity testing

Sensitivity testing is a central part of Bayesian chronological modelling and it can be used to test alternative models using different prior information. To validate the preferred site model, we test the influence of selected model constraints on posterior estimated output in two alternative site models of Aarupgaard and Søhale, respectively. The remaining model equals urnfield model B. We also test the reproducibility of the posterior estimated start and end of burial activity, because it coincides with a major plateau in the ^{14}C calibration curve c.750-400 cal BC, and an inversion c.320-200 cal BC.

In the preferred urnfield model B for Søhale, burials are grouped based on the orientation of interruptions of the circular ditches, but the three groups are not placed in any sequence. We test the chronological sensitivity of these groups in an alternative site model by constraining the start of entrance groups to follow the sequence: no interruptions, N-S, NNE-SSW. The model is acceptable ($A_{overall}$ = 84.6), permitting the possibility that the orientation of interruptions of circular ditches is time dependent, following the order as proposed by Møller et al. based on ^{14}C ages (Figure 14 lower panel) (18). Constraining the order of introduction has however, no influence on the posterior estimated output and the alternative model is therefore rejected in favour of the less constrained urnfield model B.

Bronk Ramsey (124) has shown that realistic density distributions of uniformly distributed dates can be estimated using the default KDE_Model provided in OxCal. Kernel density estimates (KDE) can also be used to visualize burial activity and changes in burial rates and a KDE plot of all posterior estimated burials from preferred urnfield model B has two peaks around the time of an inversion of the ^{14}C calibration curve c. 320-200 cal BC (Figure 15 upper panel). KDE plots of the individual urnfields all have a single peak towards the end of their use-life, but at different points in time (S1 Fig. Kernel density plot of Aarre urnfield, S1 Fig. Kernel density plot of Aarupgaard urnfield, S1 Fig. Kernel density plot of Søhale urnfield), which combined produce the two peaks. We test if the observed peaks in burial activity are mere artefacts of the ^{14}C calibration curve by creating two synthetic datasets, each with 111 simulated ^{14}C dates between 780-180 BC, drawn from a normal distribution (Sim_Norm) and a uniform distribution (Sim_Uni), respectively and summarized using the KDE_Model function (normal distribution: Figure 15 middle panel, uniform distribution: Figure 15 lower panel) (124). The KDE of the synthetic normally distributed dataset depicts the expected bell curve but bears little resemblance to the KDE of the urnfield burials. The KDE of the synthetic uniformly distributed dataset is not able to retrieve the known uniform distribution but gives a false trough in the 5th century and a false peak at c.300 BC, which are not seen in the real data, while the 4th and 3rd century peaks in the real data are not visible in the simulation and can therefore be considered as reliable. (125)

Preprints (www.preprints.org) | NOT PEER-REVIEWED | Posted: 28 November 2023 doi:10.20944/preprints202311.1702.v1

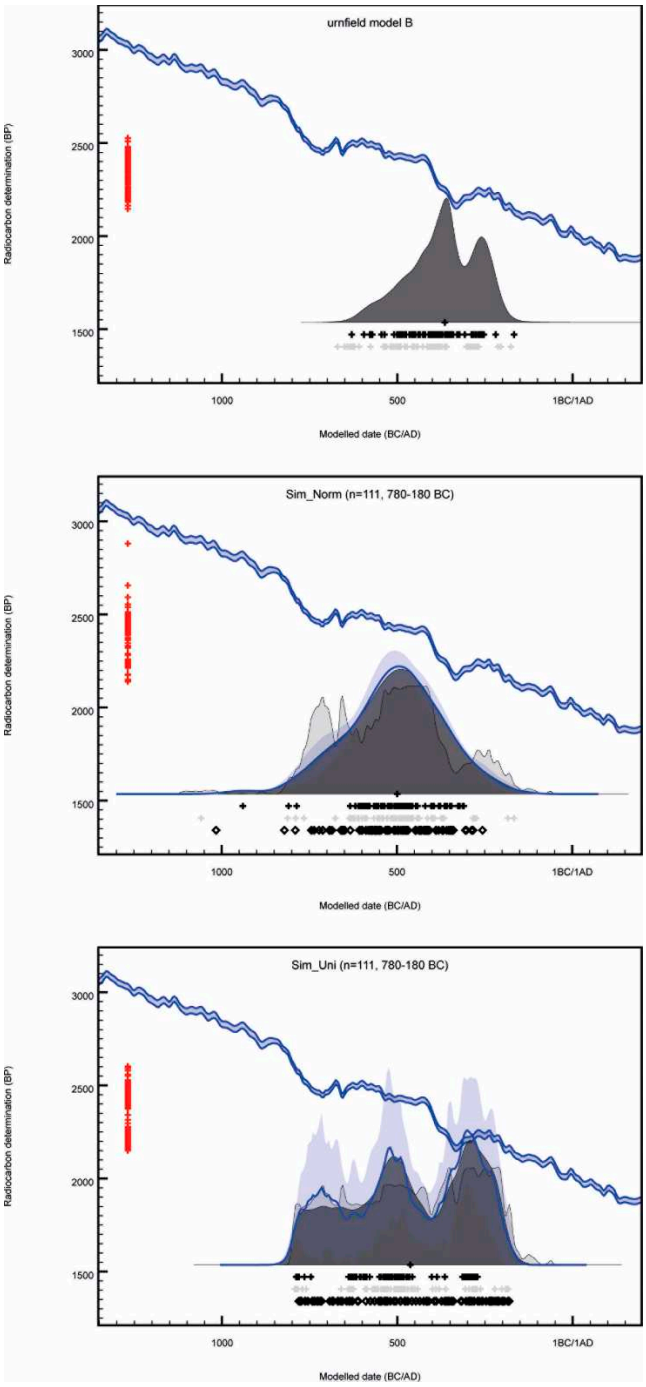

Figure 15. Kernel density estimates of actual and simulated burial activity. Upper panel: KDE plot summarizing urnfield burial activity as estimated by the preferred urnfield model B (124). Simulating burial activity of 111 simulated ^{14}C dates between 780-180 BC using the OxCal function KDE_Model with defaults parameter values (124). Middle panel: simulated ^{14}C dates drawn from a normal distribution (Sim_Norm). Lower panel: simulated ^{14}C dates drawn from a uniform distribution (Sim_Uni). Red crosses (left) show median uncalibrated ^{14}C ages, red crosses (below) show median modelled calibrated dates, grey crosses (below) show median of simple calibrated dates and diamonds (below) show known calendar ages. The relevant section of the IntCal20 calibration curve is shown for references *(64).*

We test the influence of the ^{14}C calibration inversion c.320-200 cal BC on the precision of the posterior estimated output by adding synthetic dates with +-25yr uncertainties to the real Aarupgaard dataset, using the OxCal function C_Simulate. These simulated dates are not affected by the shape of the ^{14}C calibration curve. Adding simulated calendar dates between 250-200 does not

 doi:10.20944/preprints202311.1702.v1

shift the end boundaries compared to those obtained under preferred urnfield model B, probably due to the uniform distribution favoured by the model. This implies that the latest real burials must date at least to around 200 BC, but not if they might be even later. We explore this by adding simulated calendar dates between 200-150 BC, but even though this shifts the estimated end boundary later, it still estimates the youngest simulated burials to be too early (S1 Fig. Adding simulated later burial dates to preferred urnfield model B). By repeated modelling of younger dates with slightly varying calendar dates and sampling intensity (decadal or sub-decadal) it becomes clear that adding only a few dates between 200-150 BC produces posterior estimates around 200 BC, whereas adding at least a handful of dates later than 200 BC will produce a slightly later end boundary. To recover the true calendar dates the youngest simulated dates must be later than c.150 BC, but also have a certain sampling density.

Burial U1617 from Aarupgaard has the youngest ^{14}C age BP (2163 ± 28) of the entire dataset. Calibration with IntCal20 gives a slightly later calibrated date in comparison to IntCal13, but both produce bimodal solutions with close to equal posterior probabilities on either side of the ^{14}C inversion (IntCal20: 350-305 cal BC at 31.6% probability, 208-156 at 36.7% probability). The archaeological prior information does not allow us to reject either possibility and because the urnfields were abandoned around this time, it would be difficult to sample even later burials. Our preferred urnfield model B estimates the burial date of U1617 to *322-257 cal BC* (68.3% probability), i.e. centred on the early-middle part of the ^{14}C inversion.

Based on this, we conclude that the latest real burials probably do date to around 200 BC, as also estimated by the preferred urnfield model B. We cannot reject the possibility that a few burials date to the first half of the second century BC, but we would then expect different material culture (e.g. fibulae and knives) to be present at Aarupgaard, and we therefore find this to be unlikely.

Modelling artefact currencies

The artefact currencies are modelled in a separate step. The posterior estimated burial dates from urnfield model B are saved (using the OxCal function Prior) and the currencies of types with minimum four dated cases are summarized using the default KDE_Model function in OxCal (Figure 16) (124). Though providing a first overview of the currency distributions, this is inconsistent with the archaeological expectations because, aside from the simple iron ring, there is no metalwork dating to the early 5th century BC. Overall, these KDE models also estimated that the currencies ended earlier than expected.

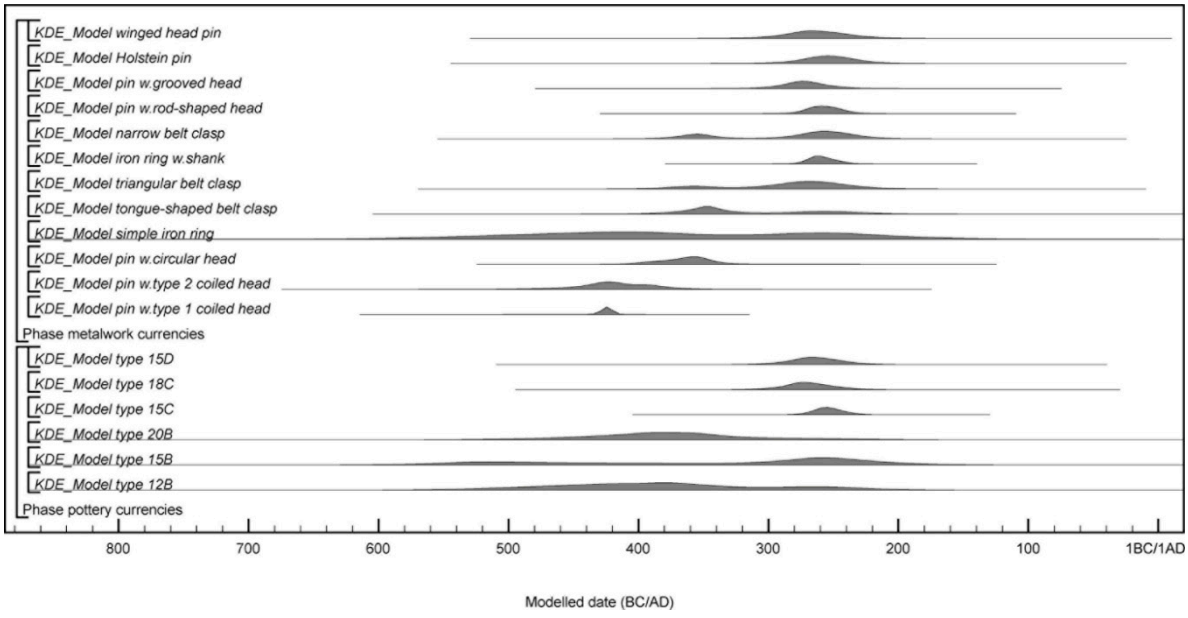

Figure 16. Artefact currencies summarized using the default KDE_Model function in OxCal (Figure 16).

 doi:10.20944/preprints202311.1702.v1

The posterior estimated burial dates (OxCal Priors) are instead modelled as dates in two separate bounded phases of pottery and metalwork currencies, which are constrained to start after the end boundary of period VI, similar to urnfield model B. Currencies dated by 1-3 cases are modelled in unbounded phases, currencies dated by 4-9 cases in uniform bounded phases, and currencies dated by ≥10 cases are modelled using trapezium boundaries (76, 78). We test and find that posterior estimates on pottery are unaffected by constraining their order of introduction as defined by correspondence analyses by Jensen (5) (starting order: 15B, 12B, 20B, [15C & 18C]). It is therefore preferable not to include prior information on pottery sequences. It is however not possible to model the metalwork currencies without constraining their order of introduction (pin sequence: pin with type 1 coiled head, pin with type 2 coiled head, pin with circular head, [pin with grooved head and pin with rod-shaped head], [Holstein pin and winged head pin]; sequence of belt equipment: simple iron ring, [tongue-shaped belt clasp and triangular belt clasp], [iron ring with shank and narrow belt clasp]). We note that artefact currencies are limited by the use-life of the urnfields, and some types might well have been in use longer elsewhere.

To identify possible heirlooms with residence-time offsets, we apply OxCal's default General Outlier_Model to the currency model, with a prior probability of 5% that all burial dates are not applicable to the associated pottery and metalwork (121). 24 artefacts from 22 graves have posterior probabilities of being an outlier higher than 5%, 13 artefacts from 12 graves are estimated to have probabilities >10% (S1 Table. Graves containing possible heirlooms, S1 Fig. Identifying residence offsets). The majority of these cannot be explained by residence-time offsets because the dates favoured by the currency model are later than their burial dates, while four outliers are caused by the model being unable to distinguish between the early and late legs of the ^{14}C calibration inversion c. 320-200 cal BC. Seven artefacts from as many graves are interpreted as heirlooms because their mean posterior dates are earlier than the respective burial dates (for artefacts with outlier probabilities >10%. Heirlooms can also be identified when graves contain artefacts of multiple types, such as U1617 from Aarupgaard, where a circular pin is estimated by the currency model to be earlier than the burial date and remaining artefacts (whose modelled dates are consistent with each other and with the burial date), clearly demonstrating that the pin must be an heirloom with a considerable residence time. In a following step, we remove the General OM and instead apply individual residence-time offsets with a normal distribution of 50 ± 25yr to the seven identified heirlooms (bold red font in S1 Table. Outlier probabilities). The currency model is acceptable ($A_{overall}$ = 104.3), and all heirlooms have acceptable indices of agreement with 41-99yr residence offsets (68.3% probability) with a mean of 67yr.

Pottery currencies

In total, 14 types of pottery from Aarupgaard urnfield are modelled: five of these in bounded phases and one using trapezoidal phase boundaries (Figure 17 upper panel, S1 Fig. Chronological model of pottery currencies). Pottery from Søhale urnfield is not included in the modelling, but results from the two urnfields are compared below. Individual currency models are provided in Supporting Information S1. The currencies evidently have large overlaps, but their order of introduction is estimated to follow the sequence: 15B, 12B, 20B, 18C, [15C & 15D], in agreement with the order given by Jensen (5). He dated type 20B to the Late PRIA, however, but the ^{14}C evidence evidently supports an earlier introduction.

Preprints (www.preprints.org) | NOT PEER-REVIEWED | Posted: 28 November 2023 doi:10.20944/preprints202311.1702.v1

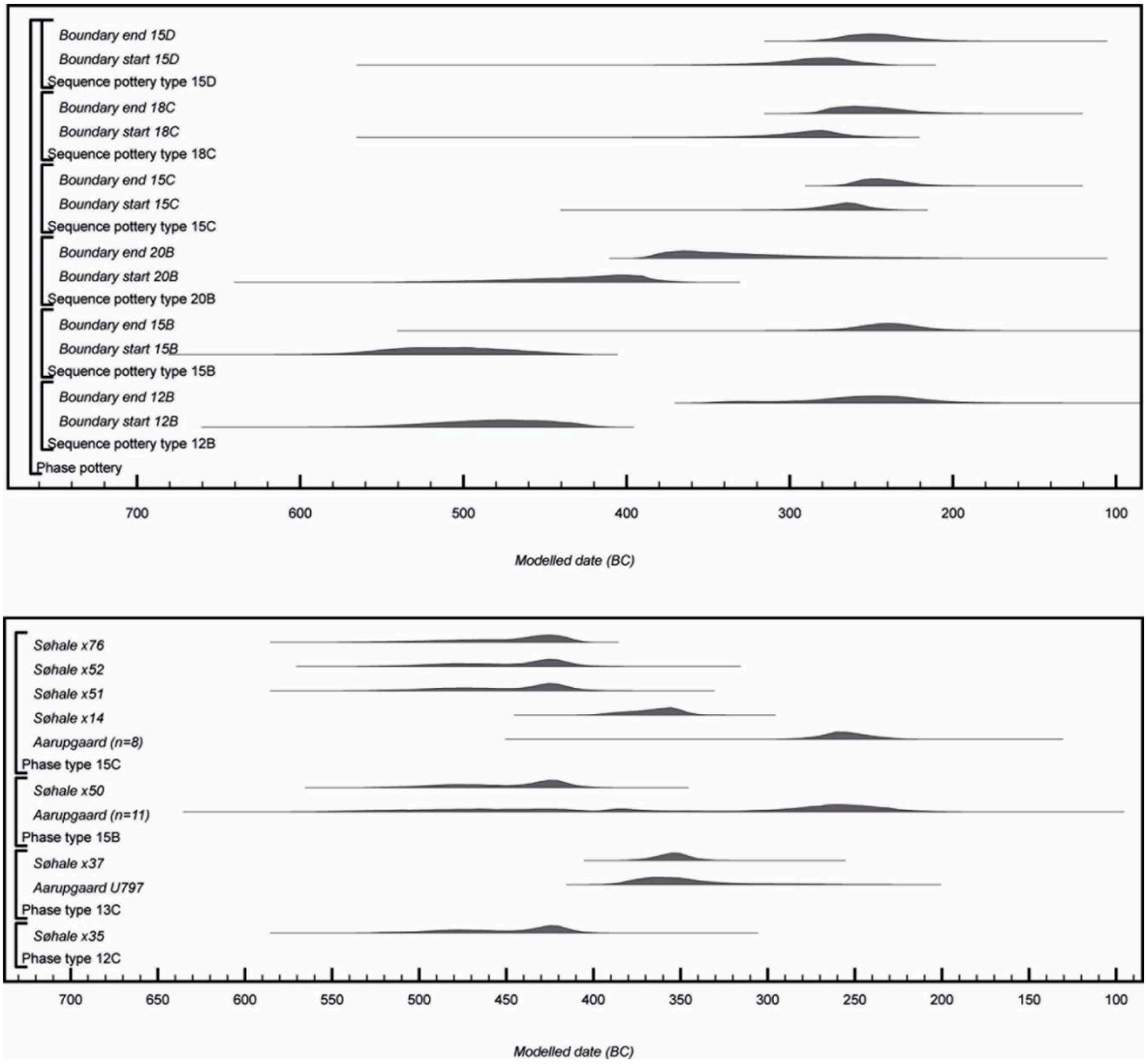

Figure 17. Posterior estimated dates on pottery from Aarupgaard and Søhale urnfields. Upper panel: posterior estimated start and end of pottery currencies from Aarupgaard with minimum four dated specimens per type. Lower panel: comparing pottery currencies from Aarupgaard to posterior estimated burial dates from graves from Søhale containing pottery.

Seven burials from Søhale urnfield contained four types of diagnostic pottery and we compare the posterior estimated burial dates of these to the estimated currencies based on burials from Aarupgaard (Figure 17 lower panel). Burial x50 contained a type 15B vessel and its date is comparable to the earlier instances of this type at Aarupgaard, four burials contained type 15C vessels that all date significantly earlier than at Aarupgaard, but burial x37 that contained a type 13C vessel is contemporary with another similar type vessel from Aarupgaard. Burial x35 contained the only type 12C in the dataset. It might be suggested that pottery types appeared at Søhale earlier than at Aarupgaard, but the present dataset is too small to reveal different temporal patterns between the urnfields.

Metalwork currencies

In total 15 types of metalwork are modelled, and 12 of these are modelled in bounded phases with predefined order of introduction (Figure 18, S1 Fig. Chronological model of metalwork currencies). Individual currency models are provided in Supporting Information S1. The currency model estimates a high degree of overlap between types. Bomb head pin, eyelet ring and bronze neck ring are only present in a few burials, but are estimated to date to the 5th century, first half of the 4th

Preprints (www.preprints.org) | NOT PEER-REVIEWED | Posted: 28 November 2023 doi:10.20944/preprints202311.1702.v1

century and to the 3rd century, respectively. Simple iron ring was probably a generic type used throughout the PRIA. Earlier, we rejected the typological differentiation between small and large pins with circular heads. This is further supported by the ^{14}C evidence that fails to show a dependency between mean ages estimated by the currency model and head size index (S1 Fig. Circular head pins from Aarupgaard urnfield).

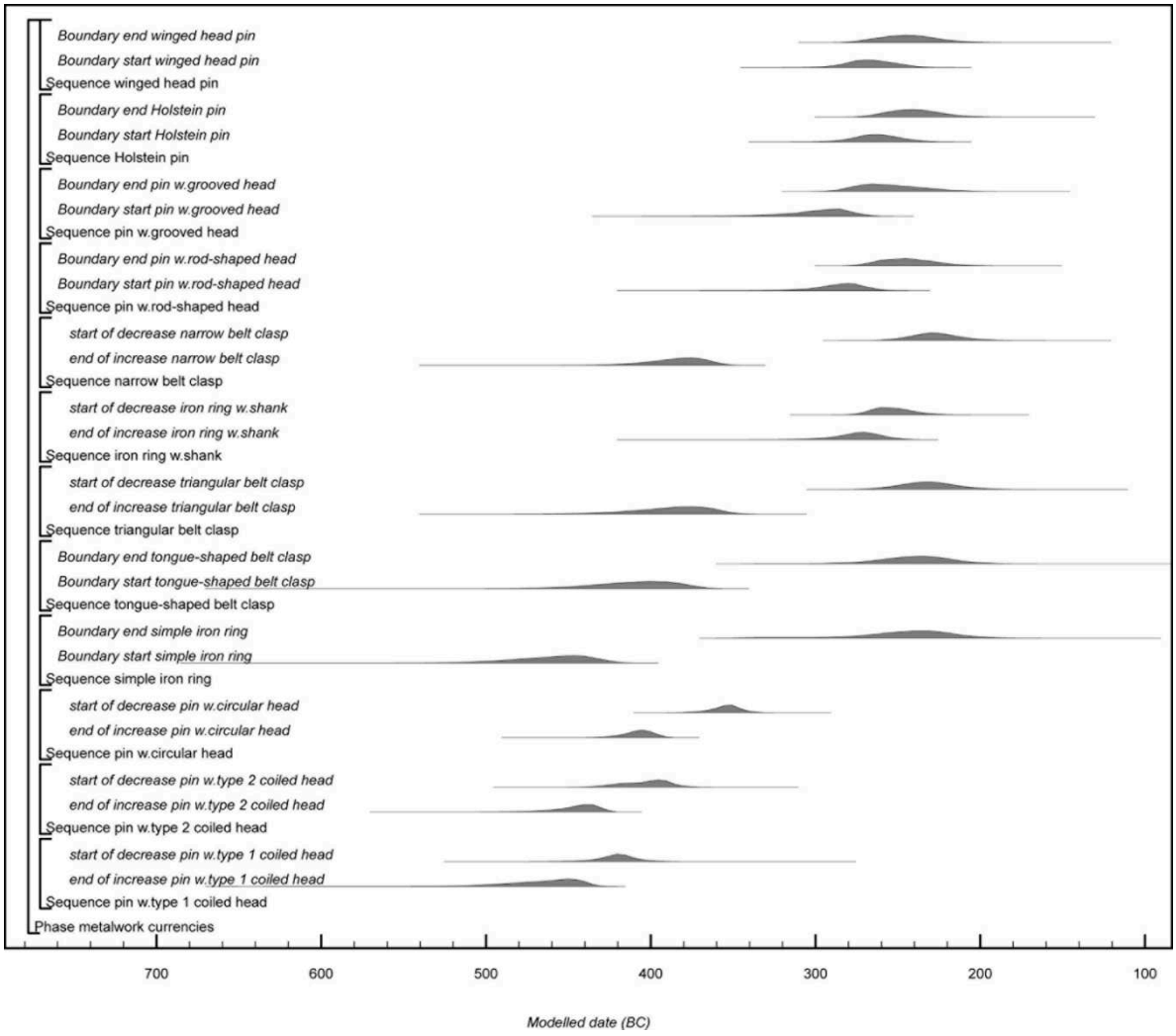

Figure 18. Posterior estimated metalwork currencies with minimum four dated specimens per type.

Discussion

Chronology construction, or situating archaeological material within space and time, is a time-honoured tradition in archaeology. It is also a prerequisite for most archaeological studies and in turn influences our resulting narrative of the past, e.g. if two key phenomena are overlapping or if one leads to the other? A good chronological resolution enables investigations not only into the material record and burial practices, but also allows us to address overarching questions regarding e.g. religious and cultic practices. The range of individual chronologies is decided by the presence of shared material culture, but can be extended or correlated by cross dating imports. In the absence of imports chronological frameworks can instead be synchronized using absolute dating. The same approach can be used to correlate different find materials, such as the many archaeological chronologies that are traditionally based on metal-based typologies, whereas ceramic types are only subsequently attributed. This is also the case for PRIA in Denmark where there are demonstrated difficulties correlating typo-chronologies of metalwork and pottery (11, 12). Here metal artefacts are practically absent from settlement contexts and without a detailed chronology for pottery, it is difficult to compare settlement and funerary evidence.

 doi:10.20944/preprints202311.1702.v1

Chronological frameworks assume change happened continuously and consequently divide the past into non-overlapping units of time, but the application of absolute dating now challenges the validity of this notion. Instead, prehistory is made up of long-term transformations, i.e. from bronze to iron technology, but any of these transformations entail a multitude of smaller-scale changes. Whether the smaller-scale changes are visible in the archaeological record depends on the resolution of the available data, but also on adopting an appropriate research approach that permits non-uniform output.

Insight into a dynamic material culture

The main new contribution of the study is the modelling approach that provides a detailed insight into the temporal dynamics of artefact currencies without *a priori* imposing the rigid boundaries of a chronological framework. Artefact typology is often used as prior information to establish site chronologies and absolute chronological frameworks (e.g. 126), but typologies are rarely the intended focus of such investigations. Important exceptions are the seminal study on British Bronze Age Metalwork (127), the 'Dating Celtic Art' project (128), and the 'Anglo-Saxon Graves and Grave Goods' project (40). Common for these are that currencies are assumed to have a uniform distribution, i.e. dated artefacts are equally likely to date to any point in between a rapid introduction and a later equally rapid abandonment. It might rightly be questioned how realistic such a scenario is and it is now possible to model artefact distributions in OxCal using the trapezium prior model, which is well suited for modelling non-instantaneous cultural changes, particular where phases are expected to be overlapping and transitional periods to have a duration (76, 78). A trapezium model divides a distribution into three parts, first an introductory period; followed by a period of maximum use; before a period of decline (43, 75). Seriation of artefacts from PRIA show individual currencies to have significant increase and decrease 'tails' and a large degree of overlap between types (5), leading us to model seven currencies using trapezoidal boundaries. We decided to focus on types with min. 10 dated cases because the model would otherwise introduce large uncertainties compared to a bounded phase model. This only includes a single pottery type, but the dynamics of type 15B appears to be comparable to the metalwork types. The periods of introduction and abandonment are estimated to last a couple of centuries, respectively, although a bimodal distribution for narrow belt clasp cannot be rejected, which leads to a longer estimated introduction period (S1 Fig. Posterior estimated parameters from currency models a). We find that letting the introduction and abandonment of the currencies have a duration, rather than being instantaneous, is a better fit with the actual artefact frequencies observed by Jensen (5).

The modelled currencies have very variable durations, with pottery being in use up to 33-313yr (68.3% probability, mean = 62yr), and metalwork up to 30-217yr (68.3% probability, mean = 48yr) (S1 Fig. Posterior estimated parameters from currency models b). Pottery types 12B and 15B were in use significantly longer than the other types, probably throughout the EPRIA, which is contextually supported by associated artefacts spanning most of the typological sequence of metalwork. The remaining three pottery types were probably in use for 2-4 generations (mean = 34yr). It has been suggested that vessel types used in the public domain are more likely to change fast over time, whereas other types appear to have remained largely unchanged for longer periods (129). The large storage vessels often reused as funerary urns probably belong in the latter category, but it is possible that currencies of smaller vessels not included in this study are more dynamic. The early pin types (pin with type 1 and type 2 coiled head and pin with circular head) were likely in use for 2-3 generations (mean= 50yr), but it is possible that several later metalwork types (iron ring w. shank, pin w. rod-shaped head, pin w. grooved head, Holstein pin and winged head pin) were in use for only 1-2 generations (mean = 19yr). The relatively long estimated durations of tongue-shaped, triangular and narrow belt clasps are at least partly caused by them coinciding with the ^{14}C calibration inversion c.320-200 cal BC.

Modelling currencies dynamically has the great advance that it becomes possible to identify periods with lower and higher rates of change during the PRIA (Figure 19). Both pottery and metalwork have considerable overlap of consecutive currencies and when combining these a pattern

 doi:10.20944/preprints202311.1702.v1

with peaks and valleys emerges. The decades around the start of the 4th century BC have a high rate of change with more types going out of use while new types are being introduced. The remaining first half of the 4th century BC has a low rate of change as these types continue to be in use, before the rate increases in the second half of the century when types are again abandoned while new types are being introduced. Followed by a period with lower rate of change in the first half of the third century BC. The start and end of the investigated period are probably also periods of rapid change, but it is difficult to demonstrate, as these are not constrained by earlier or later occurring currencies.

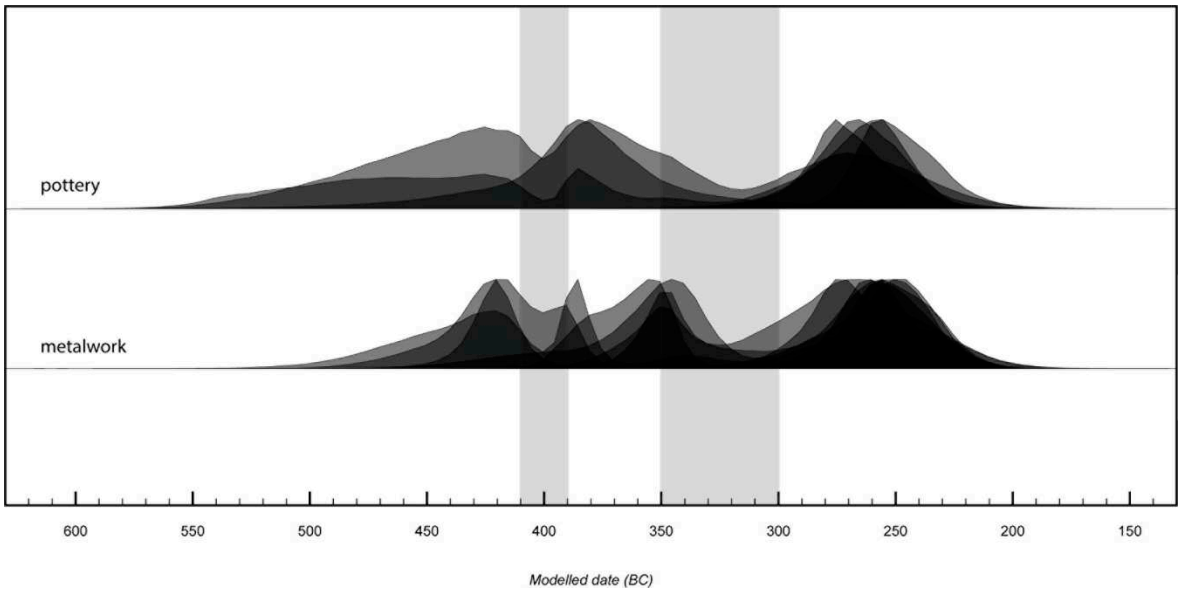

Figure 19. Currencies of pottery and metalwork are stacked, respectively, and periods with higher rate of change in material culture is marked with yellow bars.

Modelling periods of introduction, main use and decline offers a new and dynamic perspective on artefact currencies. The individual artefact types do not themselves introduce large changes to the society, but by documenting small-scale changes and demonstrating how these are concentrated in periods with a higher rate of change, it becomes clear how the redefinition of material culture is actively used in an ongoing negotiation of a dynamic society. The majority of types are introduced rather rapidly and are not in circulation long after the production ends, which demonstrates a readiness to adopt new designs of existing object forms. Particularly the metalwork types were in use for shorter periods, whereas the pottery can be divided into shorter lasting types and generic types that were in use throughout the period. Typological analyses of comparable EPRIA cemeteries from Schleswig-Holstein have demonstrated pottery to have a limited chronological sensitivity compared to metalwork (13). The Danish material share the same tendency, although it is less distinct. The difference between the Danish and German material might be caused by comparing absolute and relative dated currencies, but there are so far no large ^{14}C dataset available on German material.

Heirlooms and residence time

The production date and deposition date of an artefact are separate events that can be greatly removed from each other, i.e. the artefact has a residence time. If older individuals are buried with artefacts that they had received at a young age those artefacts will have a considerable residence time, which has led Trachsel (37) to caution against assigning currency durations shorter than a human lifetime. There is no available information on the life expectancy in the PRIA or at what age individuals would receive dress accessories such as pins and belt claps. If the artefacts were instead passed down as heirlooms, the residence time would increase significantly. Another important factor when discussing residence time of artefacts is durability of the material in question. Metalwork has a high durability is therefore considered likely to have a residence time. Pottery is more fragile and

 doi:10.20944/preprints202311.1702.v1

less likely to accumulate significant residence times. All urns from Søhale urnfield have considerable wear of the bottom and they must have been used for some time prior to being re-used as funerary urns. No experimental studies have been conducted on the use wear of PRIA pottery, but it is plausible that the bottom of a vessel would show signs of use after even a few years. It is demonstrated that some of the pottery currencies have been produced over long periods, but this does not contradict individual vessels having a short or even negligible residence time. There is a however a risk of metalwork having a residence time.

We estimate the residence offsets of identified heirloom objects by calculating the difference between the posterior estimates of the burial date, i.e., the latest possible production date, and the earliest dating artefact in the grave. It is assumed that the residence offset will be less than century (normal distribution 50 ± 25yr). We find residence offsets up to 102y*r* (68.3% probability), with a mean of 62yr (S1 Fig. Posterior estimated residence time). There is no available information on the age of the individuals buried with heirlooms, and it cannot therefore not be ruled out that some of them were older individuals buried with object they had acquired early in life. Similar to Trachsel's suggestions regarding a 40+ aged individual from the central chamber of the 'Magdalenenberg' (37). The calendar age difference between a pin with a type 2 coiled head and the burial date of Aarupgaard U928 is however larger than a single individual's lifetime (Figure 20). The burial date and a circular head pin from the same grave are estimated c.350 and c.250 BC, respectively, which correspond to before and after the ^{14}C calibration inversion. Based upon the grave placement in the urnfield (horizontal group M1-H3), the earlier solution is probably more likely, which would incidentally make the pin with type 2 coiled head less of an outlier in the burial context.

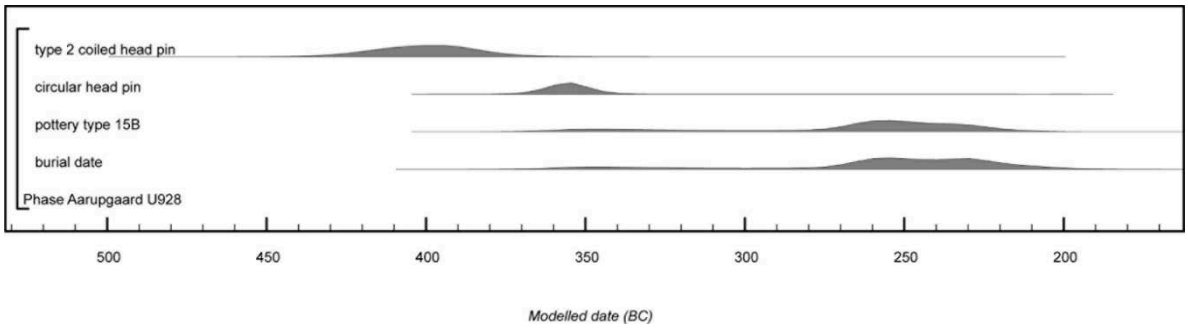

Figure 20. Burial U928 from Aarupgaard urnfield. The significant residence time of the pin with type 2 coiled head in relation to the burial date makes it a likely heirloom.

Absolute chronology

The archaeological literature contains a vast number of chronological frameworks for all time periods and regions across the globe and correlating any of these is a major task only achievable through international collaborations, and in many cases not possible without using absolute dating, such as ^{14}C dating (66, 126), or wiggle-matching dendrochronologies (130). The start of the Iron Age in Southern Scandinavia is believed to coincide Ha D in Central Europe, but the argument therefore rests on a very limited number of imports. Instead, the existing relative chronological framework is determined on typo-chronologies, largely unconstrained by absolute dating (although see 18). Recent studies have however demonstrated that the Iron Age chronology for Central Europe and possibly also Southern Scandinavia, might be in need of revisions (66, 130). In the following, we provide an absolute chronological framework of the Early Iron Age in Denmark based on posterior estimated probabilities saved as priors from the urnfield model B and the currency model.

The transformation from Bronze Age to Iron Age is usually assumed to occur around 500 BC (5, 131), or possibly in the later 6th century BC (4, 18, 132). It has been suggested that the transformation coincides with the Ha D1-D2 transition in Central Europe (16, 132), which following Rieckhoff and Biel occurs 550 BC (133). The transformation is not defined by the introduction of iron technology alone, but by a combination of small-scale changes in material culture, introduction of urnfields as a

 doi:10.20944/preprints202311.1702.v1

new funerary tradition and society structure changing from being kinship based towards more family and village orientated. Settlement structures and economy however remain relatively unchanged (132, 134). Following these observations, we model a transition period following the end of Bronze Age period VI and before burial activity at Aarupgaard, Aarre and Søhale urnfields started (Figure 21a). The model shows the transition occurred in the 7th century BC (*690-604 cal BC* at 68.2% probability), c.50-150yr earlier than usually assumed and earlier than the current date of the Ha D1-D2 transition in Central Europe. In another study (66), we found that the Ha C-D transition in Southern Germany took places some decades before the traditional 650 BC date, which incidentally extends per. D1 and possibly shifts the D1-D2 transition earlier and in the direction of the estimated Bronze-Iron Age transformation in Southern Scandinavia. This leaves little time for Bronze Age per. VI, when a new spectrum of artefact types was introduced, clearly separating it from the previous period V (39, 135). In opposition, to the continuation of artefact types across the Bronze-Iron Age transformation (5). The earlier transition date contributes to an ongoing debate, whether per. VI should instead be understood as a transitional phase between the Bronze and Iron Ages, or even if it might be incorporated into the Iron Age (5, 132, 135, 136, 137). Another possibility is overlapping phases with different geographical distributions, comparable to what has been suggested for the Hallstatt-La Téne transition in Central Europe (41), but this will need further investigation.

The typo-chronological system of Jensen (5) defines the transition between Early PRIA periods I.1 and I.2 as occurring after the introduction of pins with type 1 and type 2 coiled head and pottery type 12B, but before the introduction of pin with circular head and pottery type 18C (5). A chronological model following this construction shows the transition to occur in the late half of the 5th century (*438-410 cal BC* at 68.2% probability, Figure 21b). This is a few decades earlier than the previously suggested transition c.400 BC (18), but it is not contradicted by the archaeological information.

The transformation from Early to Late PRIA coincides with a clear break in material culture (5), and the abandonment of settlements and cemeteries across most of western Denmark (138). It is usually assumed to occur around 250-200 BC (5, 95), although Becker (4) has suggested it to occur around 300 BC and Møller et al. (18) have suggested the early-mid 3rd century BC. The typo-chronological system of Jensen defines the transformation as occurring after the introduction of pin with circular head, triangular belt clasp and pottery type 15C, and coinciding with the introduction of iron ring with shank, pin with winged head, pin with grooved head and Holstein pin (5). A chronological model following this construction shows that the transformation from Early to Late PRI probably occurred in the late 4th-early 3rd century BC (*325-286 cal BC* at 68.2% probability, Figure 21c). This is considerably earlier than usually assumed, but in agreement with suggestions by Becker and Møller et al. (cf. Figure 2), and the date is additionally supported by the transformation coinciding with the abandonments of Aarre and Søhale urnfields in the late half of the 4th century BC (cf. Figures 11 and 12).

Preprints (www.preprints.org) | NOT PEER-REVIEWED | Posted: 28 November 2023 doi:10.20944/preprints202311.1702.v1

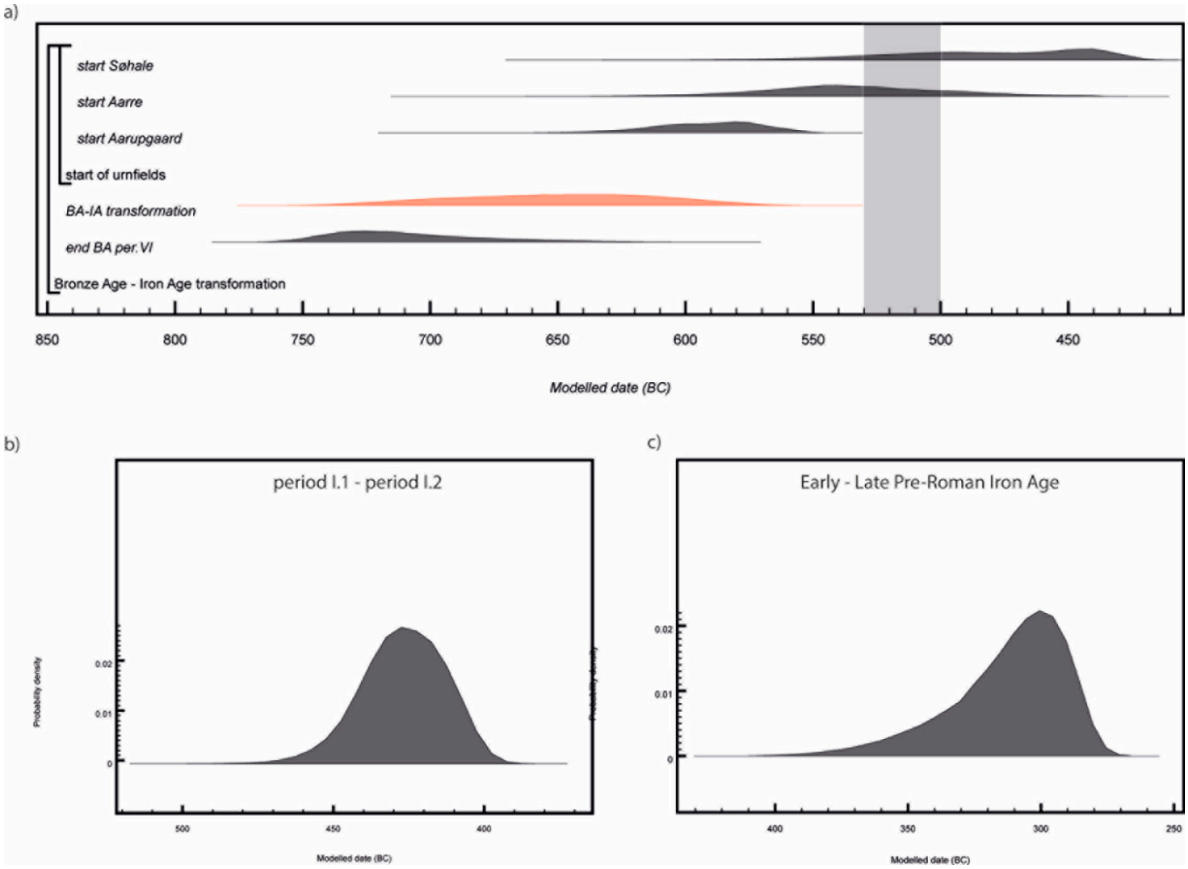

Figure 21. Chronological transitions of the Pre-Roman Iron Age, as defined by the typo-chronology of Jensen (2005). a) chronological model of the Bronze-Iron Age transformation, the red distribution is the estimated transitional period between the end of Bronze Age per. VI (690-604 cal BC at 68.2% probability) and the start of burial activity at Aarupgaard, Aarre and Søhale urnfields, the grey area marks the conventional transformation, b) per. I.1-I.2 (438-410 cal BC at 68.2% probability), c) Early-Late Pre-Roman Iron Age (325-286 cal BC at 68.2% probability).

This study demonstrates the need to adjust relative chronological frameworks using absolute dating, including the chronological framework of the Late Bronze Age and Early Iron Age in Southern Scandinavia. The introduction of the urnfield phenomenon in Denmark is a cultural marker of the start of the Iron Age and we estimate this to occur already in the 7th century BC. There is little absolute dating evidence from urnfield in Schleswig-Holstein (although see 139), but comparable material from the Netherlands is dated to Late Bronze Age-Early Iron Age, where the latter start c.800 BC (140). Urnfields in Belgium are primarily a Bronze Age phenomenon, although ^{14}C dating has also here challenged the traditional chronological framework (e.g. 141). We estimate the Danish urnfields were in use for *376-537yr* (68% probability), with Aarupgaard urnfield as the only sites that continued to be in use in the first part of the Late PRIA. There is no available absolute evidence to contradict shifting the Early PRIA chronology by c.150yr, with per.I.1 lasting above two centuries, and per. I.2 lasting above one century. Part of the shift might however be explained by considerable temporal differences in the adoption of cultural development and further investigations of the absolute chronological framework need to pay particular attention to other regions in Denmark and northern Germany.

Conclusions

Since the Danish Pre-Roman Iron Age was defined as an archaeological period in the 1890s, it has largely relied on relative typo-chronological analyses of artefact assemblages from urnfields. This study continues a long research history, but also presents the first large-scale ^{14}C investigation of regional material culture from three urnfields in Jutland. By adopting a dynamic modelling approach,

we can provide a dynamic perspective on the material culture, showing when certain artefact types were in production and primary use, how quickly types were taken up and later abandoned, and demonstrating periods with faster and slower change. We provide the first absolute correlation of metalwork and pottery artefact typologies, without which it is difficult to compare burial and settlement data.

We present the first absolute chronology for the period and demonstrate that the Bronze-Iron Age transformation took place already in the 7th century BC. This is significantly earlier than the previously assumed c.530-500 BC and revives the discussion of whether the final Bronze Age per. VI might be interpreted as a transitional phase to the Iron Age, or if per. VI and the start of the PRIA are overlapping periods, possibly with different geographical distributions. The start of the Iron Age in Denmark is correlated with Central Europe, providing the basis for future studies addressing overarching questions regarding for example social structure, economy and religion.

The last millennium BC have previously been avoided by ^{14}C researchers due to the Hallstatt plateau c.750-400 cal BC (although see 18), but by providing start and end boundaries of the urnfields within c.40-80yr (68.3% probability), and artefact currencies within c.30-70yr (68.3% probability), we successfully demonstrate that calibration plateaus are no longer a 'catastrophe' for archaeological chronologies (66, 69). We are however surprised to find that the inversion of the calibration curve c.320-200 cal BC poses a comparable challenge. Although the IntCal20 calibration dataset has an annual resolution back to 5000 cal BP it does not include high-resolution calibration data for the last centuries BC (64).

Supplementary Materials: The following supporting information can be downloaded at the website of this paper posted on Preprints.org, S1 Table. Metalwork types in English and Danish. SI Table. Pottery typology, descriptions of vessel neck shapes, after Jensen (5). S1 Table. Pottery typology, descriptions of vessel body shapes, after Jensen (5). S1 Fig. Pottery typology after Jensen (5). S1 Fig. Kernel density plot of Aarre urnfield. Estimated by the preferred urnfield model B. S1 Fig. Kernel density plot of Søhale urnfield. Estimated by the preferred urnfield model B. S1 Fig. Kernel density plot of Aarupgaard urnfield. Estimated by the preferred urnfield model B. S1 Fig. Aarupgaard urnfield divided into arbitrary horizontal groups (H1-H6) of c.200 burials. ^{14}C dated burials are marked in red, burial group M1 in light grey and burial group M2 in dark grey. S1 Fig. Posterior estimated starts of arbitrary horizontal groups at Aarupgaard urnfield. Excluding the initial 'founding phase' with burials U3330, U3341 and U3869. S1 Fig. Kernel density estimate of alternative horizontal model of Aarupgaard urnfield. **S1 Fig. Adding simulated later burial dates to preferred urnfield model B.** Diamonds are medians of true calendar dates, circles are medians of posterior estimates. S1 Table. Graves containing possible heirlooms. The table includes graves containing artefacts with posterior estimated outlier probabilities >5% as estimated by a General Outlier_Model (2). All artefacts from the respective graves are included, but only outliers are marked in red. Identified heirlooms with residence offsets are marked in bold red. S1 Fig. Identifying residence offsets. Posterior estimated dates from preferred currency model with a General Outlier_Model (121). a) circular head pin from Aarupgaard U293 estimated to be later than its burial date, b) circular head pin from Aarupgaard U1382 estimated to be earlier than its burial date, c) posterior estimated dates from Aarupgaard U1617, demonstrating the circular head pin to be an heirloom with a considerable residence offset. S1 Fig. Chronological model of pottery currencies. **S1 Fig. Currency model of pottery type 12B. S1 Fig. Currency model of pottery type 15B.** Example from grave U766 from Aarupgaard urnfield. **S1 Fig. Currency model of pottery type 15C.** Example from grave U346 from Aarupgaard urnfield. **S1 Fig. Currency model of pottery type 15D. S1 Fig. Currency model of pottery type 18C.** Example from grave U1001 from Aarupgaard urnfield. **S1 Fig. Currency model of pottery type 20B.** Example from grave U36 from Aarupgaard urnfield. S1 Fig. Chronological model of metalwork currencies. S1 Fig. Currency model of pin with type 1 coiled head. Example from grave U1186 from Aarupgaard urnfield. S1 Fig. Currency model of pin with type 2 coiled head. Example from grave U81 from Aarupgaard urnfield. S1 Fig. Currency model of pin with circular head. Example from grave U500 from Aarupgaard urnfield. S1 Fig. Currency model of simple iron ring. Example from grave U1186 from Aarupgaard urnfield. S1 Fig. Currency model of tongue-shaped belt clasp. Example from grave U1834 from Aarupgaard urnfield. S1 Fig. Currency model of triangular belt clasp. Example from grave U1363 from Aarupgaard urnfield. S1 Fig. Currency model of narrow belt clasp. Example from grave U1678 from Aarupgaard urnfield. S1 Fig. Currency model of iron ring with shank. Example from grave U2550 from Aarupgaard urnfield. S1 Fig. Currency model of Holstein pin. Example from grave U2541 from Aarupgaard urnfield. S1 Fig. Currency model of pin with rod-shaped head. S1 Fig. Currency model of pin with rod-shaped head. S1 Fig. Currency model of winged head pin. **SI Fig. Circular head pins from Aarupgaard urnfield.** Plotted are the head size index against mean ages estimated by the currency model. **S1 Fig. Posterior estimated parameters from currency models.** a) Periods of production increase and decrease estimated by trapezium prior models, b) duration of

currencies modelled in bounded phases. **SI Fig. Posterior estimated residence time. S2 Bayesian chronological models provided in the exact code in OxCal v4's Chronological Query Language (77).**

Funding: Financial support by the Deutsche Forschungsgemeinschaft (DFG, German Research Foundation – Project number 2901391021 – SFB 1266, subproject G1: Timescales of Change – Chronology of cultural and environmental transformations of the Collaborative Research Center 'Scales of Transformation: Human-environmental Interaction in Prehistoric and Archaic Societies') and the Centre for Baltic and Scandinavian Archaeology (ZBSA). The funders had no role in study design, data collection and analysis, decision to publish, or preparation of the manuscript.

Data Availability Statement: All relevant data are within the manuscript and its Supporting Information files.

Acknowledgments: The authors would like to thank Museum Sønderjylland, Sydvestjyske Museer and ARKVEST - Arkæologi i Vestjylland for access to the material and to many colleagues here for kindly helping with the sampling. Also, thanks to Anne Egelund Poulsen for helping with the archival material from Aarupgaard urnfield and to Niels Algreen Møller and Kamilla Terkildsen for access to unpublished data. The study was carried out at the Centre for Baltic and Scandinavian Archaeology (ZBSA), as part of the Collaborative Research Center 'Scales of Transformation: Human-environmental Interaction in Prehistoric and Archaic Societies', subproject G1: Timescales of Change – Chronology of cultural and environmental transformations.

References

1. Thomsen CJ. Ledetraad til Nordisk Oldkyndighed. Kjo¨benhavn: Kongelige Nordiske oldskriftselskab; 1836.
2. Gräslund B. Periodsystem i forskningshistorisk perspektiv. Hikuin. 1978; 4.
3. Neergaard C. Sønderjyllands Jærnalder Aarbøger for Nordisk Oldkyndighed og Historie. 1916; 1916: 227-302.
4. Becker CJ. Førromersk jernalder i Syd- og Midtjylland. København: Nationalmuseet; 1961.
5. Jensen CK. Kontekstuel kronologi: en revision af det kronologiske grundlag for førromersk jernalder i Sydskandinavien. Højbjerg: Kulturlaget; 2005.
6. Reinecke P. Brandgräber vom Beginn der Hallstattzeit aus den östlichen Alpenländern und die Chronologie des Grabfeldes von Hallstatt,'Mitteilungen der Anthropologischen Gesellschaft 30, Wien. 1900.
7. Kossinna G. Die Herkunft der Germanen: zur methode der Siedlungsarchäologie: Kabitzsch; 1911.
8. Sørensen MLS, Rebay-Salisbury K. The impact of 19th century ideas on the construction of 'urnfield' as a chronological and cultural concept: tales from Northern and Central Europe. In: Lehoërff A, editor. Construire le temps Histoire et méthodes des chronologies et calendriers des derniers millénaires avant notre ère en Europe occidentale Actes du XXXe (Bibracte; 16) Colloque international de Halma-Ipel, UMR 8164 (CNRS, Lille 3, MCC), 7-9 décembre 2006, Lille2008. p. 57-67.
9. Madsen A, Neergaard C. Jydske gravpladser fra den førromerske jernalder. Aarbøger for Nordisk Oldkyndighed og Historie. 1894; 1894: 165-212.
10. Neergaard C. Jernalderen. Aarbøger for Nordisk Oldkyndighed og Historie. 1892(1892): 207-341.
11. Jensen CK. Chronologische Probleme und ihre Bedeutung für das Verständnis der vorrömischen Eisenzeit in Süd-/Mitteljütland. Praehistorische Zeitschrift. 1996; 71(2): 194-216.
12. Jensen CK. Om behovet for en nyvurdering af den førromerske kronologi. Lag. 1992; 3: 53-73.
13. Hingst H. Vorgeschichte des Kreises Stormarn. Neumünster: Wachholtz; 1959.
14. Jensen J. The prehistory of Denmark: from the Stone Age to the Vikings. Kbh: Gyldendal; 2013.
15. Jensen J. Hallstattsværd i skandinaviske fund fra overgangen mellem bronze- og jernalderen. In: Poulsen J, editor. Regionale forhold i Nordisk Bronzealder 5 Nordiske Symposium for Bronzealderforskning på Sandbjerg Slot 1987 1989. p. 149-57.
16. Lorentzen A, Steffgen U. Bemerkungen zu Leitformen der älteren vorrömischen Eisenzeit nördlich der Mittelgebirge. Germania. 1990; 68: 483–508.
17. Jensen J. Ulbjerg-graven. Begyndelsen af den ældre jernalder i Jylland. Kuml. 1966; 1965: 23-33.
18. Møller NA, Harvig LL, Grundvad B. The Iron Age urnfield tradition of southwestern Jutland, Denmark. Acta Archaeologica. 2020; 91(1): 11-80. https://doi.org/10.1111/j.1600-0390.2020.12221.x
19. Baillie MGL, Pilcher JR. Some observations on the high-precision calibration of routine dates. In: Ottaway BS, editor. Archaeology, Dendrochronology and the Radiocarbon Calibration Curve. Edinburgh: University of Edinburgh; 1983. p. 51-63.
20. Lanting JN, Aerts-Bijma AT, van der Plicht J. Dating of Cremated Bones. Radiocarbon. 2001; 43(2A): 249-54. https://doi.org/10.1017/S0033822200038078
21. De Mulder G, Creemers G, Van Strydonck M. Challenging the Traditional Chronological Framework of Funerary Rituals in the Meuse-Demer-Scheldt Region: 14C Results from the Site of Lummen-Meldert (Belgium). Radiocarbon. 2014; 56(2): 461-8. https://doi.org/10.1017/S0033822200049511

22. Hüls CM, Erlenkeuser H, Nadeau MJ, Grootes PM, Andersen N. Experimental Study on the Origin of Cremated Bone Apatite Carbon. Radiocarbon. 2010; 52(2): 587-99. https://doi.org/10.1017/S0033822200045628
23. Zazzo A, Saliège J-F, Lebon M, Lepetz S, Moreau C. Radiocarbon Dating of Calcined Bones: Insights from Combustion Experiments Under Natural Conditions. Radiocarbon. 2012; 54(3-4): 855-66. https://doi.org/10.1017/S0033822200047500
24. Snoeck C, Brock F, Schulting RJ. Carbon Exchanges between Bone Apatite and Fuels during Cremation: Impact on Radiocarbon Dates. Radiocarbon. 2014; 56(2): 591-602. https://doi.org/10.2458/56.17454
25. Rose HA, Meadows J, Henriksen MB. Bayesian modeling of wood-age offsets in cremated bone. Radiocarbon. 2020; 62(2): 379-401. https://doi.org/10.1017/RDC.2020.3
26. Feinman GM, Neitzel JE. Excising culture history from contemporary archaeology. Journal of Anthropological Archaeology. 2020; 60: 101230. https://doi.org/10.1016/j.jaa.2020.101230
27. Taylor WW. A Study of Archaeology1948.
28. Binford LR. Archaeological Systematics and the Study of Culture Process. American Antiquity. 1965; 31(2): 203-10. https://doi.org/10.2307/2693985
29. Griffiths S. We're All Cultural Historians Now: Revolutions In Understanding Archaeological Theory And Scientific Dating. Radiocarbon. 2017; 59(5): 1347-57. https://doi.org/10.1017/RDC.2017.20
30. Clarke D. Archaeology: the loss of innocence. Antiquity. 1973; 47(185): 6-18. https://doi.org/10.1017/S0003598X0003461X
31. Siegmund F. How many years should chronological units cover in archaeology? In: Kars M, van Oosten R, Roxburgh MA, Verhoeven A, editors. Rural riches & royal rags? Studies on medieval and modern archaeology, presented to Frans Theuws. Zwolle: SPA-Uitgevers & the Dutch Society for Medieval Archaeology; 2018. p. 96-104.
32. Fowler C. Relational Typologies, Assemblage Theory and Early Bronze Age Burials. Cambridge Archaeological Journal. 2017; 27(01): 95-109. https://doi.org/10.1017/S0959774316000615
33. Sørensen MLS. 'Paradigm lost' – on the State of Typology within Archaeological Theory. In: Kristiansen K, Šmejda L, Turek J, editors. Paradigm Found Archaeological Theory Present, Past And Future. Oxford2015. p. 84-94.
34. Normark J. Involutions of Materiality: Operationalizing a Neo-materialist Perspective through the Causeways at Ichmul and Yo'okop. Journal of Archaeological Method and Theory. 2010; 17(2): 132-73. https://doi.org/10.1007/s10816-010-9079-7
35. Boozer AL. The tyranny of typologies: evidential reasoning in Romano-Egyptian domestic archaeology. In: Chapman R, Wylie A, editors. Material Evidence: Learning from archaeological practice. London: Routledge; 2015. p. 92– 109.
36. Gräslund B. Relativ datering. Om kronologisk metod i nordisk arkeologi1974.
37. Trachsel M. Untersuchungen zur relativen and absoluten Chronologie der Hallstattzeit. Bonn: R. Habelt; 2004.
38. Jensen CK, Høilund Nielsen K. Burial & society : the chronological and social analysis of archaeological burial data. Aarhus: Aarhus University Press; 1997.
39. Kneisel J. New chronological research of the late Bronze Age in Scandinavia. Danish Journal of Archaeology. 2013; 2(2): 95-111.
40. Bayliss A, Hines J, Høilund Nielsen K, McCormac FG, Scull C. Anglo-Saxon Graves and Grave Goods of the Sixth and Seventh Centuries AD: A Chronological Framework. J. Hines AB, editor. London: Society for Medieval Archaeology; 2013.
41. Parzinger H. Chronologie der Späthallstatt- und Frühlatène-Zeit: Studien zu Fundgruppen zwischen Mosel und Save. Weinheim: VCH, Acta Humaniora; 1989.
42. Roberts BW, Uckelmann M, Brandherm D. Old Father Time: The Bronze Age Chronology of Western Europe. In: Fokkens H, Harding A, editors. The Oxford handbook of the European Bronze Age. Oxford: Oxford University Press; 2013. p. 17-46.
43. Brainerd GW. The Place of Chronological Ordering in Archaeological Analysis. American Antiquity. 1951; 16(4): 301-13. https://doi.org/10.2307/276979
44. Plog S, Hantman JL. Chronology Construction and the Study of Prehistoric Culture Change. Journal of Field Archaeology. 1990; 17(4): 439-56. https://doi.org/10.1179/009346990791548592
45. Malmer MP. Arkeologisk positivism. Fornvännen. 1984; 79: 260-8.
46. O'Shea JM. Mortuary variability: an archaeological investigation. Orlando: Academic Press; 1984.
47. Pearson MP. The archaeology of death and burial. 2003 ed. Phoenix Mill: Sutton Publishing; 1999.
48. Zavodny E, Culleton BJ, McClure SB, Kennett DJ, Balen J. Recalibrating grave-good chronologies: new AMS radiocarbon dates from Late Bronze Age burials in Lika, Croatia. Antiquity. 2019; 93(367): 113-27. https://doi.org/10.15184/aqy.2018.184
49. Strien H-C. 'Robust chronologies' or 'Bayesian illusion'? Some critical remarks on the use of chronological modelling. Documenta Praehistorica. 2019; 46(0): 204-15.

50. Asscher Y, Boaretto E. Absolute Time Ranges in the Plateau of the Late Bronze to Iron Age Transition and the Appearance of Bichrome Pottery in Canaan, Southern Levant. Radiocarbon. 2019; 61(1): 13-37. https://doi.org/10.1017/RDC.2018.58
51. Buck CE, Cavanagh WG, Litton CD. Bayesian approach to interpreting archaeological data. Chichester: Wiley; 1996.
52. Bayliss A. Rolling Out Revolution: Using Radiocarbon Dating in Archaeology. Radiocarbon. 2009; 51(1): 123-47. https://doi.org/10.1017/S0033822200033750
53. Hamilton WD, Krus AM. The myths and realities of Bayesian chronological modeling revealed. American Antiquity. 2018; 83(02). https://doi.org/10.1017/aaq.2018.21
54. Bronk Ramsey C, Schulting RJ, Bazaliiskii VI, Goriunova OI, Weber AW. Spatio-temporal patterns of cemetery use among Middle Holocene hunter-gatherers of Cis-Baikal, Eastern Siberia. Archaeological Research in Asia. 2021; 25: 100253. https://doi.org/https://doi.org/10.1016/j.ara.2020.100253
55. Pearson GW, Pilcher JR, Baillie MGL. High-precision ^{14}C measurement of Irish oaks to show the natural ^{14}C variations from 200 BC to 4000 BC. Radiocarbon. 1983; 25(2): 179-86. https://doi.org/10.1017/S0033822200005464
56. Stuiver M, Becker B. High-precision decadal calibration of the radiocarbon time scale, AD 1950–2500 BC. Radiocarbon. 1986; 28(2B): 863-910. https://doi.org/10.1017/S0033822200060185
57. Wijma S, Aerts AT, van der Plicht J, Zondervan A. The Groningen AMS facility. Nuclear Instruments and Methods in Physics Research Section B: Beam Interactions with Materials and Atoms. 1996; 113(1): 465-9. https://doi.org/10.1016/0168-583X(95)01420-9
58. Stäuble H, Hiller A. An Extended Prehistoric Well Field in the Opencast Mine Area of Zwenkau, Germany. Radiocarbon. 1997; 40(2): 721-33. https://doi.org/10.1017/S0033822200018671
59. Hamilton WD, Haselgrove C, Gosden C. The impact of Bayesian chronologies on the British Iron Age. World Archaeology. 2015; 47(4): 642-60. https://doi.org/10.1080/00438243.2015.1053976
60. Aerts-Bijma AT, Paul D, Dee MW, Palstra SWL, Meijer HAJ. An independent assessment of uncertainty for radiocarbon analysis with the new generation high-yield accelerator mass spectrometers. Radiocarbon. 2020; 63(1): 1-22. https://doi.org/10.1017/RDC.2020.101
61. Heaton TJ, Blaauw M, Blackwell PG, Bronk Ramsey C, Reimer PJ, Scott EM. The IntCal20 Approach to Radiocarbon Calibration Curve Construction: A New Methodology Using Bayesian Splines and Errors-in-Variables. Radiocarbon. 2020; 62(4): 821-63. https://doi.org/10.1017/RDC.2020.46
62. Fahrni SM, Southon J, Fuller BT, Park J, Friedrich M, Muscheler R, et al. Single-year German oak and Californian bristlecone pine ^{14}C data at the beginning of the Hallstatt Plateau from 856 BC to 626 BC. Radiocarbon. 2020; 62(4): 919-37. https://doi.org/10.1017/RDC.2020.16
63. Park J, Southon J, Fahrni S, Creasman PP, Mewaldt R. Relationship between solar activity and Δ14C peaks in AD 775, AD 994, and 660 BC. Radiocarbon. 2017; 59(4): 1147-56. https://doi.org/10.1017/RDC.2017.59
64. Reimer PJ, Austin, W.E.N., Bard, E., Bayliss, A., Blackwell, P.G., Bronk Ramsey, C., Butzin, M., Cheng, H., Edwards, R.L., Friedrich, M., Grootes, P.M., Guilderson, T.P., Hajdas, I., Heaton, T.J., Hogg, A.G., Hughen, K.A., Kromer, B., Manning, S.W., Muscheler, R., Palmer, J.G., Pearson, C., van der Plicht, J., Reimer, R.W., Richards, D.A., Scott, E.M., Southon, J.R., Turney, C.S.M., Wacker, L., Adolphi, F., Büntgen, U., Capano, M., Fahrni, S.M., Fogtmann-Schulz, A., Friedrich, R., Köhler, P., Kudsk, S., Miyake, F., Olsen, J., Reinig, F., Sakamoto, M., Sookdeo, A., Talamo, S. The IntCal20 Northern Hemisphere Radiocarbon Age Calibration Curve (0-55 cal kBP). Radiocarbon. 2020; 62(4): 725-57. https://doi.org/10.1017/RDC.2020.41
65. Waddington K, Bayliss A, Higham T, Madgwick R, Sharples N. Histories of deposition: creating chronologies for the Late Bronze Age-Early Iron Age transition in Southern Britain. Archaeological Journal. 2019; 176(1): 84-133. https://doi.org/10.1080/00665983.2018.1504859
66. Rose HA, Müller-Scheeßel N, Meadows J, Hamann C. Radiocarbon dating and Hallstatt chronology: a Bayesian chronological model for the burial sequence at Dietfurt an der Altmühl 'Tennisplatz', Bavaria, Germany. Archaeological and Anthropological Sciences. 2022; 14(4): 72. https://doi.org/10.1007/s12520-022-01542-1
67. Jacobsson P, Hamilton WD, Cook G, Crone A, Dunbar E, Kinch H, et al. Refining the Hallstatt Plateau: Short-Term 14C Variability and Small Scale Offsets in 50 Consecutive Single Tree-Rings from Southwest Scotland Dendro-Dated to 510–460 BC. Radiocarbon. 2018; 60(1): 219–37. https://doi.org/10.1017/RDC.2017.90
68. Manning SW, Smith AT, Khatchadourian L, Badalyan R, Lindsay I, Greene A, et al. A new chronological model for the Bronze and Iron Age South Caucasus: radiocarbon results from Project ArAGATS, Armenia. Antiquity. 2018; 92(366): 1530-51. https://doi.org/10.15184/aqy.2018.171
69. Meadows J, Rinne C, Immel A, Fuchs K, Krause-Kyora B, Drummer C. High-precision Bayesian chronological modeling on a calibration plateau: The Niedertiefenbach gallery grave. Radiocarbon. 2020; 62(5): 1261-84. https://doi.org/10.1017/RDC.2020.76
70. Jørgensen E. Tuernes Mysterier. Skalk. 1975; 1975(1): 3-10.

71. Bayliss A, Bronk Ramsey C, van der Plicht J, Whittle A. Bradshaw and Bayes: Towards a Timetable for the Neolithic. Cambridge Archaeological Journal. 2007; 17(S1): 1-28. https://doi.org/10.1017/S0959774307000145
72. Deetz J, Dethlefsen E. The Doppler Effect and Archaeology: A Consideration of the Spatial Aspects of Seriation. Southwestern Journal of Anthropology. 1965; 21(3): 196-206. https://doi.org/10.1086/soutjanth.21.3.3629228
73. Lyman RL, Harpole JL. A. L. Kroeber and the Measurement of Time's Arrow and Time's Cycle. Journal of Anthropological Research. 2002; 58(3): 313-38. https://doi.org/10.1086/jar.58.3.3631180
74. Buck CE, Litton CD, Smith AFM. Calibration of radiocarbon results pertaining to related archaeological events. Journal of Archaeological Science. 1992; 19(5): 497-512. https://doi.org/10.1016/0305-4403(92)90025-X
75. Karlsberg AJ. Flexible Bayesian methods for archaeological dating [Doctoral thesis]. Sheffield: University of Sheffield; 2006.
76. Lee S, Bronk Ramsey C. Development and Application of the Trapezoidal Model for Archaeological Chronologies. Radiocarbon. 2012; 54(1): 107-22. https://doi.org/10.2458/azu_js_rc.v54i1.12397
77. Bronk Ramsey C. Bayesian Analysis of Radiocarbon Dates. Radiocarbon. 2009; 51(1): 337-60. https://doi.org/10.1017/S0033822200033865
78. Lee S, Bronk Ramsey C, Mazar A. Iron Age Chronology in Israel: Results from Modeling with a Trapezoidal Bayesian Framework. Radiocarbon. 2013; 55(2): 731-40. https://doi.org/10.1017/S003382220005788X
79. Griffiths S, Johnston R, May R, McOmish D, Marshall P, Last J, et al. Dividing the Land: Time and Land Division in the English North Midlands and Yorkshire. European Journal of Archaeology. 2022; 25(2): 216-37. https://doi.org/10.1017/eaa.2021.48
80. Martens J. Jastorf and Jutland. In: Brandt J, Rauchfuss B, editors. Internationalen Tagung zum einhundertjähringen Jubiläum der Veröffentlichung der "Ältesten Urnenfriedhöfe bei Uelzen und Lüneburg" duch Gustav Schwantes; Bad Bevensen: Archäologisches Museum Hamburg; 2014. p. 245-66.
81. Fokkens H. The genesis of urnfields: economic crisis or ideological change? Antiquity. 1997; 71(272): 360-73. https://doi.org/10.1017/S0003598X00084970
82. van Beek R, Quik C, Bergerbrant S, Huisman F, Kama P. Bogs, bones and bodies: the deposition of human remains in northern European mires (9000 BC–AD 1900). Antiquity. 2023; 97(391): 120-40. https://doi.org/10.15184/aqy.2022.163
83. Terkildsen KF. Gravpladsen Årupgård som kilde til social stratifikation i førromersk jernalder. In: Foss P, Møller NA, editors. De dødes landskab Grav og gravskik i ældre jernalder i Danmark; Ribe2015. p. 51-70.
84. Løvschal M. Emerging Boundaries: Social Embedment of Landscape and Settlement Divisions in Northwestern Europe during the First Millennium BC. Current Anthropology. 2014; 55(6): 725-50. https://doi.org/10.1086/678692
85. Eriksen P, Rindel PO. Hulbælternes funktioner. In: Eriksen P, Rindel PO, editors. Lange linjer i landskabet Hulbælter fra jernalderen. Jysk Arkæologisk Selskabs skrifter, 104. Højbjerg: Jysk Arkæologisk Selskab; 2018. p. 409-28.
86. Martens J. Fortified places in low-land Northern Europe and Scandinavia during the Pre-Roman Iron Age. In: Mollers S, Schlüter W, Sievers S, editors. Keltische Einflüsse im nördlichen Mitteleuropa während der mittleren und jüngeren vorrömischen Eisenzeit. Kolloquien zurVor- und Frühgeschichte 9. Bonn: Habelt; 2007. p. 87-105.
87. Neergaard C. Nogle sønderjydske Fund fra den ældre jernalder. Fra Nationalmuseets Arbejdsmark. 1931; 1931: 63-80.
88. Neumann H. Tuegravpladsen på Årupgårds mark, Gram sogn. Haderslev Amts Museum. 1947; 1947: 6-7.
89. Olesen LH, Schlosser Mauritsen E. Fortiden Set fra Himlen. Luftfotoarkæologi i Danmark. Holstebro: Holstebro Museum; 2015.
90. Kolstrup E. Vegetational and environmental history during the Holocene in the Esbjerg area, west Jutland, Denmark. Vegetation History and Archaeobotany. 2009; 18(5): 351-69. https://doi.org/10.1007/s00334-009-0214-x
91. Møller NA. Døde i de levendes verden. Vestjyske gravfund i kontekst. In: Foss P, Møller NA, editors. De dødes landskab Grav og gravskik i ældre jernalder i Danmark; Ribe: SAXO-insituttet, Københavns Universitet; 2015. p. 215-36.
92. Henriksen MB. Experimental cremations – can they help us to understand prehistoric cremation graves? In: Cieśliński A, Kontny B, editors. Interacting Barbarians Contacts, Exchange and Migrations in the First Millennium AD. Neue Studien zur Sachsenforschung. Warschau: Neue Studien zur Sachsenforschung Band 9; 2019. p. 289-96.
93. Harvig L, Runge MT, Lundø MB. Typology and function of Late Bronze Age and Early Iron Age cremation graves - a micro-regional case study. Danish Journal of Archaeology. 2014; 3(1): 3-18. https://doi.org/10.1080/21662282.2014.942980
94. Jørgensen E. Berigtigelse. Skalk. 1999(1): 28-31.

95. Martens J. Die vorrömische Eisenzeit in Südskandinavien. Probleme und Perspektiven. Praehistorische Zeitschrift. 1996; 71(217-243).
96. Hingst H. Neumünster-Oberjörn. Ein Urnenfriedhof der vorrömischen Eisenzeit am Oberjörn und die vor- and frühgeschichtliche Besiedlung auf dem Neumünsteraner Sander. Neumünster: Wachholtz; 1980.
97. Hingst H. Urnenfriedhöfe der vorrömischen Eisenzeit aus dem östlichen Holstein und Schwansen. Neumünster: Wachholtz; 1986.
98. Hingst H. Jevenstedt. Ein Urnenfriedhof der älteren vorrömischen Eisenzeit im Kreise Rendsburg-Eckernförde, Holstein. Neumünster: Wachholtz; 1974.
99. Hingst H. Die vorrömische Eisenzeit Westholsteins. Neumünster: Wachholtz; 1983.
100. Hingst H. Urnenfriedhöfe der vorrömischen Eisenzeit aus Südholstein. Neumünster: Wachholtz; 1989.
101. Lorange T. Det sakrale landskab ved Årre. Landskabets hukommelse gennem 4.000 års gravriter. In: Foss P, Møller NA, editors. De dødes landskab Grav og gravskik i ældre jernalder i Danmark. Arkæologiske Skrifter 13. Ribe: SAXO-instituttet, Københavns Universitet; 2015. p. 21-36.
102. Guy H, Masset C, Baud C-A. Infant taphonomy. International Journal of Osteoarchaeology. 1997; 7(3): 221-9. https://doi.org/10.1002/(SICI)1099-1212(199705)7:3<221::AID-OA338>3.0.CO;2-Z
103. Wahl J. Investigations on Pre-Roman and Roman Cremation Remains. In: Schmidt CW, Symes SA, editors. The Analysis of Burned Human Remains. Second ed. San Diego: Academic Press; 2015. p. 163-79.
104. Schulz Paulsson B. Radiocarbon dates and Bayesian modeling support maritime diffusion model for megaliths in Europe. Proceedings of the National Academy of Sciences. 2019; 116(9): 3460-5. https://doi.org/10.1073/pnas.1813268116
105. Bayliss A, Allen MJ, Healy F, Whittle A, Germany M, Griffiths S, et al. The Greater Thames estuary. In: Whittle A, Healy F, Bayliss A, editors. Gathering Time: Dating the Early Neolithic Enclosures of Southern Britain and Ireland. Oxford: Oxbow; 2011. p. 348-86.
106. Dye TS, Buck CE, DiNapoli RJ, Philippe A. Bayesian chronology construction and substance time. Journal of Archaeological Science. 2023; 153: 105765. https://doi.org/https://doi.org/10.1016/j.jas.2023.105765
107. Harvig L, Lynnerup N, Ebsen JA. Computed tomography and computed radiography of Late Bronze Age cremation urns from Denmark: an interdisciplinary attempt to develop methods applied in bioarchaeological cremation research. Archaeometry. 2012; 54(2): 369-87. https://doi.org/10.1111/j.1475-4754.2011.00629.x
108. Person A, Bocherens H, Saliège J-F, Paris F, Zeitoun V, Gérard M. Early Diagenetic Evolution of Bone Phosphate: An X-ray Diffractometry Analysis. Journal of Archaeological Science. 1995; 22(2): 211-21. https://doi.org/10.1006/jasc.1995.0023
109. Olsen J, Heinemeier J, Bennike P, Krause C, Margrethe Hornstrup K, Thrane H. Characterisation and blind testing of radiocarbon dating of cremated bone. Journal of Archaeological Science. 2008; 35(3): 791-800. https://doi.org/10.1016/j.jas.2007.06.011
110. Rose HA, Meadows J, Palstra SWL, Hamann C, Boudin M, Huels M. Radiocarbon Dating Cremated Bone: A Case Study Comparing Laboratory Methods. Radiocarbon. 2019; 61(5): 1581-91. https://doi.org/10.1017/RDC.2019.70
111. Van Strydonck M, Boudin M, De Mulder G. 14C Dating of Cremated Bones: The Issue of Sample Contamination. Radiocarbon. 2009; 51(2): 553-68. https://doi.org/10.1017/S0033822200055922
112. De Mulder G, Van Strydonck M, Boudin M, Leclercq W, Paridaens N, Warmenbol E. Re-Evaluation of the Late Bronze Age and Early Iron Age Chronology of the Western Belgian Urnfields Based on 14C Dating of Cremated Bones. Radiocarbon. 2007; 49(2): 499-514. https://doi.org/10.1017/S0033822200042429
113. Dee MW, Palstra SWL, Aerts-Bijma AT, Bleeker MO, de Bruijn S, Ghebru F, et al. Radiocarbon dating at Groningen: New and updated chemical pretreatment procedures. Radiocarbon. 2020; 62(1): 63-74. https://doi.org/10.1017/RDC.2019.101
114. Boudin M, Van Strydonck M, van den Brande T, Synal H-A, Wacker L. RICH – A new AMS facility at the Royal Institute for Cultural Heritage, Brussels, Belgium. Nuclear Instruments and Methods in Physics Research Section B: Beam Interactions with Materials and Atoms. 2015; 361: 120-3. https://doi.org/10.1016/j.nimb.2015.04.006
115. Nadeau M-J, Schleicher M, Grootes P, Erlenkeuser H, Gottdang A, Mous D, et al. The Leibniz-Labor AMS facility at the Christian-Albrechts University, Kiel, Germany. Nuclear Instruments and Methods in Physics Research Section B: Beam Interactions with Materials and Atoms. 1997; 123(1-4): 22-30.
116. Stuiver M, Polach HA. Discussion Reporting of 14C Data. Radiocarbon. 1977; 19(3): 355-63. https://doi.org/10.1017/S0033822200003672
117. Ward GK, Wilson SR. Procedures for comparing and combining radiocarbon age determinations: a critique. Archaeometry. 1978; 20(1): 19-31. https://doi.org/10.1111/j.1475-4754.1978.tb00208.x
118. Sabaux C, Veselka B, Capuzzo G, Snoeck C, Sengeløv A, Hlad M, et al. Multi-proxy analyses reveal regional cremation practices and social status at the Late Bronze Age site of Herstal, Belgium. Journal of archaeological science. 2021; 132: 105437. https://doi.org/10.1016/j.jas.2021.105437

119. Naysmith P, Scott EM, Cook GT, Heinemeier J, Van der Plicht J, Van Strydonck M, et al. A Cremated Bone Intercomparison Study. Radiocarbon. 2007; 49(2): 403-8. https://doi.org/10.1017/S0033822200042338
120. Van Strydonck M, Boudin M, Mulder GD. The Carbon Origin of Structural Carbonate in Bone Apatite of Cremated Bones. Radiocarbon. 2010; 52(2): 578-86. https://doi.org/10.1017/S0033822200045616
121. Bronk Ramsey C. Dealing with Outliers and Offsets in Radiocarbon Dating. Radiocarbon. 2009; 51(3): 1023-45. https://doi.org/10.1017/S0033822200034093
122. Dee MW, Bronk Ramsey C. High-precision Bayesian modeling of samples susceptible to inbuilt age. Radiocarbon. 2014; 56(1): 83-94. https://doi.org/10.2458/56.16685
123. Olsen J, Margrethe Hornstrup K, Heinemeier J, Bennike P, Thrane H. Chronology of the Danish Bronze Age Based on 14C Dating of Cremated Bone Remains. Radiocarbon. 2011; 53(2): 261-75. https://doi.org/10.1017/S0033822200056538
124. Bronk Ramsey C. Methods for summarizing radiocarbon datasets. Radiocarbon. 2017; 59: 1809-33. https://doi.org/10.1017/RDC.2017.108
125. Contreras DA, Meadows J. Summed radiocarbon calibrations as a population proxy: a critical evaluation using a realistic simulation approach. Journal of Archaeological Science. 2014; 52: 591-608. https://doi.org/10.1016/j.jas.2014.05.030
126. Brunner M, von Felten J, Hinz M, Hafner A. Central European Early Bronze Age chronology revisited: A Bayesian examination of large-scale radiocarbon dating. PLOS ONE. 2021; 15(12): e0243719. https://doi.org/10.1371/journal.pone.0243719
127. Needham S, Bronk Ramsey C, Coombs D, Cartwright C, Pettitt P. An Independent Chronology for British Bronze Age Metalwork: The Results of the Oxford Radiocarbon Accelerator Programme. Archaeological Journal. 1997; 154(1): 55-107. https://doi.org/10.1080/00665983.1997.11078784
128. Garrow D, Gosden C, Hill JD, Bronk Ramsey C. Dating Celtic Art: a Major Radiocarbon Dating Programme of Iron Age and Early Roman Metalwork in Britain. Archaeological Journal. 2009; 166(1): 79-123. https://doi.org/10.1080/00665983.2009.11078221
129. Whittle A, Bayliss A, Barclay A, Gaydasrka B, Bánffy E, Borić D, et al. A Vinča potscape: formal chronological models for the use and development of Vinča ceramics in south-east Europe. Documenta Praehistorica. 2016; 43: 1-60. https://doi.org/10.4312/dp.43.1
130. Kern Z, Jungbert B, Morgós A, Molnár M, Horváth E. Wiggle-match dating of a floating oak chronology from an Early Iron Age grave construction (Eresztvényi Forest, Fehérvárcsurgó, Hungary). Radiocarbon. 2021. https://doi.org/10.1017/RDC.2021.70
131. Vandkilde H, Rahbek U, Rasmussen KL. Radiocarbon dating and the chronology of Bronze Age Southern Scandinavia. Acta Archaeologica. 1996; 67: 183-98.
132. Jensen J. Fra Bronze - til Jernalder. En kronologisk undersøgelse. København: Det Kongelige Nordiske Oldskriftselskab; 1997.
133. Rieckhoff S, Biel J. Die Kelten in Deutschland. Stuttgart: Konrad Theiss Verlag; 2001.
134. Hedeager L. Danmarks jernalder: mellem stamme og stat [Doctoral dissertation]. Aarhus: Aarhus Universitetsforlag: Aarhus University 1990.
135. Schmidt J-P. Studien zur jüngeren Bronzezeit in Schleswig-Holstein und dem nordelbischen Hamburg. Bonn: Habelt; 1993.
136. Kneisel J, Dörfler W, Dreibrodt S, Schaefer-Di Maida S, Feeser I. Cultural change and population dynamics during the Bronze Age: Integrating archaeological and palaeoenvironmental evidence for Schleswig-Holstein, Northern Germany. The Holocene. 2019. https://doi.org/10.1177/0959683619857237
137. Hingst H. Grabhügelfelder der jüngeren Bronze- und der frühen Eisenzeit aus Schleswig-Holstein. Offa 1976; 33: 66–122.
138. Webley L. Iron Age households: structure and practice in Western Denmark, 500 BC-AD 200. Højbjerg: Jutland Archaeological Society; 2008.
139. Schaefer-Di Maida S. Bronzezeitliche Transformationsprozesse in Schleswig-Holstein am Beispiel vom Fundplatz von Mang de Bargen, Bornhöved (Kr. Segeberg). Kiel: Christian-Albrechts-Universität zu Kiel; 2020.
140. Louwen AJ. Breaking and Making the Ancestors. Piecing together the urnfield mortuary process in the Lower-Rhine-Basin, ca. 1300 - 400 BC. Leiden: Sidestone Press; 2021.
141. De Mulder G, Van Strydonck M, Boudin M. The Impact of Cremated Bone Dating on the Archaeological Chronology of the Low Countries. Radiocarbon. 2009; 51(2): 579-600. https://doi.org/10.1017/S0033822200055946